UNIVERSITÀ DI PAVIA

SCUOLA DI ALTA FORMAZIONE DOTTORALE

MACRO-AREA SCIENZE E TECNOLOGIE

Dottorato di Ricerca in Scienze della Terra e dell'Ambiente

Riccardo Inama

Fracture analysis and depositional geometries of a high relief carbonate platform from UAV photogrammetry and Digital Outcrop Modeling. The case of the Lastoni di Formin (Italian dolomites).

Anno Accademico 2020-2021

Ciclo XXXIII

Coordinatore	Tutor
Prof. Roberto Sacchi	Prof./Dott. Cesare Perotti

Abstract

Carbonate platforms represent an important target for hydrocarbon exploration, water resources and CO_2 sequestration and storage. In many cases, these types of sedimentary bodies are highly heterogeneous in terms of facies architecture and distribution, and are often characterized by intensive fracturing. Fractures and faults, in turn, represent preferential conducts for the fluids flow within the carbonate body and therefore their features (e.g. size, connection and distribution), strongly impact the quality of a carbonate body as a reservoir. Since most of these features are below seismic resolution, and wells, although providing key information, represent only small volumes of the rock, the study of outcrop analogues have become a powerful methodology in for the assessment of reservoirs. In particular, the analysis of outcrop analogues by the use of Digital Outcrop Modeling can provide relevant informations for the analysis and interpretation of carbonate systems, as it make it possible to collect large volumes of data from objects that for size and exposition would be otherwise inaccessibile.

In the present study we applied Digital Outcrop Modeling and Digital Photogrammetry to the study of a Triassic isolated platform (Lastoni di Formin, Dolomites, Italy), to reconstruct the platform architecture and the distribution and genesis of the fracture pattern that affect it. The photogrammetric acquisition was performed both from the ground and by the use of an Unmanned Aerial Vehicles (drone), that allowed to reach inaccessible and remote portions of the outcrop and to acquire large amounts of digital data in a quick and effective way. The obtained images were processed using Structure from Motion (SfM) techniques, producing the 3D Digital Outcrop Model (DOM). The DOM was subsequently visualized, analyzed and sampled in 3D stereoscopic environment. Furthermore, the study was supported by an intense field survey campaign, with the aim of both validating the digitally acquired data and integrating the set of measurements. The combination of remote sensing and traditional field studies has proven to be effective in achieving the objectives of the project. A first part of the study was dedicated to the reconstruction of the architecture and depositional geometries of the platform. Secondly, the structural analysis of the Lastoni platform and the characterization of the fracture network were undertaken.

Riassunto

Le piattaforme carbonatiche rappresentano un importante oggetto di studio in diversi campi applicativi delle geoscienze (ad esempio, per l'esplorazione di idrocarburi, l' approvvigionamento di risorse idriche e lo stoccaggio di CO_2). Molto spesso, questo tipo di affioramenti sono altamente eterogenei in termini di architettura e distribuzione delle facies e sono spesso soggetti a intensa fratturazione. A loro volta, fratture e faglie rappresentano dei percorsi preferenziali per il flusso dei fluidi all'interno del corpo carbonatico, esercitando un forte impatto sulla qualità del giacimento. Tuttavia, molte delle caratteristiche salienti di un reservoir sono difficilmente rilevabili tramite tecniche di indagine geofisica, e le stratigrafie dei pozzi esplorativi rappresentano solo volumi limitati di roccia. In questo contesto, lo studio di piattaforme carbonatiche affioranti rappresenta una delle metodologie più efficaci per integrare i dati di pozzo nella valutazione delle caratteristiche di un giacimento. L'applicazione di modelli digitali dell'affioramento (*Digital Outcrop Modeling o DOM*) a questo tipo di studi fornisce un'importante fonte di dati per l'analisi e l'interpretazione dei sistemi carbonatici. Questo tipo di approccio multidisciplinare combina diverse aree di competenza, (geologia strutturale, sedimentologia, stratigrafia, informatica), che contribuiscono in diversa misura allo studio e all'interpretazione delle caratteristiche geologiche dell' affioramento in esame. In questo lavoro, sono state applicate avanzate tecniche di fotogrammetria digitale e *Digital Outcrop Modeling* allo studio di una piattaforma carbonatica di età triassica e più precisamente del Carnico (Lastoni di Formin, Dolomiti, Italia). L'acquisizione fotogrammetrica è stata eseguita sia da terra che tramite l' utilizzo di un veicolo a pilotaggio remoto (drone), che ha consentito di raggiungere porzioni inaccessibili e remote dell'affioramento e di acquisire grandi quantità di dati digitali in modo rapido ed efficace. Le immagini ottenute sono state elaborate utilizzando tecniche di *Structure from Motion (SfM),* che hanno reso possibile la ricostruzione 3D dell'affioramento che è stato successivamente visualizzato, analizzato e misurato in stereoscopia 3D. Inoltre, lo studio del DOM è stato affiancato a un'intensa campagna di rilevamento sul terreno, con l'obiettivo sia di validare i dati acquisiti in digitale che di integrare il set di misure. La combinazione di telerilevamento e rilevamento geologico tradizionale si è rivelata efficace per il raggiungimento degli obiettivi prefissati. La prima parte del progetto è stata dedicata alla ricostruzione dell'architettura e delle geometrie deposizionali della piattaforma dei Lastoni; nella seconda parte dello studio sono state eseguite l'analisi strutturale e la caratterizzazione del network di fratture della piattaforma stessa.

Index

1. Introduction

1.1 Context and challenges

Carbonate bodies are one of the main targets for hydrocarbon exploitation, since 60% of the world's known oil and a huge amount of the additional gas reserves are currently hosted in carbonate reservoir (Akbar et al., 2000). Moreover, scientific and industrial interest in carbonate rocks has grown in recent years due to their increased importance for water resource management (Ford & Williams, 2007; Goldscheider et al. 2020), geothermal energy (Goldscheder et al., 2010; Montanari et al., 2017) and CO_2 sequestration (Shakiba et al., 2016). In many cases, the discontinuities represented by fractures and faults play a significant role in determining the permeability of these reservoirs and strongly impact the fluids flow. However, carbonate platforms are frequently highly heterogeneous bodies due to their complex facies organization and sedimentary architecture that influences the mechanical characteristics of the rock, and can be interested by different tectonic evolution that also determines orientation, distribution, size and connection of fractures and faults. Therefore, the fracture network in carbonate bodies shows significant lateral and vertical variability. As most of fractures are below seismic resolution, and wells, although providing key information, are representative of small volumes of the rock, outcrop analogues are one of the most important source of data on structural patterns. Moreover, they give the opportunity to investigate the geometry and the sedimentary facies distribution and variation through the platform depositional environments. The great majority of the structural studies that are performed on outcrop analogues relies on traditional field methodology and 2D analysis (scanlines). These methods are strongly conditioned by the difficulty to collect a great number of data that can be fully representative of the whole fracture network, as well as by the impossibility to reach inaccessible portion of the outcrop, such as open cliffs (Sturzenegger and Stead 2009). Moreover, compass - clinometer field measurements could be affected by some biases (Ross-Brown et al., 1973) due to the sampling technique or to local variations in orientation of measured features (e.g. waved/undulated surface). The mesurement of large-scale depositional structures (i.e. clinoforms, mounds) can be hard in the field because of their huge dimension, and this case the interpretation based on photos is mostly qualitative.

The present study aim at demonstrating how the application of advanced and well established remote sensing techniques (i.e. Digital Photogrammetry), integrated and supported by extensive fieldwork, can drastically improve the structural and sedimentological study of outcrop analogues.

The reconstruction of the depositional architecture and the structural analysis of the outcrops considered in this work were essentially performed on Digital Outcrop Models (DOMs), obtained by the use of Terrestrial Digital Photogrammetry (TDP) and Unmanned Aerial Vehicle Digital Photogrammetry (UAVDP). These techniques maket it possible to obtain georeferenced, high resolution data at a lower cost and require much easiers survey planning compared to Lidar acquisitions (Remondino & El-Hakim 2006; Westoby et al. 2012), and their application in geosciences has been increasing hand in hand with the recent development in drones and RGB cameras technologies (Colomina and Molina 2014; Bemis et al., 2014; e.g. Westoby et al. 2012; Tannant 2015; Casella et al. 2016; Salvini et al. 2016).

DOMs can be interpreted and sampled in a 3D environment, and have some substantial advantages with respect to traditional field sampling and surveying. These advantages can be summarized as follows: i) the possibility to obtain quickly a largest number of measures and more representative data with respect to the classic compass measurements; ii) the possibility for different operators to effectively check and correct the dataset at any time; iii) the creation of a virtual space where the information obtained from the DOM can be merged and combined with other geological and geophysical data, that lead to support and enhance analysis.The production of a three-dimensional dataset allows the interpretation of large structures and complex depositional geometries at the outcrop scale in a stereo 3D environment, directly on high resolution point clouds. Moreover, it overcomes many of the limitation that usually affect the 2D image analysis, and that can lead to significant errors in the interpretation of the outcrop geometries and in the reliability of quantitative measurements, as perspective deformations, occlusion of parts of the outcrops and unfavorable exposure (apparent orientations and thicknesses). The use of an Unmanned Aerial Vehicles (Drones hereafter) for the data acquisition has also some remarkable advantages with respect to ground-based techniques (mainly terrestrial photogrammetry and Laser scanner). First, it allows the inspection of large areas in a short time, significantly reducing the time spent on acquisition. Hence, it permits the acquisition of high resolution RGB images on the most remote and inaccessible outcrops, giving the possibility to measure features that would be otherwise undetectable.

Two outcrops were selected among the several Triassic isolated platforms of the Dolomites (Italy), in order to obtain a complete overview of the geological heterogeneity of these shallow-water carbonate environments. In particular, Late Ladinian - Early Carnian Cassian platforms characterized by domains (slope, margin, inner platform) with different facies organization and mechanical features laterally juxtaposed were investigated.

1.2 Thesis organization

In this thesis the research work carried out during the last three years is presented. The manuscript is divided in four main chapters that summarize and discuss the principal outcomes of the study. Each chapter deals with one of the main topic addressed: UAV digital photogrammetry and Digital Outcrop Modeling, carbonate platform architecture and geometry, and structural analysis.

Chapter 2.

A synthetic review on the general geology of the Dolomites is presented. The first part focuses on the Mesozoic stratigraphy and evolution of this sector of the Italian Southern Alps that is characterized by the development of several generations of middle Triassic carbonate platforms. Particular attention was given to the large scale depositional geometries and the interrelationship between subsidence, shallow water carbonate production and basinal deposition. In the second part of the chapter, the main tectonic events that occurred from Permian to Neogene times are discussed. Finally, the geology of the study area is introduced.

Chapter 3.

In this chapter, the methods for the application of digital photogrammetry to the reconstruction of Digital Outcrop Models (DOMs) are discussed. In the first paragraph the principles of photogrammetry and Structure from Motion technique (SfM) are introduced, followed by a complete step - by - step description of the workflow used for the generation of the Digital Outcrop Models of the examined outcrops, from the UAV survey to the post processing operations and the sampling of the 3D model. Advantages and limitations of these techniques are highlighted.

Chapter 4.

This chapter corresponds to the manuscript published in *Marine and Petroleum geology* (Inama et al., 2020), and mainly focuses on the reconstruction of the depositional architecture of the *Lastoni di Formin* carbonate platform, through the application of Digital Outcrop Modeling and field studies. Moreover, a relationship between fractures and compaction - induced deformation has been investigated.

Chapter 5.

Chapter 5 represents the last part of the study, and is focalized on the structural characterization of the *Lastoni di Formin* outcrop. The origin and timing of the several tectonic features that form the fracture pattern of the platform are discussed. The results were acquired by means of a combined approach of field and remote sensing observations. A paper that reassumes the principal outcomes of this chapter is in preparation, and will be soon submitted to a peer reviewed scientific Journal.

2. Geological Setting

2.1 The dolomites: general geology

The Dolomites are a mountain range located in northeastern Italy and part of the Italian Southern Alps. The area is relatively well confined from the geological point of view and consist of a portion of upper crust uplifted in the Neogene by a large pop-up syncline, limited to the north by the Insubric Lineament and to the south by the Neogene south-vergent Valsugana Overthrust, that is responsible of a crustal shortening up to 10-15 km (Doglioni, 1987, Bosellini 2003) (fig 2.1). During the Mesozoic, this domain of the Southern Alps was part of the passive continental margin of the Ligurian - Tethys Ocean (Winterer & Bosellini, 1981; Berra & Carminati, 2010). During the Alpine Orogeny the sedimentary cover was only gently deformed by tectonics and escaped high-grade metamorphism.

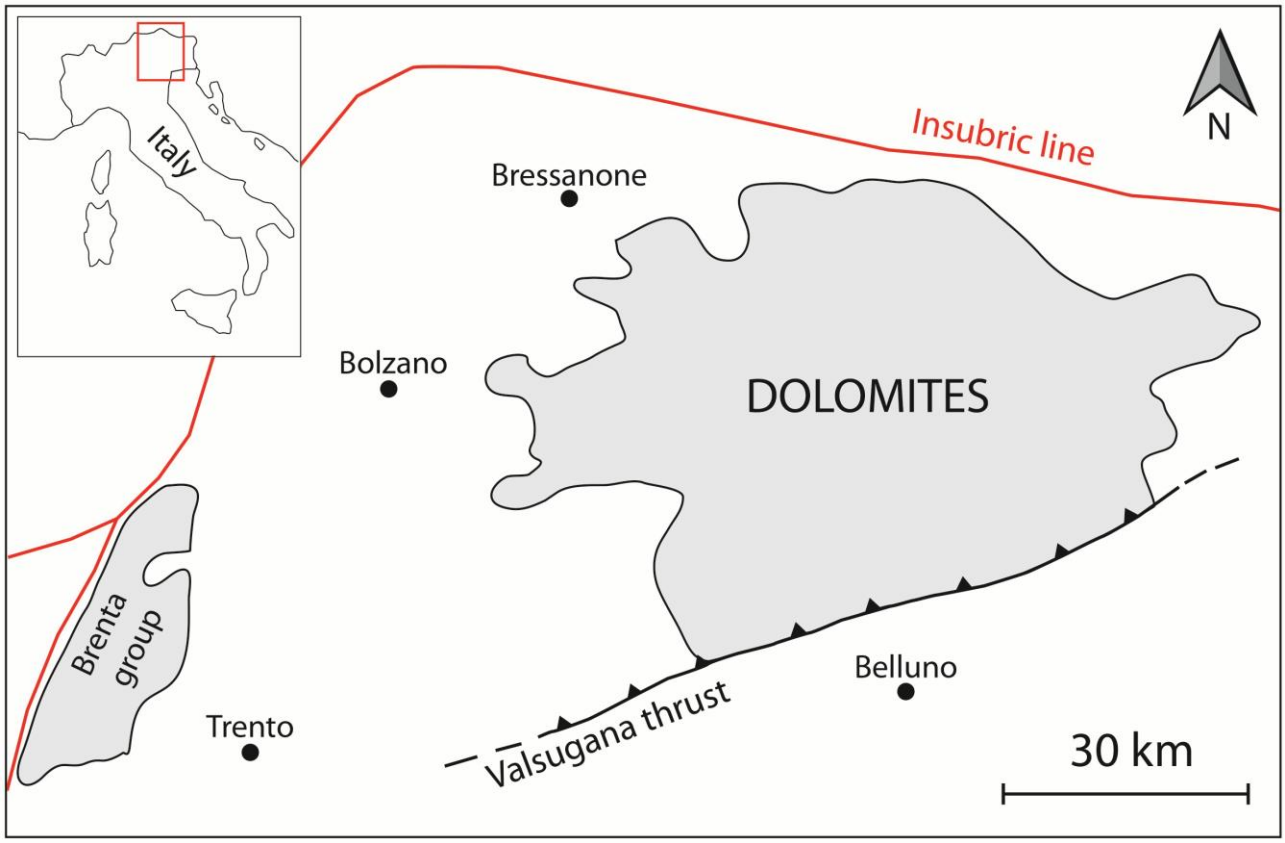

Fig. 2.1 Location map of the Dolomites region (northern Italy), showing its northern and southern boundaries.

The peculiarity of the Dolomites region can be found in its extremely articulated topography and geological variability that contributed to shape one of the most outstanding landscape in the world. This incredible variety of valleys, rivers, gentle meadows and vertical peaks takes its name from the French naturalist and explorer Deodat de Dolomieu (1750-1801), who firstly studied the particular characteristics of the rock that constitutes large parts of the most impressive mountains of the area. Thanks to the exceptional exposure and preservation of seismic-scale depositional geometries, the unique depositional history, the abundant fossil record and the relatively slight deformation, the Dolomites has become a worldwide reference area for the Triassic period, a time that witnessed mass extinctions (i.e. Permian - Triassic), global climate changes, volcanic events and tectonic evolution. Furthermore, the Dolomites are one of the few easy accessible places where large Mesozoic carbonate platforms and their adjacent basinal deposits can be observed in natural transects (Gianolla, 2008a). The region can be schematically subdivided into Western and Eastern Dolomites, virtually separated by the axis Badia Valley – Campolongo Pass – Cordevole Valley (Agordino) and recording different tectonic, stratigraphic and burial evolution (Gaetani et al., 1981). Although the regional stratigraphic framework comprises terrains of different origin that ranges from Permian to Cretaceous, the landscape is dominated by Triassic. In spite of the late pervasive diagenetic dolomitization that affects many of the carbonate bodies of the Dolomites, some of the Anisian-Ladinan buildups escaped this process and preserved the original facies.

2.1.1 The Early and Middle Triassic: development and evolution of the carbonate platforms

At the beginning of the Triassic (Induan-Olenekian), the Dolomites area were dominated by an eastward-dipping, mixed terrigenous-carbonate marginal marine ramp system (Werfen Fm.). The formation records the recovery of marine ecosystems after one the most severe mass extinction of the entire Phanerozoic, which marks the boundary between Permian and Triassic. This event triggered the demise of large marine biological communities affected the carbonate production, which in the Early Triassic consists mainly in loose micritic mud, bioclasts and lacks of bioconstructions. The Middle Triassic (Anisian - Ladinian) is characterized by the development of the spectacular carbonate edifices that shape the geological landscape of the Dolomites region. At the beginning of the Anisian, the carbonate sediments were deposited on a tidal flat which is testified by the Lower Serla Dolomite (Bosellini 2003). The homogeneous paleogeography and the relative uniformity of the depositional environment were broken by the tectonic reactivation of older Permian structures, which generated a complex pattern of structural highs and subsident area. Two generations of independent carbonate platforms developed in the eastern, more subsiding part

of the Dolomites (Monte Rite Fm and Upper Serla Fm): these buildups represent the first recovery of bioconstructors (dasycladacean algae and tubiphithes) in this part of the Triassic Tethys after the P-T crysis (Neri et al., 2007; Gaetani et al., 1981; Bosellini, 2003). These carbonate systems drowned because of a general sea-level rise and deep marine condition set up in the areas, as recorded by mixed terrigenous-carbonate basinal successions (Dont, Bivera and Ambata formations) (Assereto et al., 1977; Pisa et al., 1979; Gaetani et al., 1981, Bosellini, 2003). At the same time, the western Dolomites were uplifted and eroded up to Permian deposits (Bosellini, 1968) and a subsequent transgression restored shallow marine conditions and allowed the re-establishment of carbonate deposition (Contrin formation). This unit reached an average thickness of 50/ 150 m, locally higher, with the platform-top deposits characterized by peritidal stromatolites, dasycladacean algae, and encrusting and problematica organisms (Tubiphytes) and flanked by large clinostratified slopes, that prograded over the basinal terrigenous-carbonate Morbiac Formation (Bosellini et al., 2003; Neri et al., 2007).

2.1.2 Pre volcanic platforms

During the Late Anisian, a renewed, extremely fast subsidence involved the Dolomites area, and general deep-water conditions were established. The carbonate producing environments survived only at the top of few, small (1-2 km-order of extension) structural highs. These buildups were able to aggrade very quickly and compensate the increasing accommodation space. Some of these isolated carbonate bodies eventually drowned, especially in the eastern, more subsiding sector: the rapid sea-level rise is documented by the backstepping geometry of some of these platforms (i.e. Monte Cernera) (Blendinger et al., 2004). To the west, the carbonate build-ups were able to catch up with the relative sea level rise aggrading very fast, and becoming the nucleus of much larger platforms (Marmolada, Sciliar, Latemar and Catinaccio) that progressively raised over the adjacent basins (fig. 2.2). At this stage, subsidence rate was about 200/400 m/Ma, and these platforms rapidly reached 800/900 m of thickness, while in the basins only few meters of sediments accumulated. During the early Ladinian (240-239 Ma), subsidence almost stopped; the buildups were forced to expand laterally, developing steep, clinostratified breccia slopes (40/45°) that prograded very fast (1400 to 2700 m /Ma in the western Dolomites, according to Bosellini, 2003) for several km over the adjacent basins: in the western Dolomites, the early phreatic marine cementation is pervasive along the narrow margin and the upper slopes, essentially dominated by automicrite (in situ-produced micrite) Late diagenetic dolomitization (Wilson et al., 1990, Stefani et al., 2010; Ferry et al., 2011; Jaquemyn et al., 2014) affect most of these platforms (Sciliar

dolomite), although a limited number preserved the original carbonate texture (i.e. Marmolada limestones).

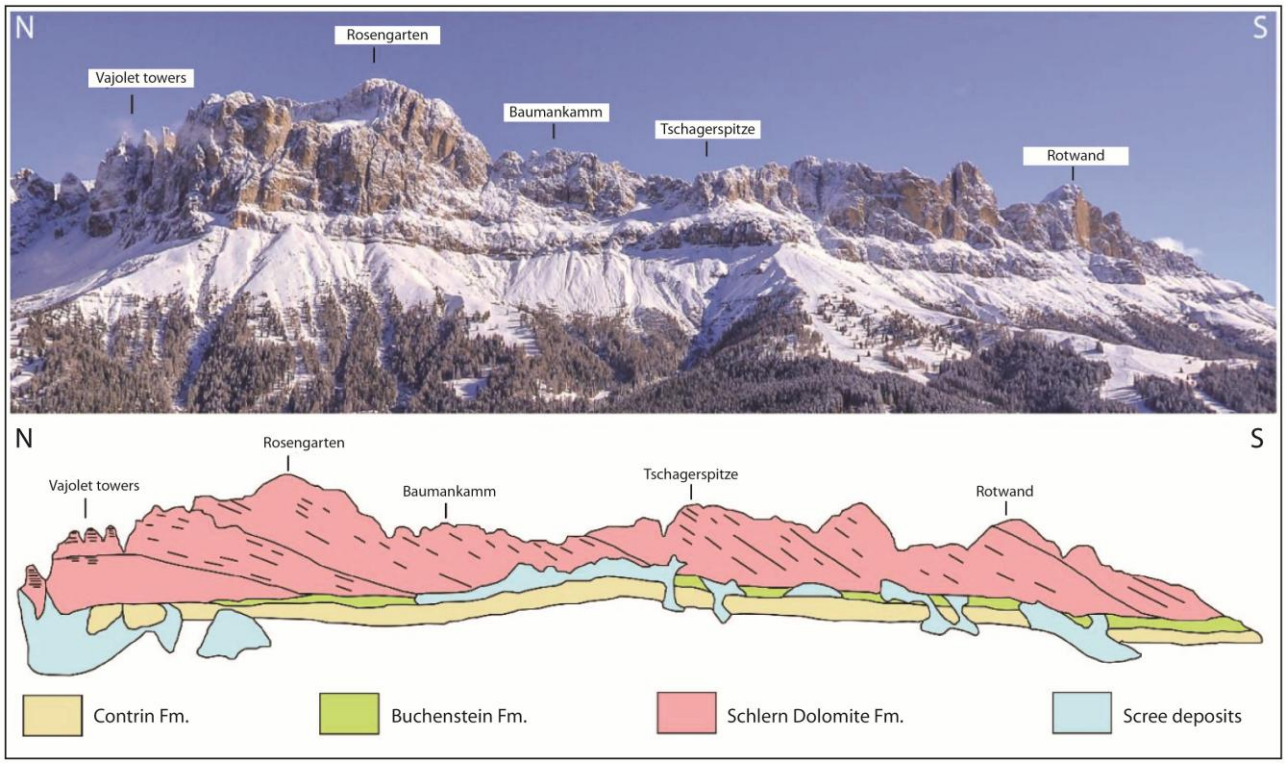

Fig. 2.2 Sketch (modified after Maurer, 2000) of the Rosengarten Group, showing the geometrical relation between the highly prograding slopes of the Sciliar Dolomite, the basinal Buchenstein Fm and the Contrin carbonate bank (image modified by Silvia Passoni, tesi di Laurea).

2.1.3 The Middle Triassic volcanic event

An important tectono-magmatic event characterized the Middle Ladinian in the western area of the Dolomites (fig. 2.3). Large parts of the region were struck by major volcanic eruptions, mainly into submarine environments, where they originated pillow lavas and hyaloclastites (Calanchi et al., 1978). Few subaerial episodes of volcanism are recorded at the Monte Agnello (Fiemme Valley) and Sciliar mountains in the form of diatremes, lava flows, tuffaceous layers and pyroclastic breccias (Nemeth & Budai, 2009). In the western Dolomites magma was able to rise up along inherited structures from the Permian extensions, and a few small bodies were intruded at shallow depths (Predazzo and Monzoni intrusions) (Castellarin., 1988; Abbas et al., 2018). The onset of the magmatic activity largely interfered with the platforms growth: in some cases (Latemar, Marmolada), the volcanic rocks directly onlapped the platform slopes, causing the demise of the buildup and "freezing" the original morphology.

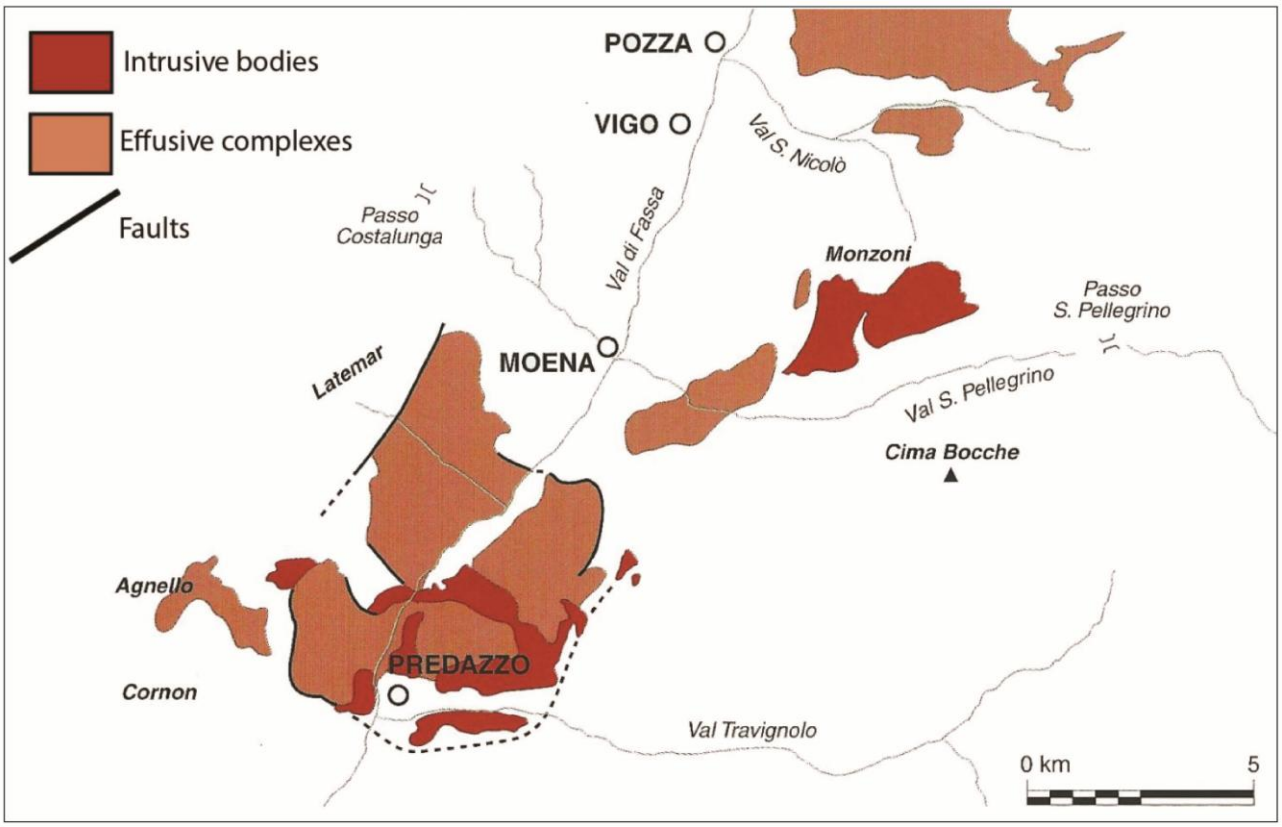

Fig. 2.3. Distribution of effusive and intrusive rocks of the Monzoni and Predazzo complexes (from Bosellini, 1996).

At the end of the volcanic activity the volcanic edifices were progressively eroded, and the products of the dismantling accumulated in the basins: in the vicinity of the volcanic reliefs they are represented by the coarse deposits of the Marmolada Conglomerate, whilst large volumes of finer sediments could reach further distances (Wengen Fm.), also in the form of turbidites (Zoppè Sandstones, Fernazza Fm.). The depositional "break" in the platform succession, created by the volcanic and volcanoclastic deposits, allows to distinguish two different generations of platforms: "pre-volcanic" and "post-volcanic" (Bosellini & Rossi, 1974). However, in areas far away from the volcanoes, the carbonate sedimentation was not interrupted and some kind of production was active even close to the major magmatic areas (i.e., Sciliar, Col Rossi/Padon; Brandner, 1991; De Zanche et al., 1993; De Zanche & Gianolla, 1995).

2.1.4 Cassian Platforms

At the fading of the magmatic activity (Late Ladinian), a stability phase followed and the environmental conditions suitable for shallow water carbonate deposition were re-established. A

new generation of platforms (Cassian Dolomite, Assereto et al., 1977, Neri et al., 2007) nucleated on topographic highs, represented by remnants of Ladinian platforms or partially dismantled low volcanic reliefs, and prograded into the basins (Bosellini, 1996). These post-volcanic platforms are characterized by the presence of ooids, absent since the Early Triassic, and progressive colonization of the margin environment by Techosmilia-like branching corals, which were however always subordinated to smaller sediment-producing organisms (Bosellini, 2003). In western Dolomites, the low subsidence rates forced these buildups to grow mainly through lateral progradation over the adjacent basins. Conversely, platform-top successions of the more subsiding eastern Dolomites aggraded moderately (e.g., Picco di Vallandro), and a vertical accumulation rates of about 200m/Myr were recorded (Gianolla, 2008a). In the central and eastern Dolomites, two generations of Cassian buildups have been identified (Cassian I and II, fig. 2.4), separated by a break of the progradation, marked by the onlap of the basinal beds onto the Cassian slopes (Richtofen riff, Lagazuoi - Col dei Bos) (De Zanche, 1993; Gianolla et. al 1998; Neri et al., 2007; Trombetta 2016).

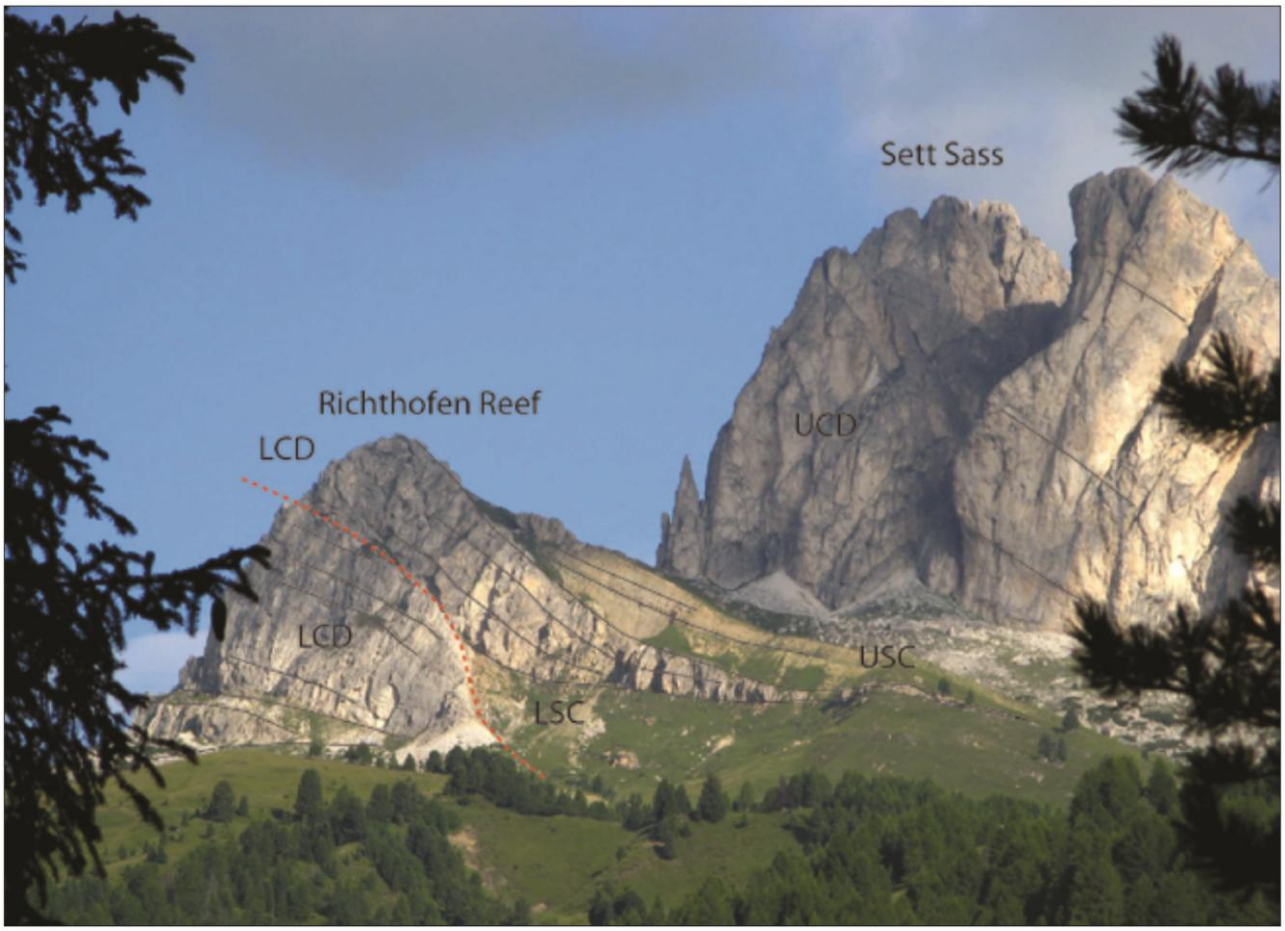

Fig. 2.4. Cassian Dolomite I (LCD) and II (UCD) at the Richtofen reef - Setsass. The Lower and Upper Cassian Dolomite represent two highstand phases of platform progradation over the basinal San Cassiano fm. The basinal unit onlap the slopes of the Cassian dolomite I. (From Roghi et al 2014.)

The clinostratifications of the Cassian slopes are generally less steep (30-35°; Kenter, 1990) than those of the pre-volcanic platforms, and the high basinal sedimentation rates, fed by large amount of volcaniclastic sediments) produced a shallowing evolution of the basinal areas, that results in climbing base-of-slope progradation. Despite the almost complete dolomitization of the Cassian platforms, the original facies of the margin/platform top can be inferred from the "Cipit boulders", calcareous olistolithic bodies of platform origin fallen and embedded in adjacent basinal units (the schematic depositional profile of the Cassian platform is shown in fig. 2.5). The fine-grained matrix (clays, marls, silt), which results impermeable to diagenetic fluids (Biddle, 1981; Russo et al., 1991), preserved the Cipit boulders from dolomitization. The intra-platform basins deposits (San Cassiano Fm.) consist in an alternation of thin layers of mixed, fine grained siliciclastic sediments and swarms of bioclastic calcarenites collapsed from the platform margin.

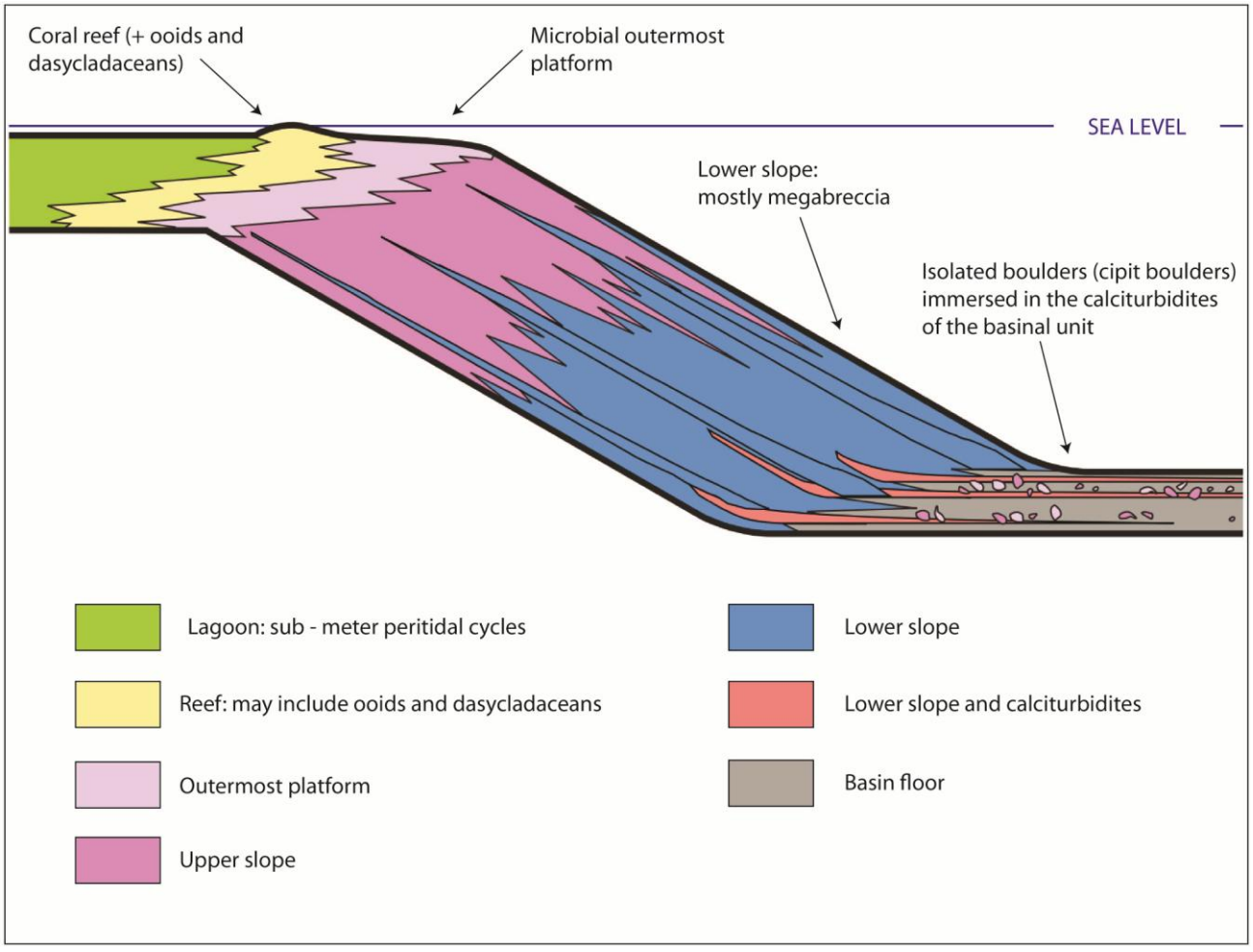

Fig. 2.5. Depositional profiles of the Cassian Sella platform. Modified from Preto et al 2017.

During the early Carnian, the slope angles of the Cassian buildups progressively decreased, due to the almost complete filling of the basins. The sedimentological record of the Dolomites witnesses a change in the carbonate facies architecture, matched with a worldwide crisis of rimmed carbonate platforms. After the demise of the last high relief platforms, shallow-water loose terrigenous-carbonate sediments (Heiligkreuz Fm.) started to accumulate, at first in the centre of the former basinal areas and onlapping onto the Cassian slopes. The base of the Heiligkreuz is composed by organic-rich claystones and marls, with freshwater influences and strongly impoverished faunae, that grades upward in a carbonate unit recording the growth of carbonate biostromes, and the appearing of the first "modern" patch reef (Gianolla et al., 2008). This unit is followed by a terrigenous - carbonate arenites that show cross and hummocky stratification, and the top of the formation is represented by a competent oolitic-bioclastic carbonate unit that close the sequence. These complex depositional systems witness important climatic fluctuations, marked by the development of humid phases (Bosellini, 2003). The Heiligkreuz Formation is the physical expression in the Dolomites of the Carnian Pluvial Episode, a complex phase of climate and environmental change likely associated to a global perturbation of the carbon cycle (Dal Corso et al., 2020).

2.1.5 The Late Triassic and Jurassic evolution

Between the Middle Carnian and the Early Norian, the deposition of the Heiligkreutz formation progressively leveled the complex topography that characterized the area in Lower-Middle Triassic. During the upper Carnian (Tuvalian), in this environment the Travenanzes formation deposited, a terrestrial to shallow marine, mixed siliciclastic succession (Breda e al., 2008) composed of dolomites beds, reddish, whitish and greenish mudstones with sandstone and conglomerate intercalations. This unit deposited in a wide flat coastal area, fed emerged lands located southward of the dolomites, and represents the interfingering between alluvial plain, flood basin and shallow lagoon. Near the end of the Carnian, subsidence increased and a renewed marine transgression that brought back shallow marine condition is testified by the onset of the Dolomia Principale, a unit deposited in a thousand of km - wide lagoon that covered large part of the Italian Southern Alps. The Dolomia principale is characterized by regular cycles of subtidal to peritidal whitish and grayish dolomites, with abundant stromatolites and fossils of bivalves (*megalodon gumbelii*) and gastropods. During Norian times, disoxsic-anoxic intraplatform depressions, rich in carbonate mud and organic matter, developed in different parts of the large Dolomia Principale platform producing potential source rocks for hydrocarbons. During the Early Jurassic (Hettangian), the Dolomites

underwent E-W extensional tectonics that caused the brake - up of the topographical uniformity, generating a series of basins (Lombardy and Belluno basins) and structural highs (Friuli and Trento platform) delimitated by N-S trending normal faults. At the top of the Trento platform subtidal and peritidal environments (together with emerged lands) survived, and the deposition of the shallow-water carbonate succession of the Calcari Grigi took place. Finally, from the Sinemurian the Trento platform started to sink during a renewed subsidence phase, driving the deposition of pelagic fine sediments, (Rosso Ammonitico) over the Calcari Grigi. The following lithostratigraphic scheme summarizes the variety of lithologies that make up the Mesozoic stratigraphic succession of the Dolomites (Fig. 2.6).

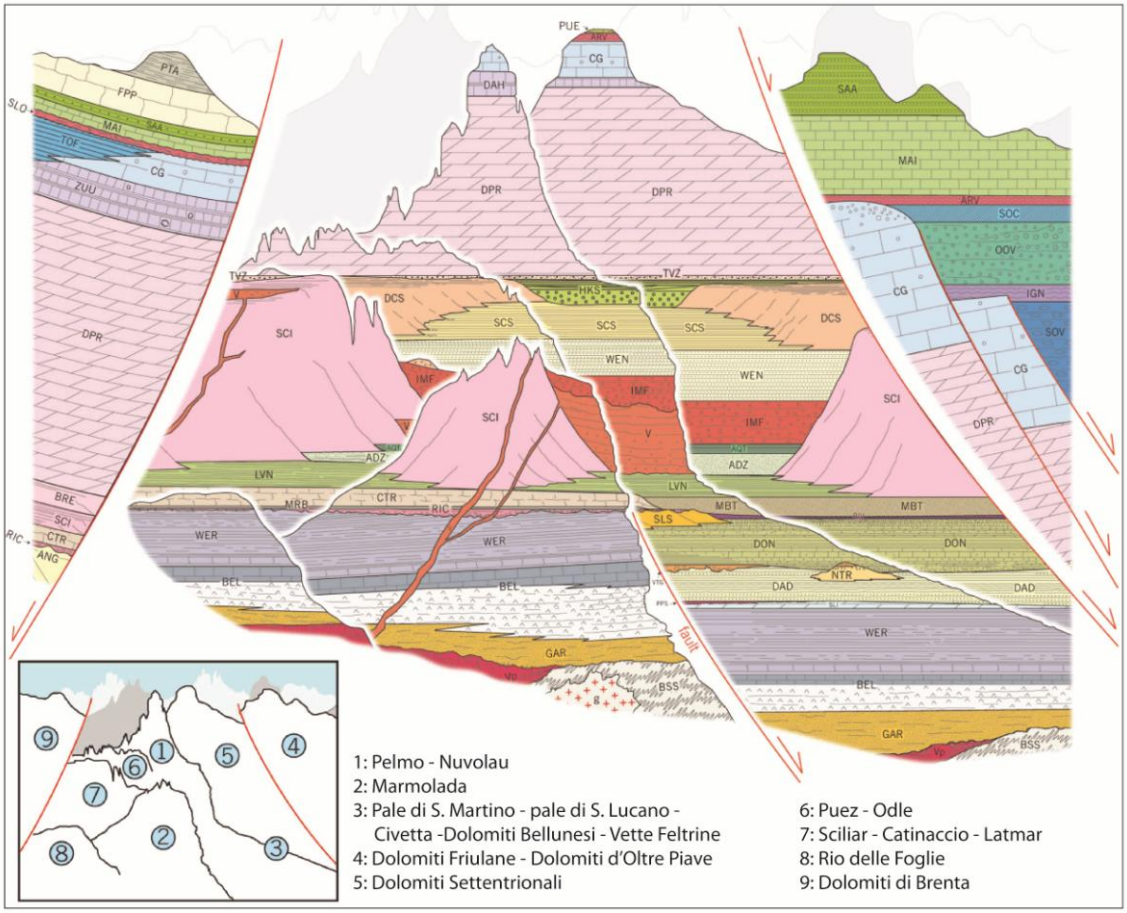

Fig. 2.6. E-W geological sketch showing a lithostratigraphic scheme of the Dolomites region (modified from Gianolla et al., 2019). ADZ Zoppè Sds; ANG Angolo Lms; ARV Ammonitico Rosso Veronese; BEL Bellerophon Fm; BIV Mt. Bivera Fm; BRE Breno Fm; BSS Metamorphic basement; CG Calcari Grigi; CTR Contrin Lms; DAH Dachstein Lms; DAD Gracilis Fm; DCS Cassian Dm; DON Don't Fm; DPR Dolomia Principale; FPP Ponte Pià Fm; g granites; GAR Val Gardena Sds;HKS Heiligkreutz Fm; LVN Livinallongo/Buchenstein Fm; IGN Igne Fm; IMF Mt. Fernazza Ignimbrites; MAI Maiolica; MRB Morbiac Fm; NTR Mt. Rite Fm; OOV Vajont Lms; PTA Ponte Arche clays; PUEPuez marls; RIC

Richtofen Cgm; SAA Scaglia Rossa Fm; SCI Sciliar Dm; SCS San Cassiano Fm; SOCSoccher Lms; SLO Selcifero Lombardo; SOV Soverzene Fm; TOF Tofino Fm; TVZ Travenanzes Fm; VLadinian volcanics; Vp Permian porphyries; WEN Wengen Fm; WER Werfen Fm; ZUU Zu Limestones.

2.2 The dolomites: structural setting

The region of the Dolomites is bounded to the south by the Neogene south-vergent Valsugana and Belluno thrusts, and to the north by their antithetic Funes - Passo delle erbe line (Fig.2.7). The domain is part of a south vergent thrust belt (Doglioni & Castellarin, 1985) and, despite it has avoided intense deformations, recorded a number of magmatic and tectonic events (Bosellini et al., 2003) that goes from the Varisican orogeny to the Neogene compression, including both rifting and compressional phases. The main shortening occurred during Neogene times (Venzo, 1939; Massari et al., 1986). Most of these events inherited and reactivated previous structures, causing inversion of the kinematics (Doglioni, 1987). All the different tectonic phases developed at low temperatures and essentially correspond to brittle deformations (with the exception of the evaporitic and marly rocks that show ductile behavior at low temperature, i.e., Bellerophon Fm, Travenanzes Fm).

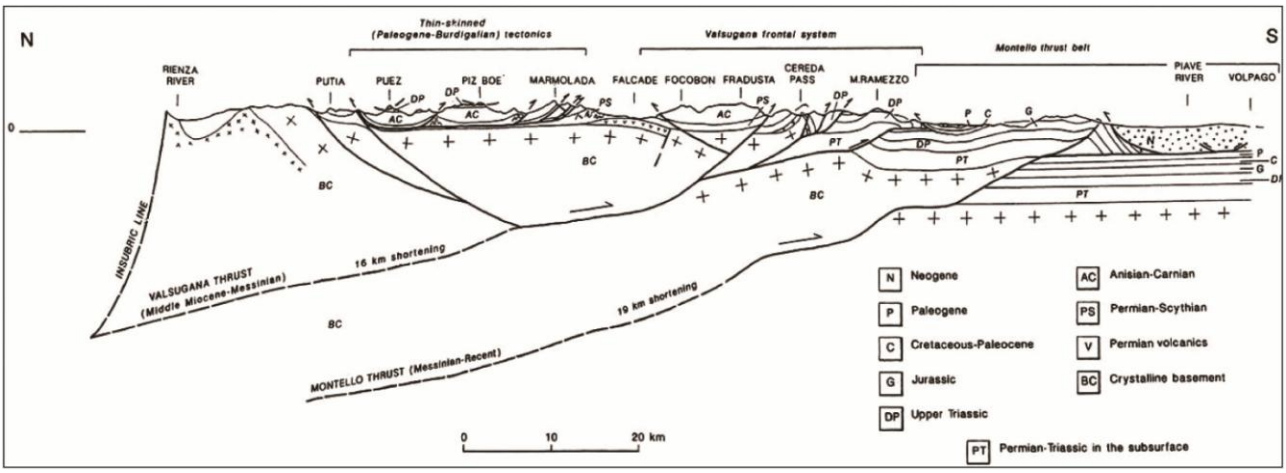

Fig. 2.7 N- S geological profile of the western Dolomites (from Castellarin et al., 1998).

The structural setting of Dolomites was also controlled by their particular stratigraphic succession, characterized by the alternation of stiff carbonate buildups with steep slopes and less competent formations such as Bellerophon, Werfen, Livinallongo and Travenanzes Fm. The slopes of Ladinian and Carnian platforms acted as ramps for overthrusts, while the evaporitic sediments, shales and marls behaved as décollement horizons for low angle thrust faults (Doglioni, 1987, Doglioni &

Carminati, 2008). In the following paragraphs, the main tectonic phases that occurred during the geological evolution of the Dolomites area are summarized.

2.2.1 Permian and Early Triassic evolution

Permian and Triassic transtension and rifting broke the Dolomites area into North-South trending blocks with different degrees of subsidence. The most prominent elements were the eastern Atesina Platform and the western Carnico-Bellunese basin, separated by the Passo Rolle Line; the change in thickness of the sedimentary cover range from ~ 2 km in the west, to 4-5 km in the east. During the Permian, the Southern Alps were affected by intensive magmatic activity that produced basic to acid vulcanic and plutonic rocks; the magma emplacement controlled by postorogenic lithospheric extension, generating normal and transtensional faulting (Marocchi et al., 2008). In the Dolomites, Permian magmatism is witnessed by the Athesian Volcanic Group characterized by lithologies that range from andesites to rhyolites (Marocchi et al., 2005). Together with the intrusive bodies of Cima d'Asta, Bressanone, and Monte Croce, it constitutes the major Permian volcanoplutonic system of the central and eastern Southern Alps (Marocchi et al, 2008). The tectonic models for the generation of the Permian magmatism of the Southern Alps involve the following processes: i) magmatism originated in response to lithospheric extension, without any relation to subduction processes (Boriani et al. 1995; Quick et al. 2003) and ii) magmatism originated in an Andean - type continental margin at the southern flank of the Variscan Belt (Visonà 1982; Lorenz & Nicholls, 1984).

2.2.2 Ladinian - Carnian tectonics

After a phase of general subsidence trend, a restricted region in the central Dolomites (Fiemme and Fassa valleys), was subject to local sinistral transpressive tectonics, that is responsible for the formation of structures aligned in N70 - 90 ° direction (Stava and Trodena Lines). Some of the most prominent structures found along this axis are diapirs (Passo S. Nicolò, Col Becher), that develop in the evaporitic Bellerophon Formation, and flower structures (Monte Rocca, Malga Fosse) generated by systems of inverse faults with opposite vergence (Doglioni et al., 1984) and deforming the basement. The dating of these structures is possible because folds and thrusts are cut by volcanic dykes and plutonic bodies of Late Ladinian age (Doglioni, 1987). Subsequently, this alignment was the preferential locus of the emplacement of the Middle Triassic magmatism associated to intrusive

(Predazzo, Monzoni) and effusive (Sciliar, Monte Agnello) complexes. The radial arrangement of faults and volcanic dykes in the area suggests a genetic relation between these features and the presence of a domal uplift, associated with the upcoming magmatism (Doglioni & Carminati, 2008).

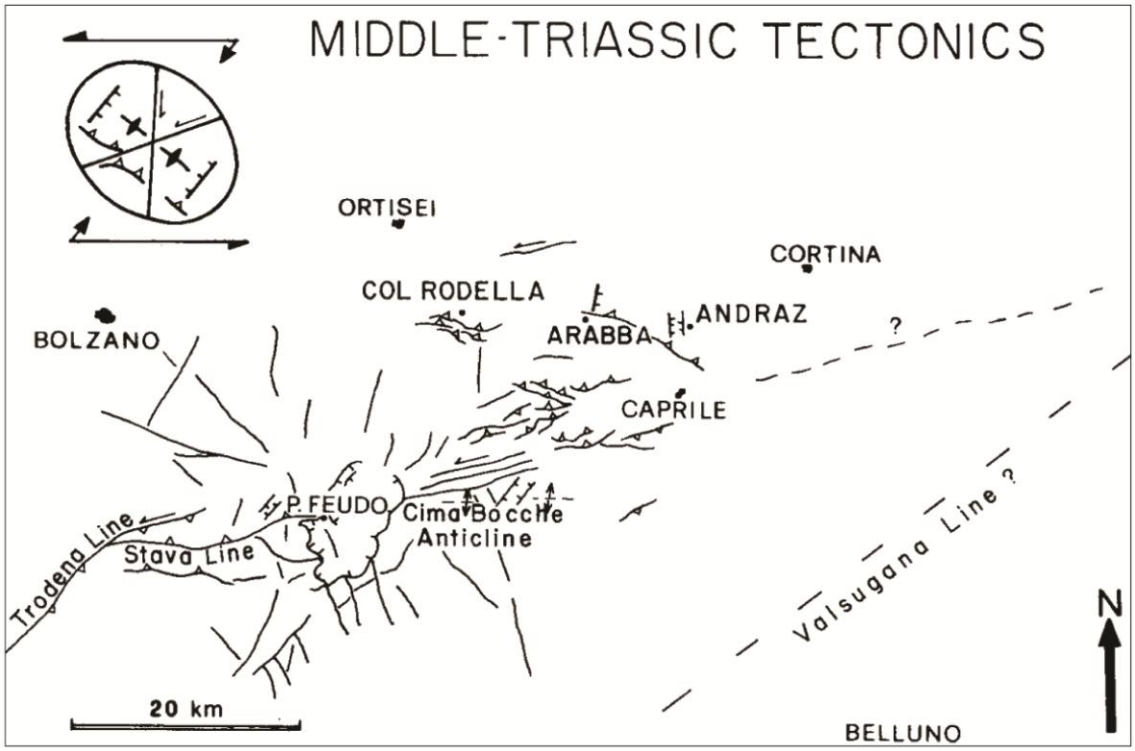

Fig.2.8. Main features of the transpressive Middle - Triassic tectonic in the Dolomites. Form Doglioni, 1987.

2.2.3 Jurassic rifting

During Upper Triassic and Jurassic the Dolomites and the entire Southern Alps domain were involved in a prominent rifting phase culminated in the Middle-Upper Jurassic, connected to the break-up of the Pangea megacontinent (Bertotti et al., 1993; Santantonio & Carminati, 2011) and the opening of the Piedmont-Ligurian Ocean (western Tethys) (Doglioni, 1987). The Dolomites were part of the passive continental margins of the Adria plate (Bertotti, 2001; Berra and Carminati, 2010). This tectonic setting induced a generalized subsidence and the fragmentation of the large Dolomia Principale platform in N-S trending structural highs and basins by normal faults (fig. 2.9.): from east to west: the Lombard Basin, the Trento Platform, the Belluno basin and the Friuli Platform (Bernoulli et al., 1979; Winterer & Bosellini at al. 1981).

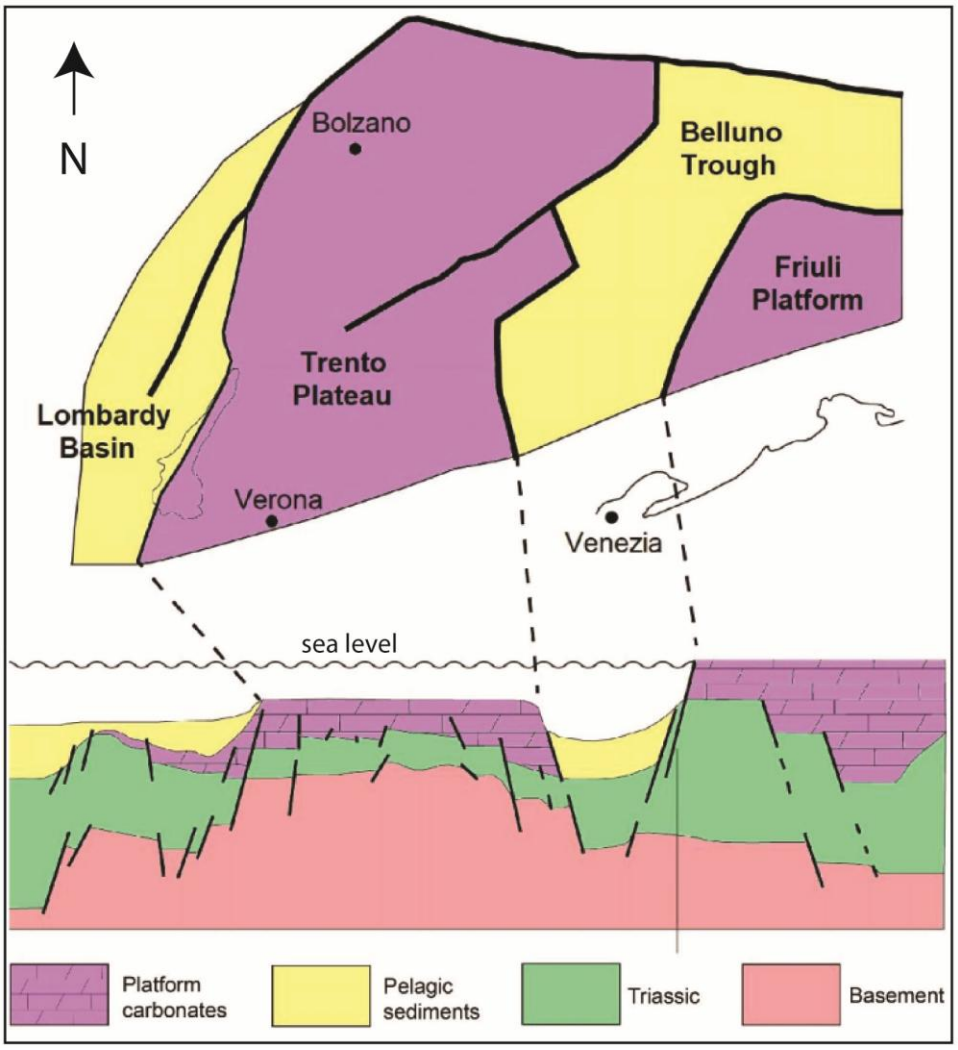

Fig.2.9. Simplified cross section of the Southern Alps domain at the end of the Jurassic. The Dolomites are dissected by N-S striking normal faults that generate a system of platforms and basins. Modified from Cau & Fanti, 2014.

2.2.4 Paleo-Alpine tectonics

The Cenozoic evolution of eastern Dolomites is strictly related to the Africa - Europe plate kinematics. During Paleogene and Neogene times the Southern Alpine domain was involved in the Alpine Orogeny, and the Dolomites were subject to different tectonic phases. Four main compressional events were recognized by Caputo (1996) and dated by comparison with the results obtained from studies in other sectors of the Southern Alps. The average $\sigma 1$ axes of these events is oriented, from older to younger: N58° (pre-Oligocene), N26° (Chattian-Burdigalian), N346° (Serravalian-Tortonian) and N307° (Late Messinian to Early Pliocene), depicting an anticlockwise rotation of the main compressive direction from NE-SW to NW-SE (Mazzoli & Helman, 1994).

While the first of these events is considered pre-alpine in age (Doglioni, 1987; Doglioni & Carminati, 2008) the post Oligocene tectonics is consistent with the evolution of the convergence direction between Africa and Europe plates. In the Dolomites region, the occurrence of a tectonic phase with a main compressive axis oriented – E-W (known as the "Dinaric Phase"), is supported by the presence of N-S and ENE-WSW trending thrusts and fold axes (Doglioni, 1987, fig.2.10). These structures that are well documented in the eastern sector of the South Alpine chain (Cousin, 1981), are likely related to the Late Cretaceous-Paleogene events that led to the formation of the Dinaric Range, and of which they could represent the westernmost external deformation of the belt (Doglioni, 1987).

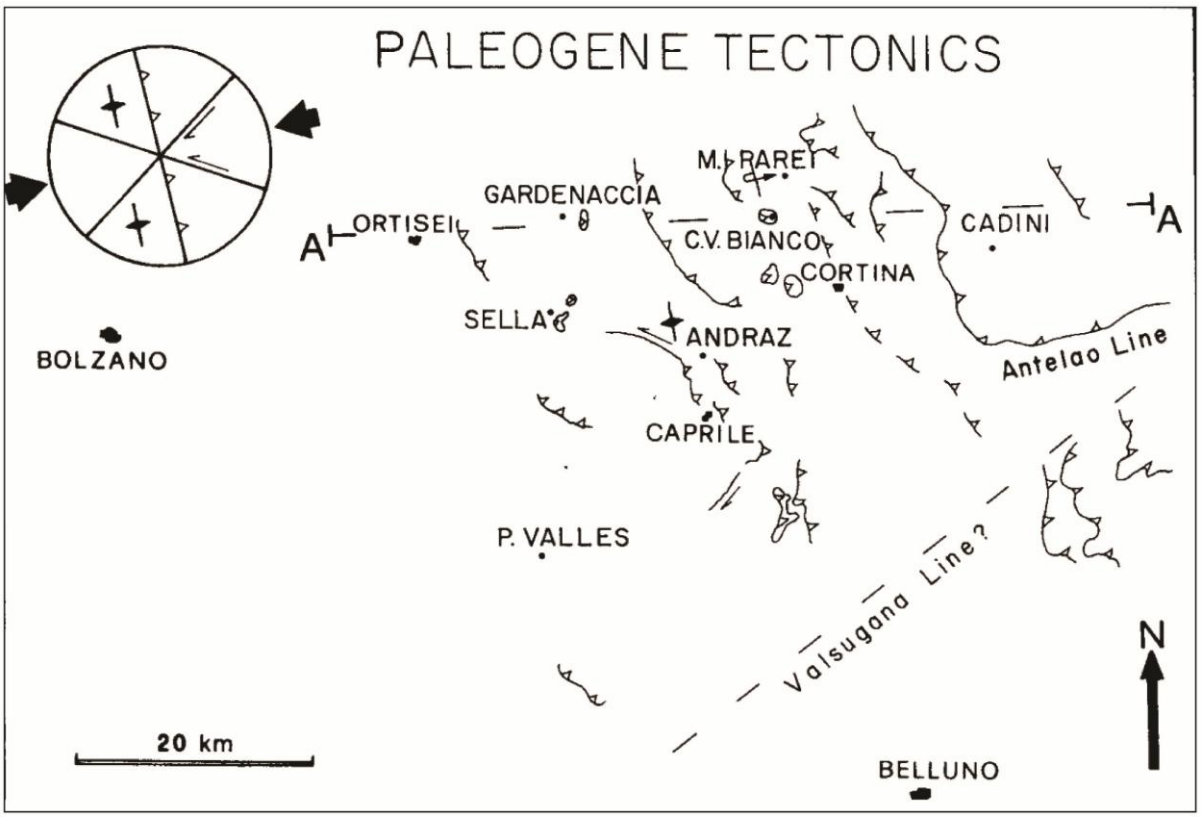

Fig.2.10. Direction of the main compressive stress and relative tectonic features developed during the pre-Neogene phase of shortening. From Doglioni, 1987.

2.2.5. Alpine tectonics

As previously mentioned, three main tectonic phases have been distinguished within this orogeny (Fig. 2.11): 1) the first one (Chattian-Burdigalian) can be considered as the continuation of the Dinaric Phase, characterized by a compressive axis oriented NNE-SSW; 2) the Alpine -

Valsuganense Phase (Serravalian - Tortonian), characterized by a NNW-SSE shortening; 3) The Schledrense Phase(Messinian-Lower Pliocene), shows a NW-SE axis orientation.

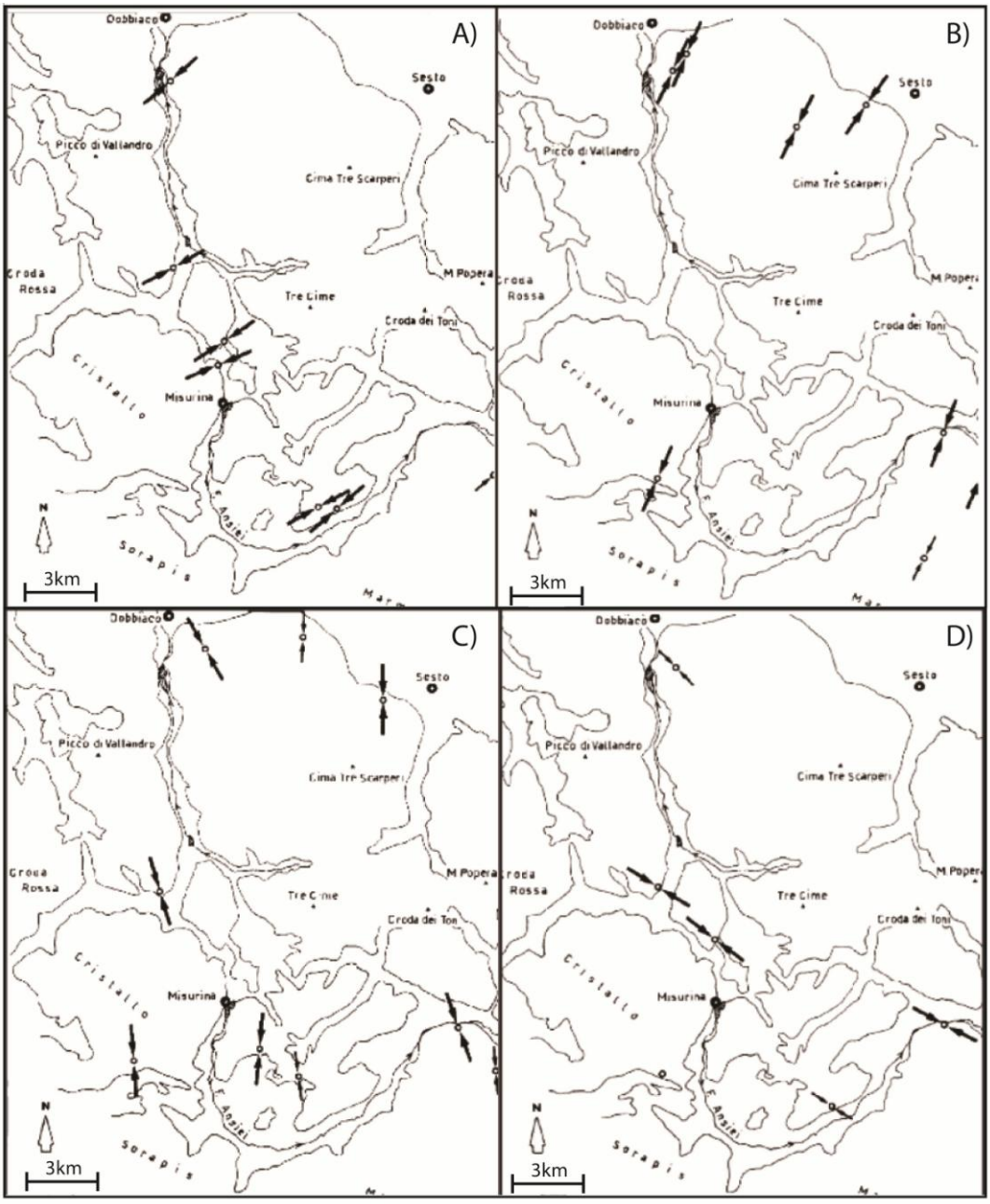

Fig.2.11. Convergence direction of the four compressional tectonic events of the Alpine Orogeny identified by Caputo (1996) in the Cortina d'Ampezzo area. Clockwise: A) NE-SW, B) NNE-SSW, C) NNW-SSE and D) NW-SE phases. From Caputo (1996).

The Neogene evolution of the Dolomites domain is characterized by the development of a south verging thrust belt (Doglioni, 1987; Berra & Carminati, 2010; Doglioni & Castellarin, 1985; Caputo, 1996) which main thrusts are the Valsugana and Belluno Line, the Moline Line, the Tezze

Line, and the Bassano Line: most of the them trend from N90° to N50-60°. The crystalline basement was involved, outcropping in the hanging wall of the Valsugana Overthrust, which is responsible for a southward shortening of about 8-10 km (Bosellini & Doglioni 1986). With its antitethic N-verging backthrusts, (Funes and Passo delle Erbe Lines), is responsible for the present-day tectonic configuration of the Dolomites: a large pop-up synclinorium, that have been uplifted by 3-5 km. Flexural slip faulting developed in the overlying sedimentary cover, as a response to the basement folding (Doglioni, 1987). Within the sedimentary cover, the development of thrust is controlled by the particular stratigraphic succession, where poorly competent lithologies (marls, evaporites and shales), interspersed with thick and stiff carbonates units acted as preferential decollement layers. Besides the low angle thrusts, the main Neogene tectonic features of that characterize the sedimentary cover are conjugate strike-slip faults, trend N30°-60°W and N0°-30°E. These strike-slip faults often show both positive and negative flower geometries.

2.3 Geology of the passo Giau Area

2.3.1 The stratigraphic succession

The Passo Giau (el. 2236 m.) is located in the Central- Eastern Dolomites (Belluno province), on the main route that connects the Ampezzo Valley and the town of Cortina with the Agordino Valley. The breathtaking geological view of the surroundings clearly illustrates the Triassic evolution of the area, especially at the turn between pre and post - volcanic carbonate depositional systems (fig.2.11).

The area is closed to the south by the thick Upper Anisian Cernera Platform, whose slopes are clearly onlapped by the erodible volcanoclastics and basinal deposits, which shapes the vast mountain pastures around the pass. Towards the north, the landscape is dominated by the post-volcanic carbonate slopes of Nuvolau and Averau that prograde northward over these deposits. Few km east from the pass, another Cassian platform outcrop, the Lastoni di Formin, that consists in a high carbonatic plateau bounded by steep and subvertical rock walls. The southern and central parts of the massif correspond to platform interior facies, while in the northern part northward-dipping thick clinoforms outcrop (Fig.2.12).

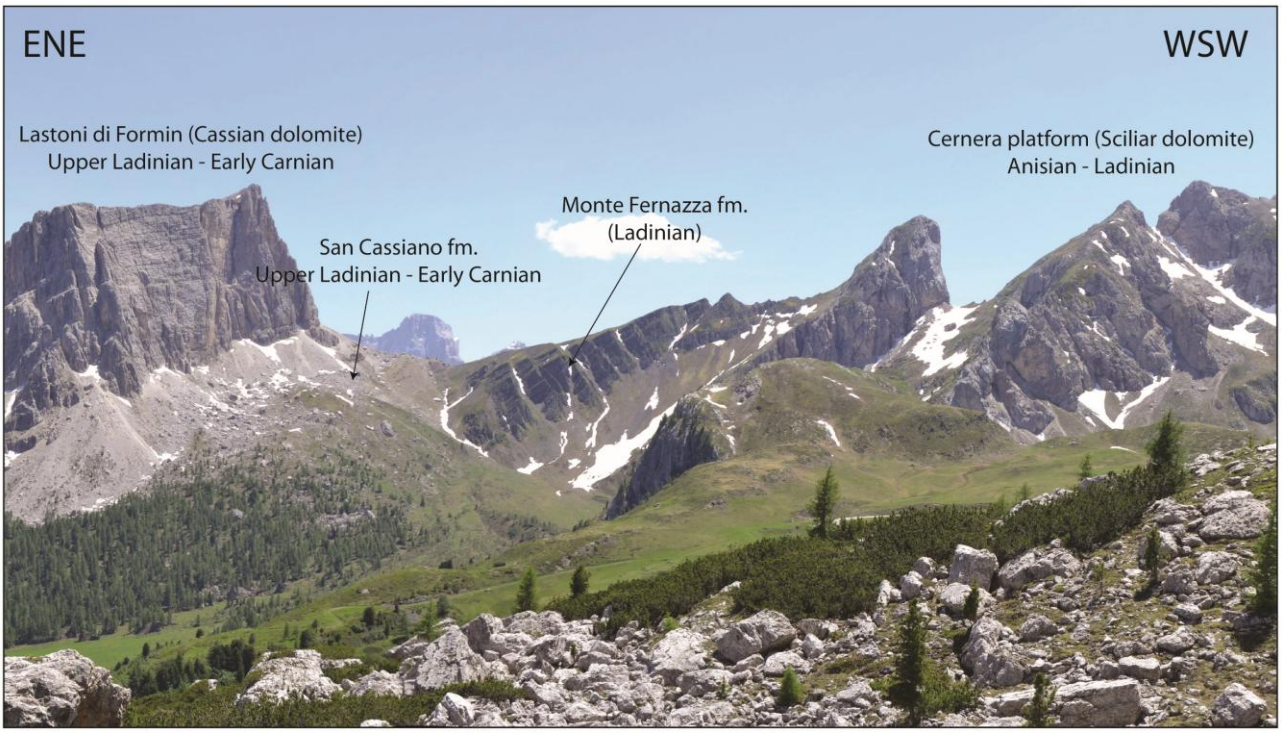

Fig. 2.11. Panoramic view of the passo Giau area (picture taken from the base of the Nuvolau). The area clearly show the turn between pre - volcanic (Cernera) and post - volcanic (Lastoni di Formin) carbonate depositional systems. The two platform are separated by the basinal volcanoclastic deposits of the Fernazza fm, constituted by the product of the dismantling of the middle- Triassic volcanic edifices, onlapping the eastern flank of the Cernera platform.

Deep-seated gravitational deformations affects this sector of the massif, triggering lateral spreads, block slides and toppling phenomena (Soldati & Pasuto, 1991). The summit plateau of Lastoni is topped near its southern sector by a remnant of Heiligkreutz and Travenanzes Formation, witnessing the last filling phase of the Cassian basins. On the background, the steep pinnacles of the Croda da Lago are cut in the Carnian/Norian Dolomia Principale, consisting of flat lying regional wide peritidal deposits. Despite the presence of minor regional Alpine lineaments that dissect the area, the main stratigraphic relationships between platforms and basins are well preserved. Both the Lastoni di Formin and the Nuvolau platforms are gently tilted toward NE of about 10°/15, and provide superb examples of the evolution of the platform-to-basin relationships: the slope angles progressively decrease upward and with the shallowing up evolution of the basinal San Cassiano successions, testify the progressive filling up of the small intraplatform basins from the latest Julian (early Carnian) (Breda et al., 2009: Gattolin et al., 2015).

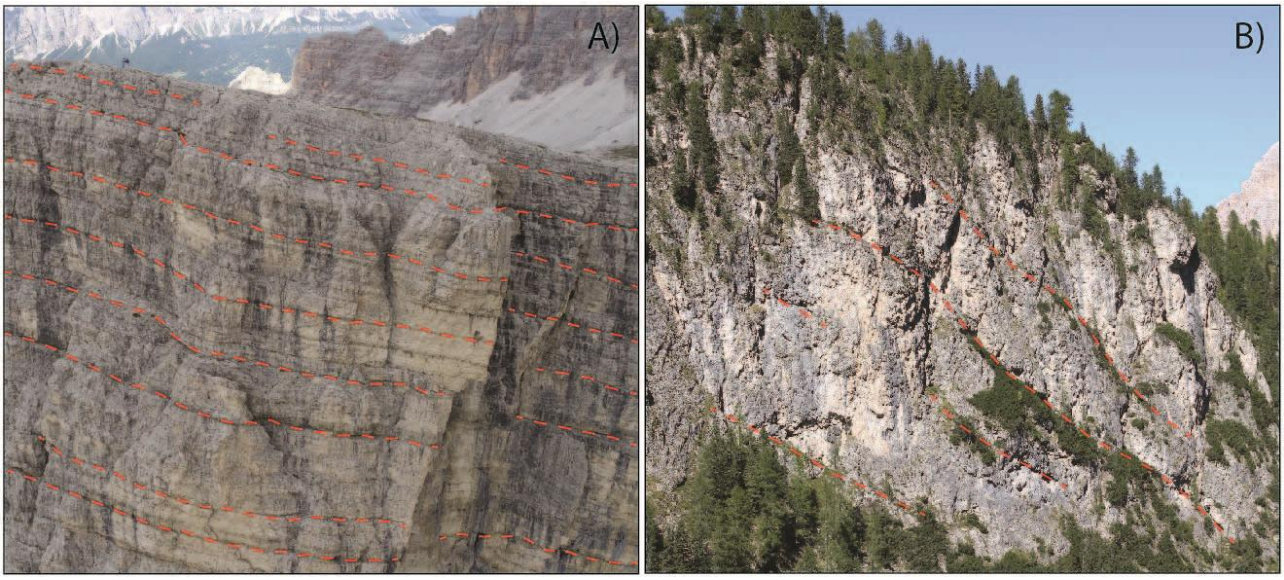

Fig. 2.12. A) Platform interior facies, clearly recognizable on the wide and open outcrop's cliffs, which characterize the southern and central part of the Lastoni Mountain. B) Slope facies outcropping in the northern sector of Lastoni di Formin.

The definition of the Cassian platforms stratigraphy in the eastern Dolomites has been debated by several authors for a long time. The controversy is related to the nature and the attribution of the Dürrenstein dolomite (sensu Bosellini et al., 1996; De Zanche et al., 1993; Preto and Hinnov, 2003). The "old" and the "new" stratigraphic interpretation are well resumed by Bosellini (1996) and Neri (2007) respectively. According to Bosellini, a general lowering of the sea level induced the deposition of the shallow water carbonates that took place within the Carnian basins and onlapped on the slopes of the Cassian platforms. Eventually, the residual basins where then completely filled by the Raibl formation, and the paleotopography was leveled.
The new stratigraphic model, proposed by Neri (2007) introduced substantial differences that can be summarized as following:
- The lower part of the Dürrenstein Dolomite has been reinterpreted as the inner platform facies of the Cassian Platform.

- The introduction of the Heiligkreutz formation (already proposed by Keim et al., 2001 and Stefani et al., 2004), that corresponds to the upper part of the Durrenstein Fm. and the lower members of the former Raibl Fm. (Trombetta 2006); this formation represents a shallowing upward terrigenous-carbonatic sequence deposited in a ramp environment, onlapping the Cassian slopes.

- The introduction of the Travenanzes formation, which corresponds to the former "Argilliti di Travenanzes", previously included into the Raibl group.

The facies descriptions and lithological characterizations described in this thesis are referred to the more recent interpretation of the Upper Ladinian - Lower Carnian stratigraphy of the area proposed by Neri (2007). The main units outcropping in the Passo Giau area are listed in the following figure (Fig. 2.12).

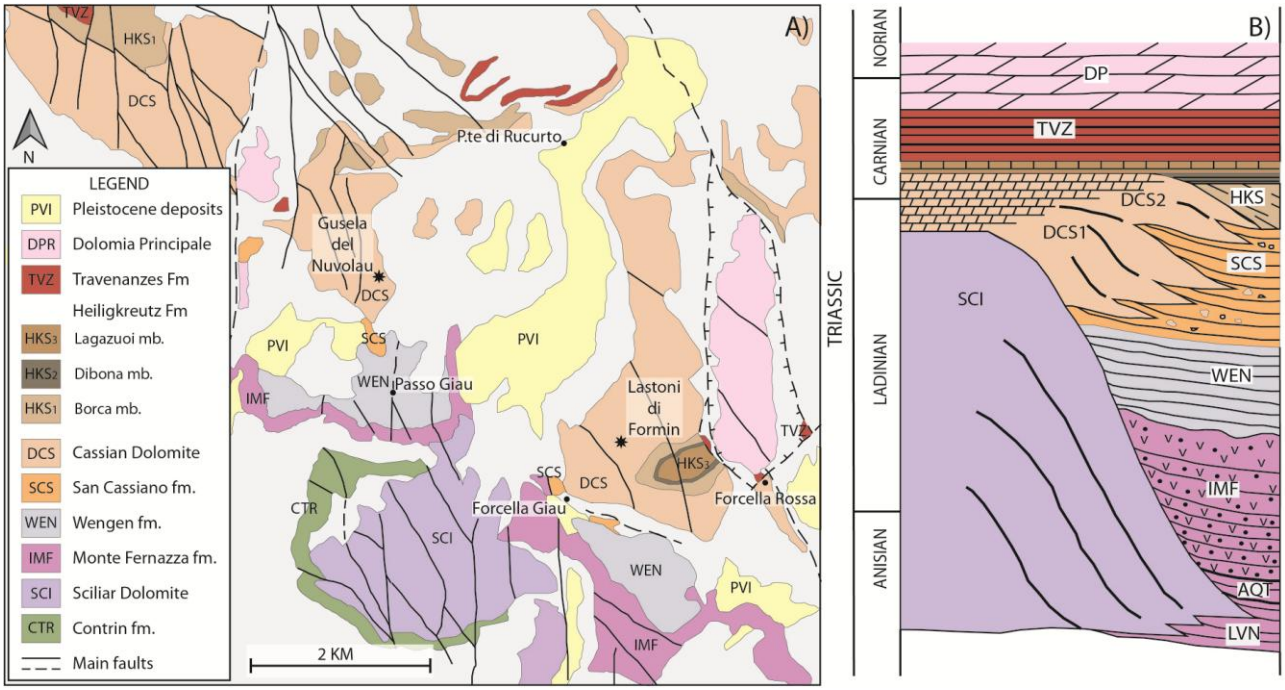

Fig. 2.13 A) Geological map of the passo Giau area (modified from Carta Geologica d'Italia. Foglio Cortina d'Ampezzo 029. Scala 1:50.000.). B) Ladinian - Norian stratigraphic scheme of the outcropping units in the central - western Dolomites according to the interpretation of Neri et al., (2007). (Modified from Trombetta, 2016).

2.3.2 Main tectonic features

Major south verging Alpine thrusts are located north and south of the study area, corresponding roughly to the E-W trending valley that goes from Cortina to Passo Falzarego to the north, and to the WNW - ESE Val Fiorentina to the south. The main tectonic elements of this section of eastern Dolomites are described in the Foglio 029 – Cortina d'Ampezzo (Carta Geologica d'Italia – 1:50.000). Some regional-scale tectonic lineaments are reported. The main structure is present in the easternmost part of the area, and consists of a N-S graben-like structure that lowers the Dolomia Principale. The western fault of this structure separates the Lastoni di Formin plateau from Croda da Lago, and near Forcella Formin it divides in two branches, that obliterate most of the original thickness of the Travenanzes formation, here outcropping only for few meters (the whole

undisturbed sequence reaches ~ 150 - 200 m in the area of Cortina, Neri et al., 2007; Breda et al., 2009). Nearby the Forcella Rossa (South of Croda da Lago, see image 2.13 for the location) the Heiligkreutz Fm is completely eroded, and the upper part of the Travenanzes and Dolomia Principale are in contact with the top of the Cassian platform. In Val Cernera, the contact between the volcanoclastic deposits and the Ladinian Cernera escarpment has been likely weakly reactivated by a S-W-vergent thrust fault (Stefani, 2004; Doglioni & Carminati, 2008). At the Forcella Giau, a minor fault apparently down throw the eastern side, putting the volcanoclastic unit in contact with the S. Cassiano Fm. The Cernera Mountain, as well as the Averau - Nuvolau massif in the north-eastern part of the area, is dissected by several vertical strike slip faults, oriented with a N-S trend.

3. Methodology

3.1 Introduction

The last two decades have marked the rise of laser scanning (LS) and digital photogrammetry (DP) as useful tools in many fields of geosciences (Chandler et. al., 1999; Hodgetts et al., 2004; Rarity et al., 2014; Burnham et al., 2018; Cawood et al., 2017; Menegoni et al., 2019). In particular, photogrammetry - based Digital Outcrop Modeling has become one of the most attractive survey techniques for the analysis of fractured outcrop analogues (Bistacchi et al., 2015; Casini et al., 2016; Corradetti et al., 2017a; Franceschi et al., 2015) since it allows the detailed quantitative description of large scale depositional structures and the collection of great volumes of data directly at a reservoir scale. The use of DOMs gives the possibility to explore outcrops and navigate around the model in a 3D stereo mode, that sometimes results in different interpretations than the more limited view that a geologist can have by studying only restricted parts of outcrops (Hodgetts, 2013; Bistacchi, 2015). Moreover, this technique allow to overcome the significant biases of the traditional 2D interpretation of fractures based on orthorectified photomosaics, that suffer from the reduction of a 3D surface to a 2D plane image (i.e.fractures with different angles produce traces on the outcrop surface that can be misinterpreted a quasi-perpendicular set) (Minisini et al.,2014).

The recent technological improvement of Unmanned Aerial Vehicles (drones), high-resolution digital cameras and computer processors, together with the development of new processing procedures (Structure from Motion, SfM) have made this method of survey easier and more accurate, enhancing the quality of structural and sedimentological data that can be collected also in large and inaccessible areas. Moreover, whereas Laser Scanner could be very expensive and complex in term of survey planning (heavy and bulky equipment), the use of Digital Photogrammetry has a greater flexibility and yields to extremely high resolution data with a lower cost and a more user-friendly survey planning (Remondino and El-Hakim 2006; Westoby et al. 2012; Bemis et al., 2014). The Passo Giau area (Central Dolomites, Italy) provides spectacular remnants of dolomitized Middle-Triassic carbonate platforms, different in dimensions and expositions, where these techniques can be tested and exploited for the characterization the depositional geometries and tectonic features. In particular, the study has been performed on two outcrops that represent the remnants of a Cassian platform (late Ladinian/early Carnian): the *Gusela del Nuvolau* and the *Lastoni di Formin* (see fig. 2.13 A for the locations). The *Gusela* is dominated

by the massive clinoforms of the slope facies. The *Lastoni* consists in a high carbonatic plateau corresponding in the southern and central parts of the massif to platform interior facies, while in the northern part northward-dipping thick clinoforms outcrop (see fig. 2.12).

In this chapter the methodology and the workflow for the developments of the Digital Outcrop Models, based on Unmanned Aerial Vehicles Digital Photogrammetry (UAVDP) and Terrestrial Digital Photogrammetry (TDP) are described. The process consists in two distinct parts: the photogrammetric survey and the data processing and development of the DOM. The study has demonstrated the advantages and the effectiveness of UAVDP as a reliable method of investigation, highlighting, at the same time, some critical issues in the DOM generation and georeferencing of such extensive outcrops.

3.2 Principles of Digital Photogrammetry and Structure from Motion

The argument has been exhaustively treated by Birch (2006), according to which photogrammetry can be defined as *the science of determining 3D data from two or more 2D images of a scene*. This is achieved by determining the position of homologue pixels that are recognized in two or more images, taken from different angles, of the same object, in function of the position and the parameters (focal length, imaging size, lens distortion) of the camera (fig.3.1).

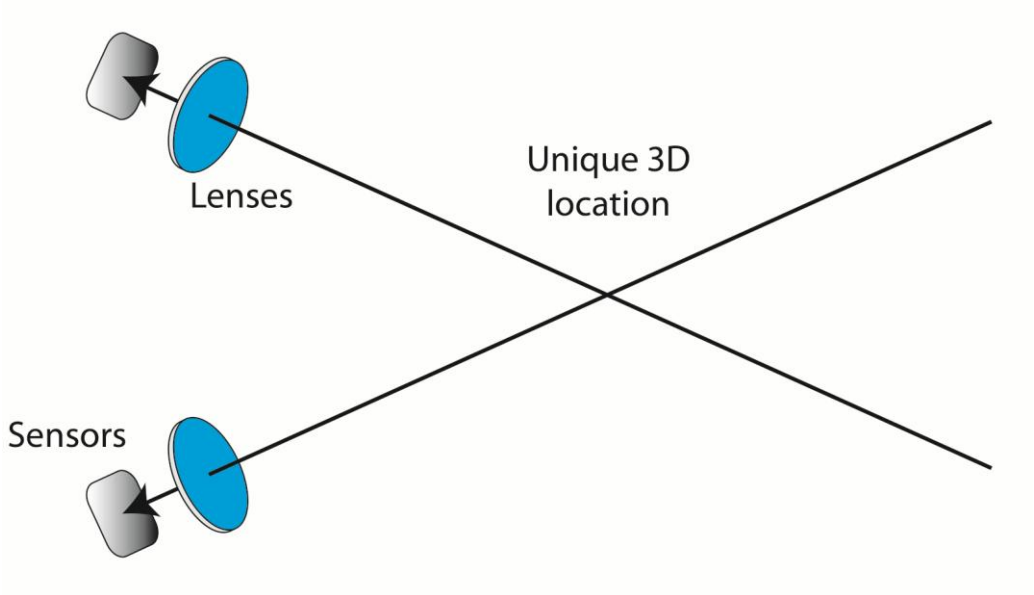

Fig. 3.1 The light that arrived at a particular pixel of an image could have originated at any point along the ray depicted. The intersection of two rays determines a unique 3D location where the light for that point must have originated (from Birch, 2006).

In practice, this technique allows the reconstruction a 3D surface of an outcrop starting from a series of overlapping RGB images (Remondino and El-Hakim, 2006; Sturzenegger & Stead, 2009). The output of the reconstruction process is a RGB point cloud dataset, that can be used directly for the geological interpretation or further implemented by triangulation to obtain a textured surface model of the object.

The photogrammetric acquisition can be performed from the ground (Terrestrial Digital Photogrammetry) or from aerial position, with the camera placed on an aircraft device (Aerial Digital Photogrammetry). When Aerial DP is performed using Unmanned Aerial Vehicle (UAV), also called Remote Piloted Aerial System (RPAS), it is defined as UAV-based Digital Photogrammetry (UAVDP, less commonly RPASDP). Moreover, Digital Photogrammetry is divided in Close range DP and long range DP according to the camera - object distance, lower or higher than 300 m respectively (Wolf and Dewitt, 2000). This distance, together with the focal length of the camera, directly influence the resolution of the image (defined as the ground-pixel size), according to the equation defined by Birch (2006).

$$pixelsize_{ground} = \frac{Distance}{focal\ length} \times pixelsize_{sensor}$$

The distance between pixel centers on the ground (i.e. ground-pixel size) is also called Ground Sampling Distance (GSD) and represents the available resolution of the generated DOMs. In traditional photogrammetry the position and orientation of the camera, as well as accurate 3D information on control point in the scene of interest, needs to be known prior of processing the images (Cullen et al., 2018).

However, over the last decade, the photogrammetric techniques underwent a significant evolution; today, many of the software for the photogrammetric reconstruction (e.g. Pix4D and Agisoft Photoscan) are based on the Structure from Motion algorithm (SfM), a computer vision technique for the reconstruction of 3D object from pictures (Spetsakis & Aloimonos, 1991). It works estimating simultaneously the 3D scene and the orientation and position of the images by the identification and matching of common points in multiple overlapping images (Fig. 3.2), by using the scale-invariant feature transform algorithm (Lowe, 1999; Lowe, 2004) and the bundle adjustment process (Triggs et al., 1999). The result is a "sparse" point cloud that can be used to optimize the camera alignment before the processing of the "dense" point cloud.

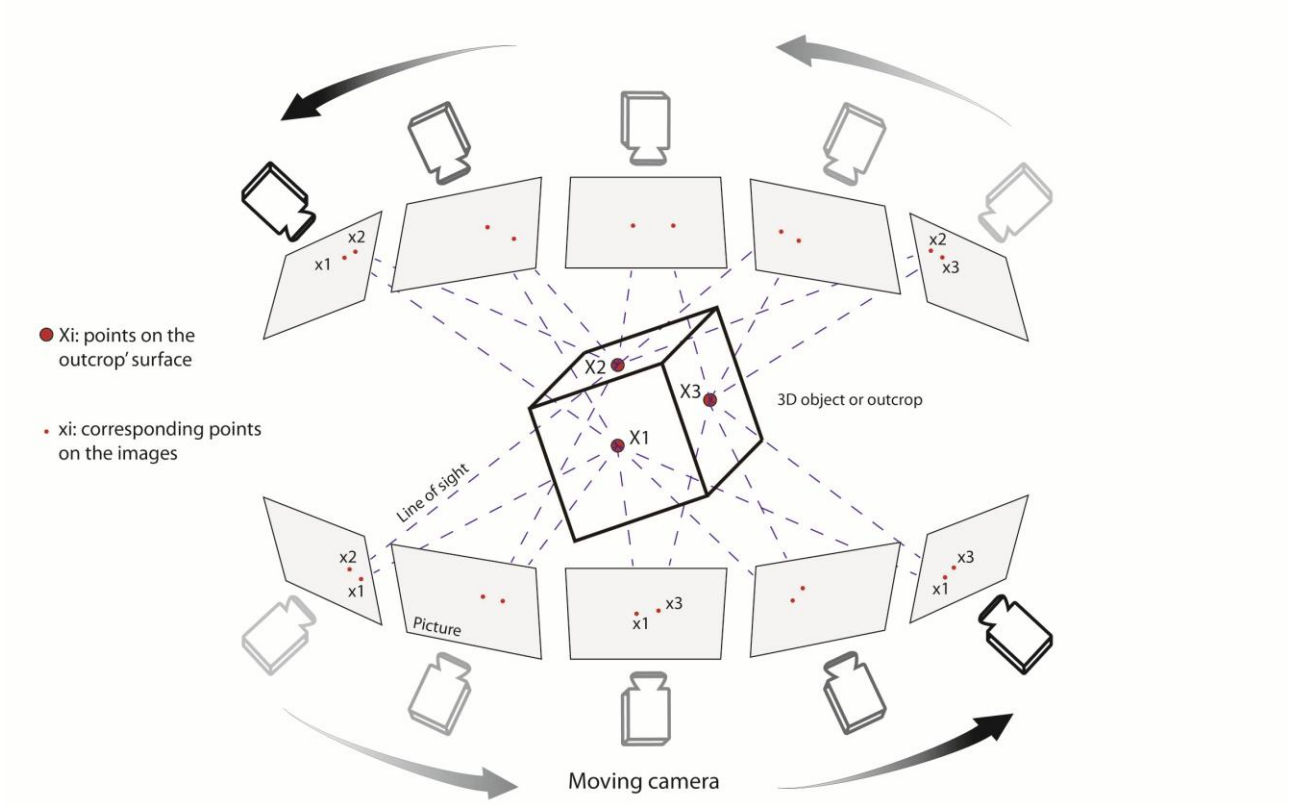

Fig. 3.2 Principles of SfM techinque. The 3D reconstruction of an object is achieved by determining of orientation and position of the images by the matching of common points in multiple overlapping images.

3.3 UAV Survey and processing

As previously mentioned, the survey was conducted on two outcrops that are representative of the different depositional environments of the same carbonate depositional system. The two areas, although located at a short distance from each other, are very different in size and geometry. The *Gusela del Nuvolau* is a prominent rocky spur that represents the remnants of a Mesozoic Cassian slopes: main target of the survey is the south-east cliff, that displays a section almost parallel to the depositional profile of the platform. It rises of about 150 m over the surrounding meadows, dipping towards the north. The *Lastoni di Formin* massif crops out few km east from "Passo Giau" and covers an area of approximately 2.8 km^2. It consists in a carbonate edifice bounded on three sides by steep vertical walls that can rise up to 300 m. The top of the massif is represented by a wide inclined plateau, dipping to north-east and interspersed by deep crevasses. The outcrop is dominated by regular peritidal cycles referable to the inner platform environment (Chapter 2, Fig.2.12 A); the slope facies are visible at the bottom of the cliffs and in the northern sector. Due to the

characteristics of the outcrops, the surveys have been conducted using Ummanned Aerial Veichles, that allowed to obtain detailed aerial images with various angles even along the wide cliffs of the massifs. This had also the advantage to minimize some of the limits of ground-based acquisition, such as truncation and occlusion effects (fig.3.3).

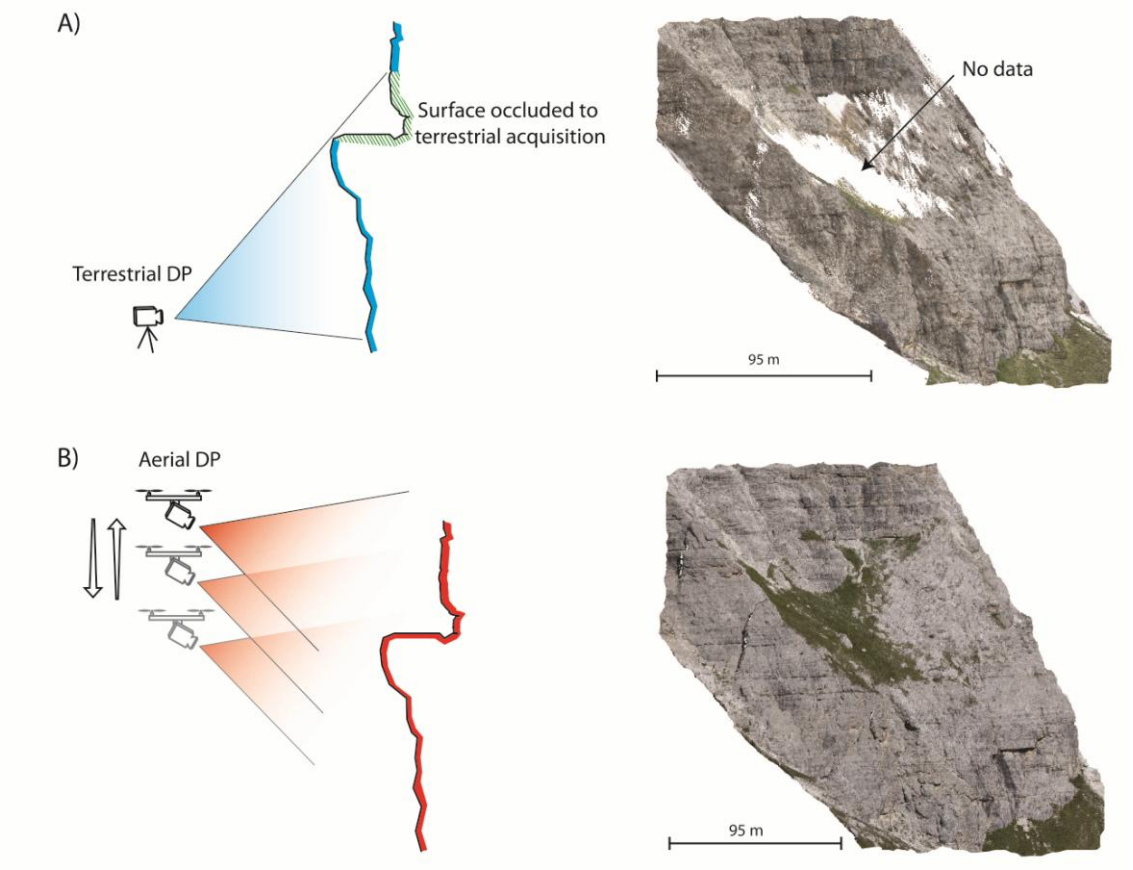

Fig. 3.3 Example of the occlusion effect that usually occur during acquisition from the ground. Occlusion can be easily reduced by the use of UAV photogrammetry.

During the flights, the orientation of the camera was maintained orthogonal to the outcrop surface, and the images were acquired with an overlap and a sidelap greater than 90%. The exact position and orientation of the camera during each shot have been recorded by the on-board GNSS-IMU instrumentation, (e.g. GPS, compass, gyroscope, and accelerometer). Another benefit of DP is that the ground resolution is mainly controlled by the camera - object distance. In both the outcrops this distance was maintained around 200 m, (with possible variation due to the shape of the outcrop), in order to keep a reasonable balance between the final resolution of the model and its size. Terrestrial digital photogrammetry have been performed only on small selected sampling windows, with a camera-object distance < 10 m, realizing some very high-resolution models of specific points of interest. The photogrammetric acquisition was carried out in several missions using a DJI Matrice

200 quadcopter, equipped with a 20 Megapixel Zenmuse X4S camera (Lastoni di Formin) and a DJI phantom 4 with a 20 Megapixel CMOS camera and high precision Real Time Kinematic (RTK) positioning system.

Further specifications about UAV platform and sensors are illustrated in the table 3.1. Since the morphology of the outcrops can influence the type of aircraft and camera settings fit for purpose (Giordan et al., 2015) the choice of operating with relatively "compact" multi-rotors drones was considered optimal for the mapping of the vertical cliffs of the massifs, because they can move easily (with respect to, for example, fixed wings drones) in vertical and lateral direction, as well as closer or further from the walls. Moreover, they are stable also in windy and severe weather conditions, allowing to work in high mountain areas.

Table 3.1. *Unmanned Aerial Vehicles specifications.*

UAV platform specifications					
	UAV type	*Empty weight*	*Engines*	*GNSS*	
Dji Matrice 200	X shaped quadricopter	3.8 kg	4 brushles	GPS+GLONASS	
Dij phantom 4 RTK	X shaped quadricopter	1.4 kg	4 brushles	High precision RTK	
Camera specifications					
	Sensor type	*Image size*	*Focal lenght*	*Resolution (pixels)*	*Pixel size*
Zenmuse X4S	1" CMOS 12.8 x 9.6 mm	4864×3648 (4:3) 5472×3648 (3:2)	8.8. mm	20 mpx	2.3 x 2.3 µm

The survey of the Lastoni di Formin outcrop was carried out during different days by flying and capturing images in automatic mode. The operations were preceded by an accurate flight planning on the base of previous data (1m resolution Digital Elevation Model) using a dedicated software. The flights were planned to scan the outcrops along several horizontal strips at progressive increasing elevations (an example from the Nuvolau oucrop is shown in img.3.4 A); on the flat top of the massif, the camera orientation was maintained in zenithal position, and the flights were designed to investigate the surface following a flat horizontal grid (img.3.4 B): in total, 16 drone missions with four different take-off positions were carried out, that lead to the acquisition of more than 12 000 images.

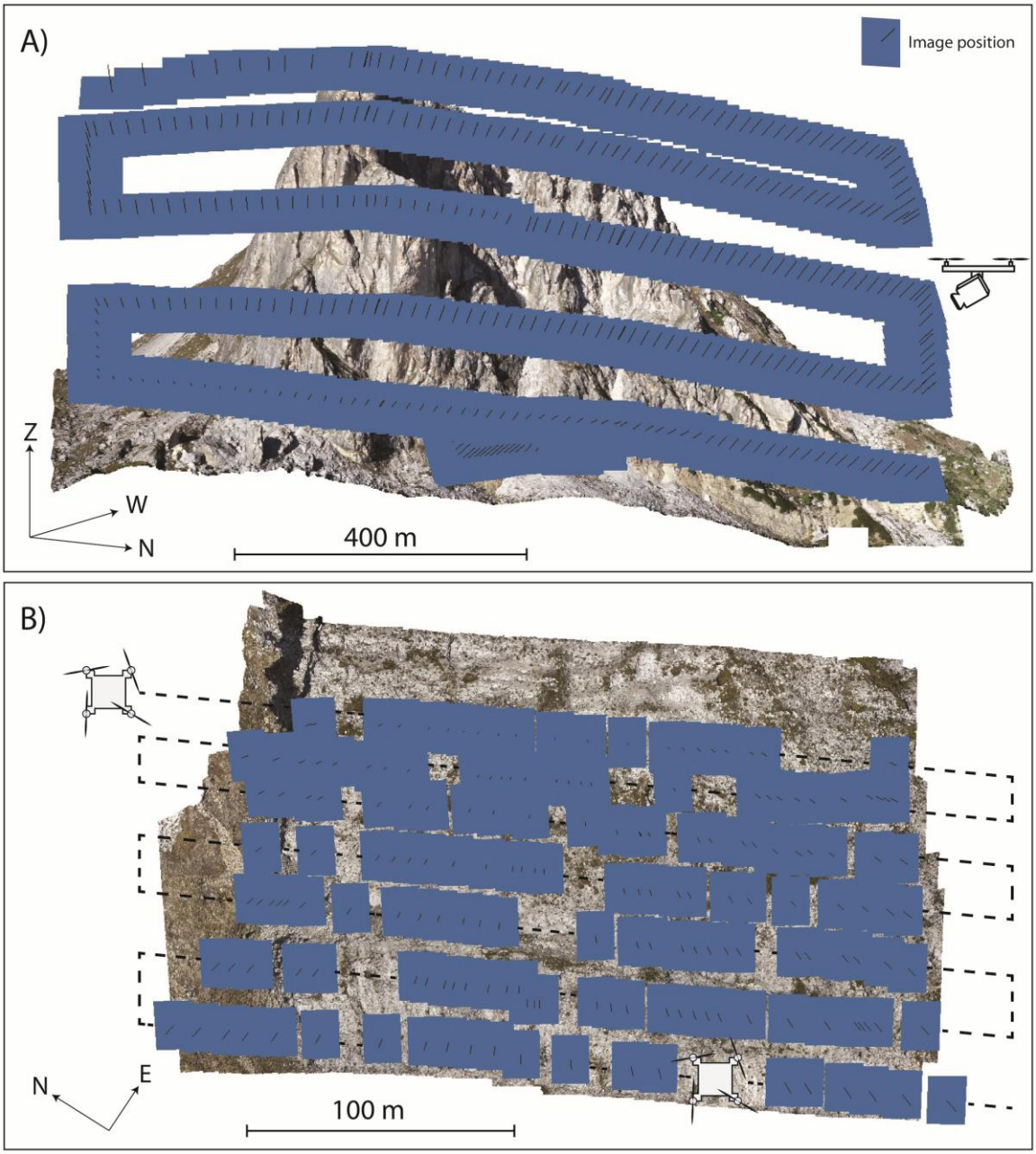

Fig. 3.4 Example of UAV survey in the case of A) vertical cliffs and B) zenithal acquisition of plane surfaces (e.g the top of the Lastoni outcrop).

The considerably smaller dimensions of the Gusela del Nuvolau outcrop, compared to the Lastoni, allowed to complete the acquisition in few-days; in this case, the morphology of the relief required the manual control of the UAV. Four drone missions were planned for the acquisition of the total morphology of the outcrop; moreover, few highly detailed flights were performed at the base of the cliff with the purpose to obtain high resolution data (1 cm pixel size) of the transect that show the platform - to - basin transition. The dataset was then processed using the software *Photoscan*

(Agisoft). The Photoscan workflow that was used to generate the DOM can be summarized in the following steps:

- Pre-processing: removing of unwanted, blurry or defective images (for example, images involuntary taken during the drone's take off, "burned" or overexposed, or with the object partially covered by haze).

- Image matching, using the GNSS/IMU information recorded by the RPAS on-board GPS, and bundle block adjustment, including the GCPs position measured in the field with Real Time Kinematic GPS. Generation of the sparse point cloud;

- Reconstruction of the dense point cloud using the high-quality setting of Photoscan;

- Mesh and texture generation and developing of georeferenced orthophoto mosaic, based on the dense cloud and the high face count suggested by Photoscan. The results were exported in WGS 84 metric coordinate system. In particular, the dense PC was exported as a .las file including the RGB color value for each point. The textured model was exported as an OBJ file including the vertex normal and texture. The parameters used during the processing are indicated in *Table 3.2.*

***Table 3.2**. Processing parameters used in Photoscan software*

Process	**Processing parameters**		
Image alignment and sparse point cloud generation	**Accuracy**	**Tie Point**	**Key Point**
	High	40000	100000
Dense point cloud generation	**Quality**	**Depth filtering**	
	High	Mild	
Mesh generation	**Source data**	**Surface type**	**Face count**
	Dense cloud	Arbitrary	High
Texture generation	**Mapping mode**	**Blending mode**	
	Generic	Mosaic	

3.4 Georeferencing

The global position and the orientation of the camera during of the acquisition are recorded by the onboard GNSS/IMU onto the EXIF header of the digital image and used by the SfM algorithms to georeference directly the 3D model. Since most of the drones are equipped with low-grade GNSS

systems the absolute accuracy of the positioning of the camera could reach tens of meters and this kind of georeferentiation is generally not accepted by the scientific community. Therefore, it is strongly recommend the use of *Ground Control Points* (GCPs) for the correct georeferentation of the DOM.

This is particularly evident in the *Lastoni di Formin* case of study, where sets of photos acquired in different missions and take-off position are affected by a significant vertical shift. Therefore, the UAVDP acquisition of this outcrop was preceded by the measurement of 22 Ground Control Points (GCPs), represented by artificial targets, placed at the top of the massif and at the base of the cliffs, whose position was decided on the base of aerial photos in order to have a uniform distribution. The survey was conducted with a differential Real Time Kinematic (RTK) GPS (type Topcon Hiper Pro), that has a theoretical accuracy of 0.01 m and 0.015 m for horizontal and vertical measurements, respectively.

The position of GCP were then included automatically in the processing workflow, enhancing the image matching and the adjustment of the camera positions. Despite the drone used for the acquisition on the *Gusela del Nuvolau* was equipped with GPS RTK, few GCP were measured to have additional control. For a further validation of the developed DOM, some direct-contact control measurements have been taken in portion of the outcrop clearly visible onto the images of the UAV and then compared. Accuracy and precision assessment for the Lastoni DOM are addressed in the paragraph 4.3.2 of the chapter 4.

3.5 Results

Several digital models were generated for each of the studied outcrops and georeferenced in WGS 84 UTM 33 coordinates. The overall point clouds of Lastoni and Nuvolau has a resolution generally around 5 cm/pixel and can vary from 2.7 to 7.9 cm/pixel, largely sufficient for the interpretation of the depositional characteristics of the platform and the acquisition of quantitative structural data at the reservoir scale. Few high-resolution (0.7 cm/pixel) DOMs and orthophotos were realized on specific areas, especially on the summit plateau of the Lastoni and at the slope - basin transition on the Nuvolau platform, in order to perform more detailed structural (fractures arrangements and relationships) and sedimentological analyses.

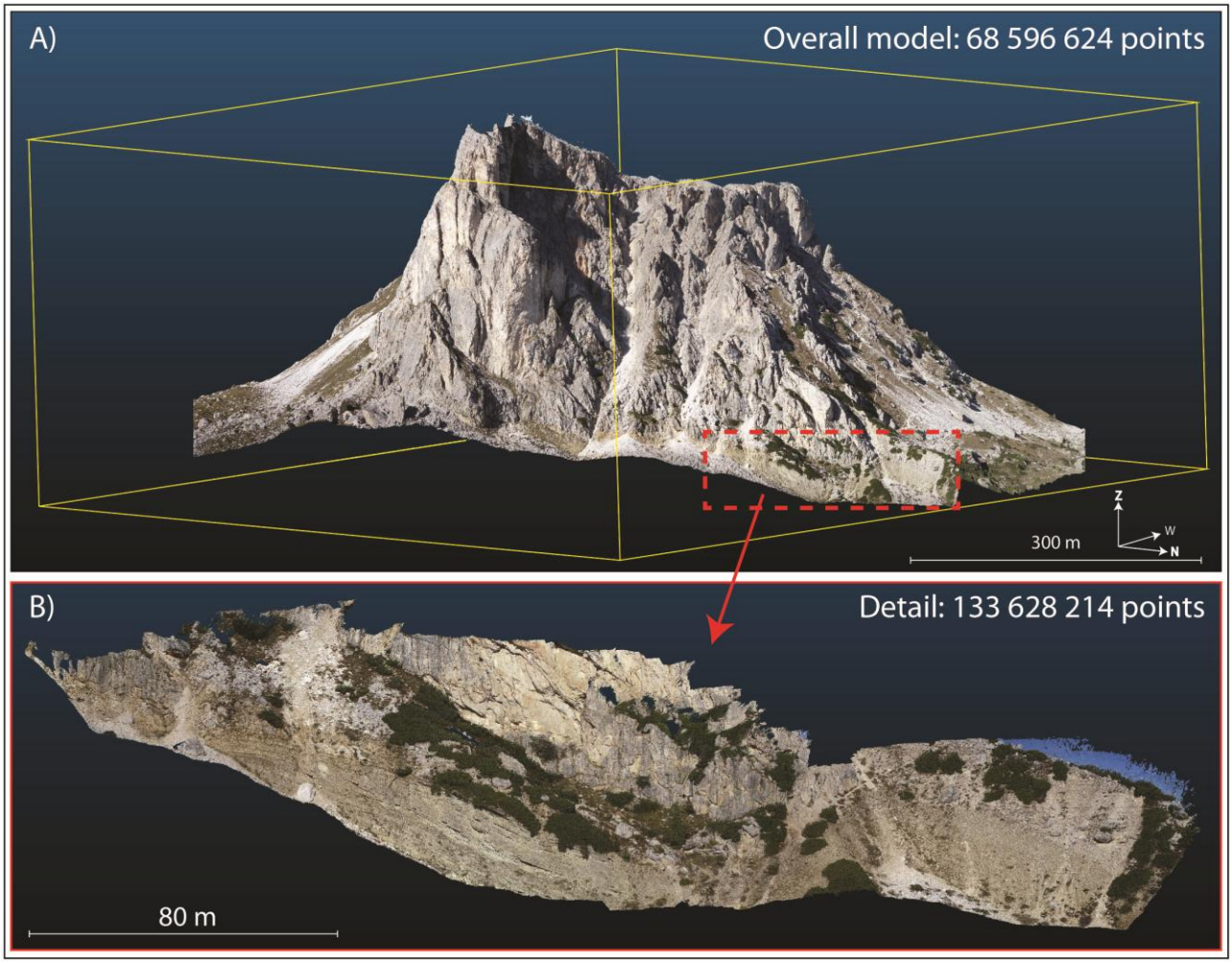

Fig. 3.5 Example of UAV survey in the case of A) vertical cliffs and B) zenithal acquisition of plane surfaces (e.g the top of the Lastoni outcrop).

3.6 Accuracy assessment

To evaluate the effectiveness of the georeferencing for the *Lastoni di Formin* case study and quantify the effect of errors on the measurements, the accuracy of the models was assessed. According to Chesley et al., (2017), accuracy of a DOM can be distinguished in absolute and relative. The absolute accuracy of the Digital Outcrop Model is defined as the difference between the real coordinates of the GCPs marked with GPS RTK in the field and their position detected on the DOM. The relative accuracy was evaluated by comparing the lengths and azimuths of vectors joining pairs of GCP with the lengths and azimuths measured from the corresponding points in the model. For geological and structural outcrop studies, evaluating the relative accuracy is of a key importance to verify the reliability of the measurements. The mean absolute accuracy is about 120 cm and 72 cm for the planar and the vertical positioning, respectively. The maximum angular

differences in orientation and length of the 231 measured vectors are below ±1° and 0.17%, respectively. These values fall within the range of errors of the manual compass-clinometers orientation measurements; this range (ca. ±2°) depends mainly on the instrumentation accuracy, expertise of the operator or statistical significance of field measurements on non-planar and irregular surfaces (Cawood et al., 2017; Jordá Bordehore et al., 2017).

3.7 Digital mapping of features

The DOMs developed using SfM algorithms were managed and analyzed in a 3D environment by the use of the CloudCompare software and a 3D Pluraview UHD stereoscopic hardware (e.g. stereoscopic monitor, Virtual Reality glasses, specific video card). The hardware used in this research for the Stereoscopic Vision (SV), is a Planar SD2220W 3D LCD screen, composed by two separate polarized display monitors placed one above the other at 90° and half-silvered glass at 45° in the middle (fig. 3.6). The application of stereoscopic vision to 3D DOM is particularly advantageous for the interpretation of large scale depositional geometries, since prevent biases due to 2D visualization on standard monitors of 3D objects. CloudCompare is a free 3D processing software that allow to handle point clouds and triangular meshes.

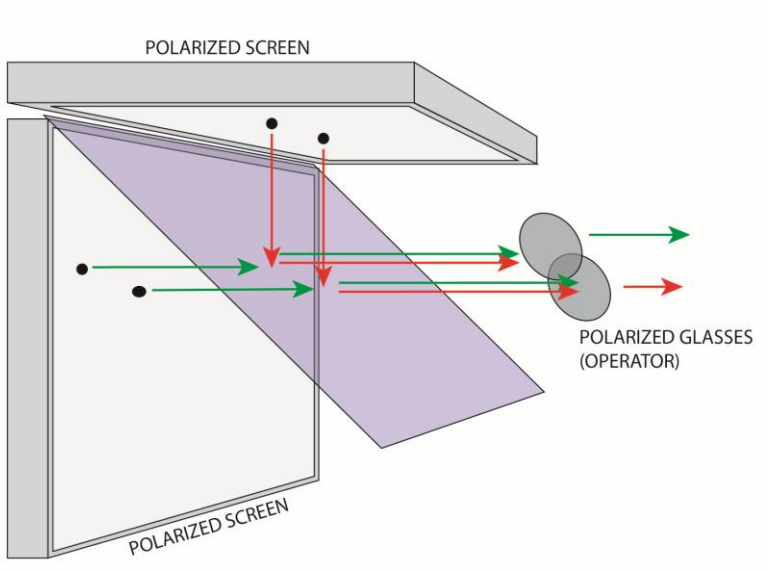

Fig. 3.6 Simplified sketch of the Planar SD220W stereoscopic screen.

The software is open source and is subject to a continuous implementation of plugins and developments. CC provides advanced algorithms for editing and rendering DOMs, as well as a set

of tools for manual and automatic extraction of information and statistic computations, periodically implemented and updated (e.g. Dewez et al., 2016; James et al., 2017; Thiele et al., 2018).

The software allows the digital mapping of geological features directly onto the dense point cloud (thicknesses, volumes and dimensions of rocks, orientations of the bedding and fractures, fault displacements). As previously mentioned, gathering data from the DOM has some unequivocal advantages with respect to the traditional field mapping, such as:

- To obtain data of inaccessible parts of the outcrop;

- To obtain quantitative data that does not suffer of limitations, such as orientation biases and trace truncation;

- To allow checking and managing of the data at any time and by different users;

- To gather digitalized data that can be directly exported and managed with suites for statistical analysis (i.e. R, Matlab).

Despite several procedures for the automatic data extraction have been developed in the last decade (Slob et al., 2004; Jaboyedoff et al., 2007; Chen et al., 2016; Gomes et al., 2016; Jordá Bordehore et al., 2017), mostly manual and, in some cases, semi-automatic (Qcompass plugin, Thiele et al., 2018) methods for the measurements of orientations and thicknesses were applied. The manual procedure used to measure orientation of bedding and fracture planes consists on the point-picking on the feature's trace that intersect the outcrop surface, with the *trace polyline* tool. This tool permits the sampling on both the point cloud or on the triangular mesh. In the first case, the picked node of the polyline is positioned onto the closest point of the cloud; when the point picking is performed on the triangular mesh, the node is positioned by the algorithms on the nearest available positions (vertices of the picked face of the mesh, center of the picked face or the middle position between two vertices of the face). The 3D polyline was successively fitted with a 3D plane that is calculated as the best fit plane of the XYZ coordinates of the polyline nodes, and embody the values of deep and deep direction and the coordinates of the feature. Together with the manual sampling, the semi - automatic extraction was performed, when possible, by the use of the Qcompass plugin (Thiele et al, 2017), that works only on the point cloud (fig. 3.7). In particular, the tools used for the analysis are:

-Plane tool: measure surface orientations of fully exposed planar structures. A plane circle is shown in the 3D window, which radius can be changed with the scroll wheel of the mouse. After picking

on a surface of the DOM, a plane is fitted to all points sitting within the circle, giving an orientation estimate.

- Trace tool: allows the estimation of a structure orientation based on its intersection with a non-flat surface. It is similar to the manual point-picking, but it uses different algorithms to "follow" the trace between the nodes, connecting points of the cloud, on the base of their similarity (i.e darkness, RGB value, curvature, distance). The advantage of the tool is that it is sufficient to select the first and last node of a feature to define the entire trace.

- One-point/two-point thickness: can be used to measure the true-thickness of geological units by selecting a plane representing the orientation of a unit and one or two points on its boundary. It is particularly useful to measure the real bed thickness (which can be confused with the apparent thickness in a 2D interpretation) and the fault displacements. One-Point Thickness measures the perpendicular distance between the selected plane and a chosen points. Two-Point Thickness measures the perpendicular distance between pairs of successively chosen points.

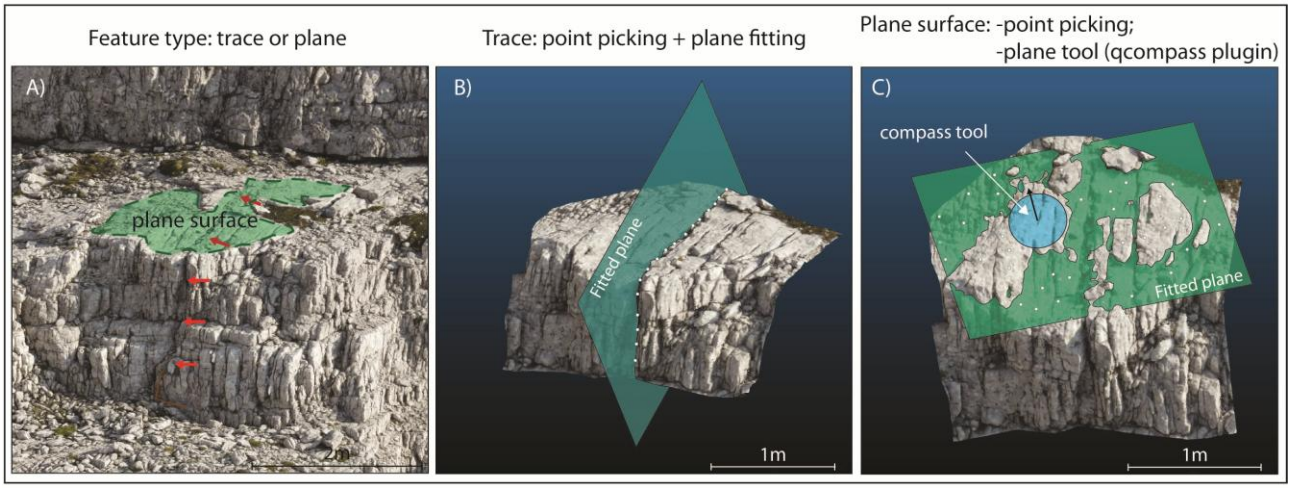

Fig. 3.6 Workflow of the tools for the sampling of the point cloud and mesh, according to the feature studied (A): B) point picking and plane fitting of a fracture trace; C) point picking and qCompass semi - automatic acquisition on a plane surface. The qCompass plugin (Thiele et al., 2017) only works on point clouds.

3.8 Discussion

The reconstruction of a high-quality Digital Outcrop Model has been accomplished despite the technical and logistic difficulties that came up working in a high mountain environment. In general, the advantages of the approach adopted for the study has been highlighted and the centimeter-scale

resolution of the DOM satisfies the aims of the study and revealed to be appropriate for the definition of bedding, fractures and faults. In the scheme of fig.3.7 the entire workflow for the analysis of outcrops using Digital Outcrop Modeling and photogrammetry is reassumed. The ability to perform measurements directly on the 3d models drastically increases the amount of data that can be collected from an outcrop, providing a solid base for the interpretation. At the same time, it significantly reduces the time required for the measurements, if compared with the field activities (quicker sampling of a single feature, measures automatically digitalized, applications of semi-automatic methods). Nevertheless, the photogrammetric survey and the 3D model development can be relatively time-consuming operations.

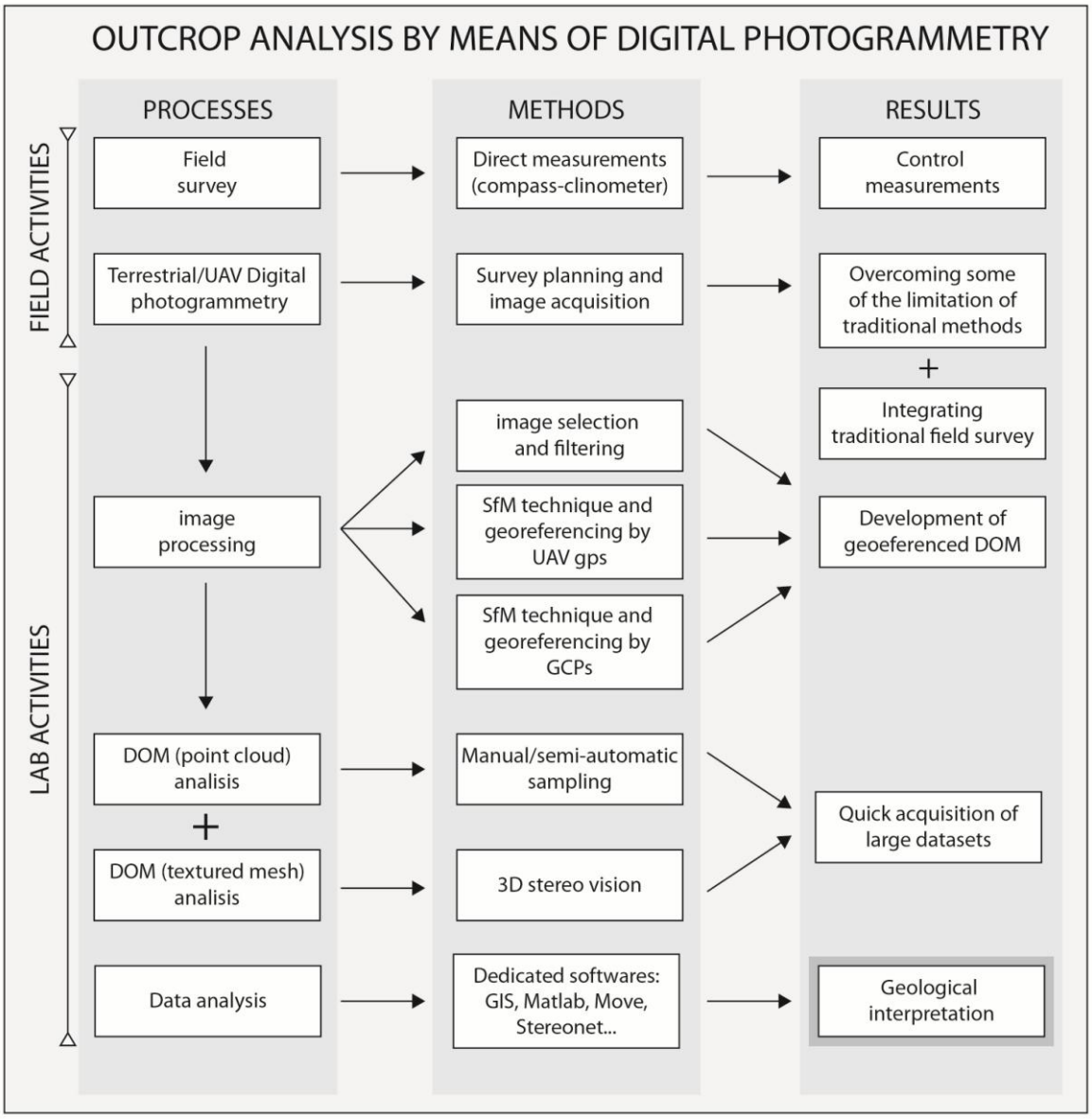

Fig. 3.7 Processes, methods and results of the methodological workflow presented in this research for the outcrop analysis using digital photogrammetry (Modified from Menegoni, tesi di dottorato, 2019).

The UAVDP survey on Lastoni di Formin required 4-5 days in the field, mainly due to: - logistic issues (i.e. access to the outcrop only with several hours of walk, limited availability of drone's batteries) - difficulty in the image acquisition (i.e. variable light and wind conditions, outcrop's geometry) and ground control points acquisition. All of these disadvantages are largely counterbalanced by the benefits of having the outcrop at hand, allowing to analyze it at any time and in every moment. Moreover, in the case of the Gusela del Nuvolau, the use of UAV equipped with high-precision RTK GNSS significantly reduced the time required to perform the survey, avoiding the acquisition of several Ground Control Points; the DOM in this case was directly georeferenced using the image position and orientation recorded by the on board GNSS instrumentation.

The processing time for the DOM generation strongly depends on the computational performances of the workstation used for the elaboration. An incorrect calibration between the quantity of data simultaneously computed and the machine performance can lead to a critical slowdown in the DOM developments (days - weeks). Also the visualization of the 3D models depends mainly on the hardware (CPU and Video Card) and could be problematic in the case of very extensive or highly resolute models (several millions to billions of points); all these aspects needs to be considered before the decision to perform DP for the investigation of wide outcrops.

4) Manuscript A: Syndepositional fractures and architecture of the Lastoni di Formin carbonate platform: insights from Virtual Outcrop Models and field studies.

Manuscript published on Marine and Petroleum geology, Elsevier, Volume 121, November 2020.

Riccardo Inama[1], Niccolò Menegoni[1], Cesare Perotti[1]

[1] Università di Pavia

Abstract

The recent rapid improvement of Unmanned Aerial Vehicles, together with advances in photogrammetry and Structure from Motion techniques, have enhanced the role of Digital Outcrop Models in many field of geology, due to the possibility to obtain quantitative information from large and inaccessible areas. In this study we integrated Digital Outcrop Modeling techniques and field survey to investigate the architecture of the Middle Triassic platform of *Lastoni di Formin*. (Italian Dolomites). The research highlighted the presence of two superimposed carbonate bodies. The lower unit (Cassian I) is dominated by low-angle clinoforms dipping north-northeastward and prograding over the basinal San Cassiano Fm. The upper unit (Cassian II) is characterized by a thick sequence of peritidal cycles connected northward to another generation of clinoforms. The inner platform beds of the upper unit display a lateral thickening that is particularly evident near the shelf break, and that has been interpreted as due to the increased subsidence and the consequent down-to-basin tilting of the outermost part of the platform. Moreover, the structural analysis performed on the Digital Outcrop Models and supported by field observations, highlighted the presence of an early generation of faults and joints that indicate an early gravitational deformation of the platform possibly caused by the platform progradation and compaction-induced subsidence of the San Cassiano basinal deposits. These WNW-ESE synsedimentary structures are formed by normal faults and extensional joints that are oriented nearly perpendicular to the direction of the carbonate platform.

4.1 Introduction

This study aims reconstruct the architecture of the carbonate platform of Lastoni di Formin, a beautifully exposed Cassian carbonate buildup of the Italian Dolomites. The research was carried out integrating extensive field studies with the advantages of the Digital Outcrop Modeling techniques. Differently from modern carbonate platforms, the peculiarity of the Middle Triassic carbonate edifices of the Italian South-Alpine domain is their prevailing microbial nature: the Dolomites are considered one of the best places to study typical examples of "microbial platforms", highly productive mud-mound factories that developed flat top and relatively steep slopes (Blendinger, 1994; Russo et al., 1997; Schlager, 2003; Schlager & Keim, 2009; Preto et al., 2017, Franceschi et al., 2020). Despite the scarcity of this particular type of buildups in the present-day marine environments, they were widespread during the Mesozoic, and currently constitute important hydrocarbon reservoirs all over the world. In the absence of a standardized facies model for this kind of platforms (Preto et al., 2017), particular attention is given to outcrop analogue studies, in order to unravel the geometries of subsurface bodies.

Moreover, this study aims to provide insights on the occurrence of compaction-driven syndepositional deformations affecting a prograding carbonate platform. Syndepositional deformation is considered an important feature of carbonate systems, controlling the variation of stratal geometry, platform architecture (Doglioni & Goldhammer, 1988; Saller 1996; Rusciadelli et al., 2007; Berra & Carminati, 2016; Nolting et.al., 2018) and synsedimentary fracturing. In particular, synsedimentary fractures play significant role in the migration of early diagenetic fluids, triggering karst development and enhance permeability (Kosa & Hunt, 2005; Frost & Kerans, 2009; Berra & Carminati, 2012). Early lithification is crucial for the development of these fractures, since it is responsible for brittle behavior shortly after deposition (Grammer et al., 1999; Frost & Kerans, 2010).

The structural analysis and the reconstruction of the platform architecture were highly improved by the analysis of detailed Digital Outcrop Models that were realized using unmanned aerial vehicles (drones) photogrammetry and Structure from Motion process (SfM) This technique allowed to acquire fundamental quantitative information along the vertical and inaccessible cliffs of the Lastoni di Formin, and to interpret the seismic-scale geometries of the outcrop. In recent years, digital photogrammetry has emerged as an important source of data in many fields of geosciences (Hodgetts et al., 2004; Burnham et al., 2018; Bistacchi et al., 2015; Casini et al., 2016; Cawood et al., 2017; Corradetti et al., 2017a; Menegoni et al., 2019), permitting the reconstruction of georeferenced high-resolution 3D surfaces, and avoiding the use the more expensive, complex and

time-consuming LiDAR acquisitions and processing (James and Robson, 2012). The use of drones allows remote or inaccessible portions of the outcrops to be reached (Sturzenegger et al., 2009; Menegoni et al., 2018) and, with respect to terrestrial Digital Photogrammetry, overcome limitations of structure exposure, giving the possibility to orthorectify images and observe structures without perspective distortion (Gattolin et al., 2015; Tavani et.al., 2016, Corradetti et.al., 2017b), and significantly reducing occlusions and vertical orientation biases.

4.2 Geological setting

The study site is the well exposed outcrop of *Lastoni di Formin*, located in the eastern Dolomites, in the central portion of the Italian Southern Alps (Fig. 4.1). The Dolomitic domain is a relatively coherent slab of upper crust that form a large pop-up syncline of Neogene age (Castellarin, 1979; Doglioni & Castellarin, 1985; Doglioni & Bosellini, 1987; Bosellini et al., 2003) that is limited to the south by the Valsugana overthrust and to the north by its antithetic Funes-Passo delle Erbe line (Doglioni, 1987). This domain exhibits a spectacular sequence of Permian to Cretaceous rocks, including several generations of different Triassic carbonate platforms: the incredible preservation of the platform-to-basin depositional geometries, due to the relatively slight alpine deformation, has made the Dolomites a very attractive area for researchers in carbonate geology (e.g. Kenter, 1990; Schlager & Keim, 2009; Stefani et al., 2010). The relief of *Lastoni di Formin* appears as a wide isolated plateau, extended for over 2 km^2, gently dipping toward N/NE and bordered to west and south by vertical cliffs up to 250- 300 m high (Fig. 4.2). This outcrop represents the easternmost part of a broader carbonate system that extended approximatively E-W, including the outcrops of Sass de Stria, Col Gallina and Nuvolau-Averau (Leonardi, 1968; Bosellini et al., 1982; Blendinger & Blendinger, 1989). These buildups belong to the so-called Cassian platforms (Assereto et al., 1977; Neri et al., 2007), a generation of carbonate edifices that develop from Late Ladinian to Carnian, recording the first recovery of carbonate production after the fading of the Middle - Triassic magmatic event (Bosellini et al., 2003; Stefani et al., 2004) and the demise of the pre-volcanic Late Anisian - Ladinian buidups (Sciliar Fm.). The nature of the Cassian platforms has been a matter of debate for a long time: their pervasive dolomitization often obliterates the original texture of the rock, and the reconstruction of the biota is largely based on studies of isolated and undolomitized olistholites (Cipit boulders), and swarms of carbonate material embedded in the coeval basinal sediments of the san Cassiano Formation (Russo et al., 1997). In general, the origin of the dolomite is an open question in carbonate sedimentology (McKenzie & Vasconcelos, 2009):

the presence of different generation of Triassic carbonates, with various grades of dolomitization, has made the Dolomites region suitable for this kind of studies.

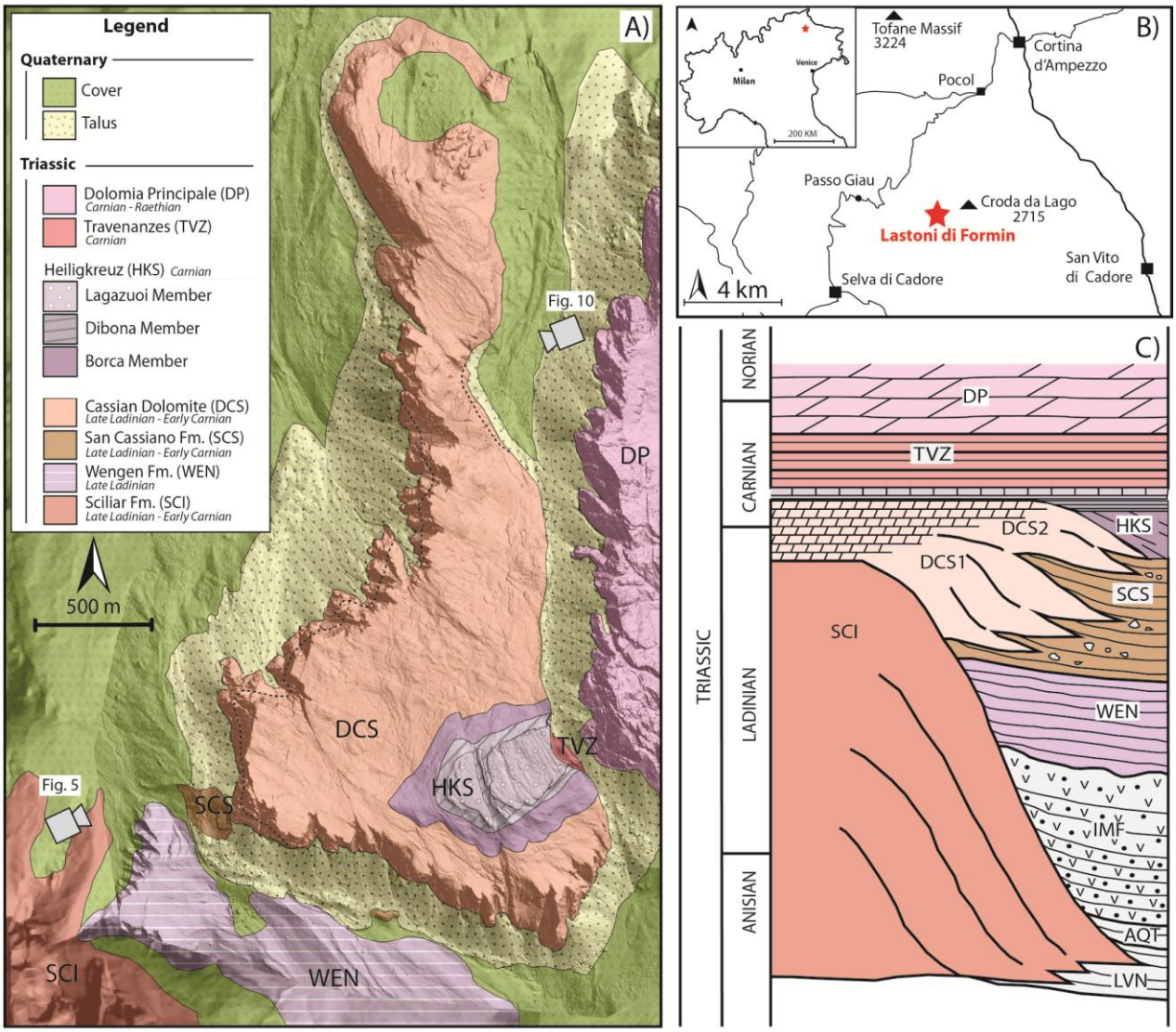

Fig. 4.1 A) Geological map of the Lastoni di Formin area (modified from Neri et.al., 2007) where the viewpoints of Figs. 5 and 6 are shown. B) Location map of the study site. The red star indicates the position of the Lastoni outcrop. C) Stratigraphic sketch of the middle/upper Triassic in central-eastern Dolomites (modified from Neri et al., 2007).

Nevertheless, a general model of dolomitization that can be applied to a wide spectrum of platforms has yet to be established. The Anisian-Ladinian pre-volcanic platforms (Sciliar platform, Latemar platform and the older nucleus of Sella) are generally assumed to be dolomitized by secondary replacement (Wilson et al., 1990, Stefani et al., 2010; Ferry et al., 2011; Jaquemyn et al., 2014), whereas studies on the Pale di San Lucano (Sciliar fm.) suggested that the dolomitization derives from recrystallization of a very high Mg-Calcite (Blendiger et al., 2015). Moreover, the

Carnian/Norian Dolomia Principale is likely related to microbial activity and could be considered of primary origin (Mastandrea et al., 2006; McKenzie & Vasconcelos, 2009). Despite the several attempt to unravel the origin of dolomitization that have been carried out in the region, none of the models convincingly adapts to the case of Lastoni di Formin. The nature, timing and evolution of dolomitization of the Cassian platforms has yet to be explained, and only few studies report these buildups as affected by extensive and pervasive dolomitization (Keim & Schlager, 1999; Antonellini & Mollema, 2000; Russo et al., 1997). However, some well preserved primary textures have been recognized also within dolomitized Cassian platforms (i.e. Sella massif): quantitative compositional analysis carried out on these outcrops by Keim & Schlager (1999, 2001), together with the studies of Russo (1997) on the cipit boulders derived from the Sassolungo massif, revealed the mud-mound nature of the Cassian carbonate factories of the dolomites: the main component of these buildups is fine-grained carbonate muds that mainly precipitate in situ (automicrite), and abiotic marine cements (Keim & Schlager, 1999).

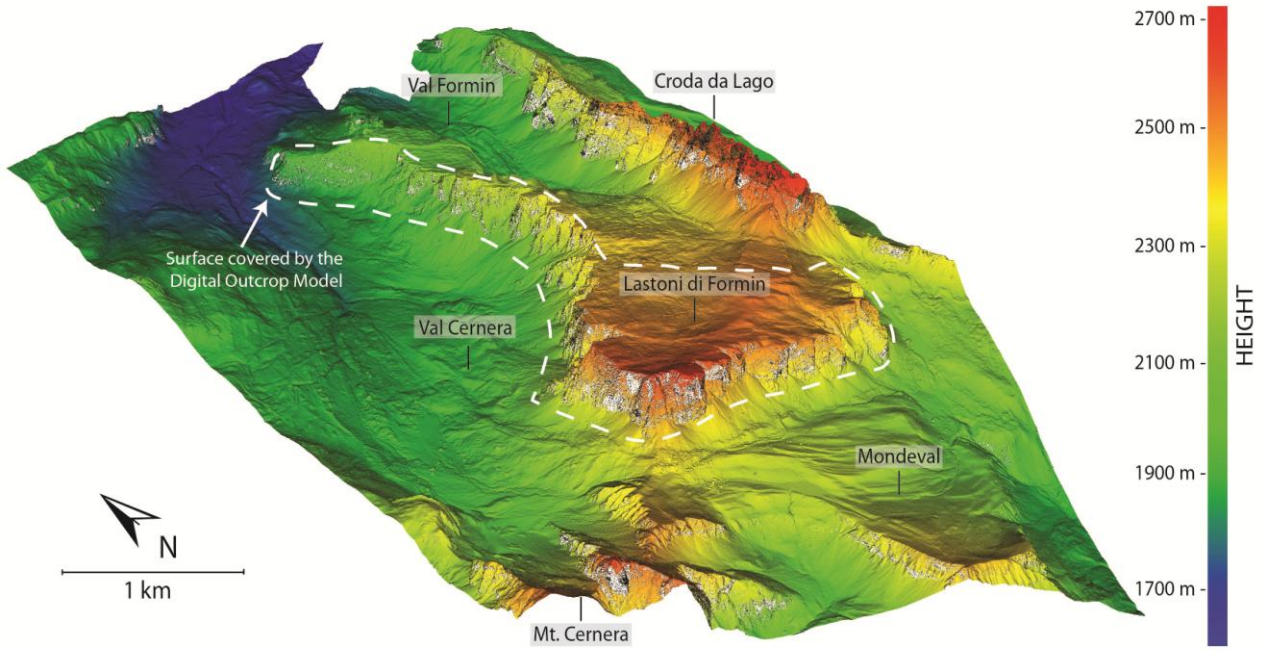

Fig. 4.2 DTM (1 m of resolution) of the Lastoni area, derived from aerial LIDAR. The main reliefs and valleys are represented. The Lastoni di Formin outcrop forms a wide plateau gently dipping toward NE that rises about 400 meters above the surrounding areas. Data from Ministero dell'Ambiente: Geoportale Nazionale, 2019.

In this type of buildups skeletal carbonate may occur, but it is not characteristic (Schlager, 2003). Furthermore, the estimated facies composition of the Sella platform revealed that the presence of automicrite is not limited to the top of the platform, but is extended to the margin and the slope

(Keim & Schlager, 2001). The association of automicrite, micro-organisms and marine cement helps to create a rigid framework that underwent early diagenesis, shortly upon formation (Russo et al., 1997; Keim & Schlager, 1999). Notwithstanding the dominance of mud-mound production mode during the whole Triassic of the Dolomites), the Cassian buildups form platforms, with flat and wave-swept tops and relatively steep slopes, that can reach an inclination of 30°-35° (Kenter, 1990). According to the model of Bosellini & Rossi (1974), the generation of post-volcanic platforms is coeval with the deposition of the basinal San Cassiano Formation, that consist of shales and marls alternating with volcanoclastic materials and gravity-displaced swarms of oolitic-bioclastic calcarenites, derived from the upper part of the platforms. In the central and eastern Dolomites, two generations of Cassian buildups have been mapped (Cassian I and II), separated by a break of the progradation, marked by the onlap of the basinal beds onto the Cassian slopes (Richtofen riff, Lagazuoi - Col dei Bos) (De Zanche, 1993; Gianolla et al., 1998; Neri et al., 2007; Trombetta, 2016).

4.3 Methods

4.3.1 Photogrammetric acquisition

The photogrammetric acquisition was performed using an Unmanned Aerial Vehicle (UAV) type DJI Matrice 200 quadcopter, equipped with a 20 Megapixel Zenmuse X4S camera. The technical features of the UAV platform and camera are reported in Table 1.

***Table 1**: camera and drone specifications*

UAV platform specifications					
UAV type	Dimension	Engines	Rotor Diameter	Empty weight	Payload
X-shaped quadcopter	89 x 88 x 38 cm	4 brushless	381 mm	3.8 kg	6.2 kg
On-board camera specifications					
Camera	Sensor type	Sensor size	Image size	Pixel size	Focal length
Zenmuse X4S	CMOS	12.8 × 9.6 mm	5472 × 3648 px	2.3 x 2.3 µm	8.8 mm

16 drone flights with four different take-off positions were carried out: three were located at the base of the rock walls and one on the summit plateau.

During the flights, 12000 images were acquired with an orientation of the camera that was mostly orthogonal to the outcrop surface (horizontal for the cliffs and nadiral for the plateau), and an overlap and a sidelap of the images greater than 90%, covering a total surface of ca. 2.2 km^2. The camera-outcrop distance was maintained around 200 m for the entire survey, even if it may have varied within ±100 meters due to the shape of the outcrop, such as near edges or recesses of rock walls. According to Birch (2006), the image resolution was therefore generally around 5 cm/pixel (camera-outcrop distance ~ 200 m) and can vary from 2.7 to 7.9 cm/pixel (camera-outcrop distance from 100 - 300 m). Few high-resolution (0.7 cm/pixel) models were realized along some specific outcrops by acquisition flights very close to the rock walls. Due to the presence of on-board GNSS-IMU instrumentation (e.g. GPS, compass, gyroscope, accelerometer) it was possible to record the position and orientation of the photographs. The photogrammetric acquisition was preceded by the measurement of 22 Ground Control Points (GCPs). The survey was conducted with a differential Real Time Kinematic (RTK) GPS (type Topcon Hiper Pro), that has a theoretical accuracy of 0.01 m and 0.015 m for horizontal and vertical measurements, respectively. The positions of the GCPs were previously decided on the base of aerial photos, and highlighted with a series of visible colored targets distributed along the outcrop.

4.3.2 *Image Processing, Digital Outcrop Model (DOM) development and accuracy assessment*

The dataset was pre-managed, removing blurry and unwanted images (<100 photos), and then processed using the *Photoscan* software (Agisoft). Differently from traditional photogrammetric methods, in the Structure from Motion (SfM) approach, used by *Photoscan*, the camera position and orientation are determined by the identification and matching of common features in multiple overlapping images, using the scale-invariant feature transform algorithm (Lowe, 1999; Lowe, 2004). Subsequently, the orientation and position of the images and the 3D Digital Outcrop Model (DOM) were calculated through the bundle adjustment process (Triggs et al., 2000; Westoby et al., 2012). The Photoscan workflow that was used to generate the DOM can be summarized in four stages: 1) image matching, bundle block adjustment, and generation of sparse Point Cloud (PC); 2) dense PC generation; 3) mesh generation; 4) texture generation (Fig.4.3). The parameters used during the processing are indicated in Table 2.

***Table 2**. Processing parameters used in Photoscan software*

Process	**Processing parameters**		
Image alignment and sparse point cloud generation	**Accuracy**	**Tie Point**	**Key Point**
	High	40000	100000
Dense point cloud generation	**Quality**	**Depth filtering**	
	High	Mild	
Mesh generation	**Source data**	**Surface type**	**Face count**
	Dense cloud	Arbitrary	High
Texture generation	**Mapping mode**	**Blending mode**	
	Generic	Mosaic	

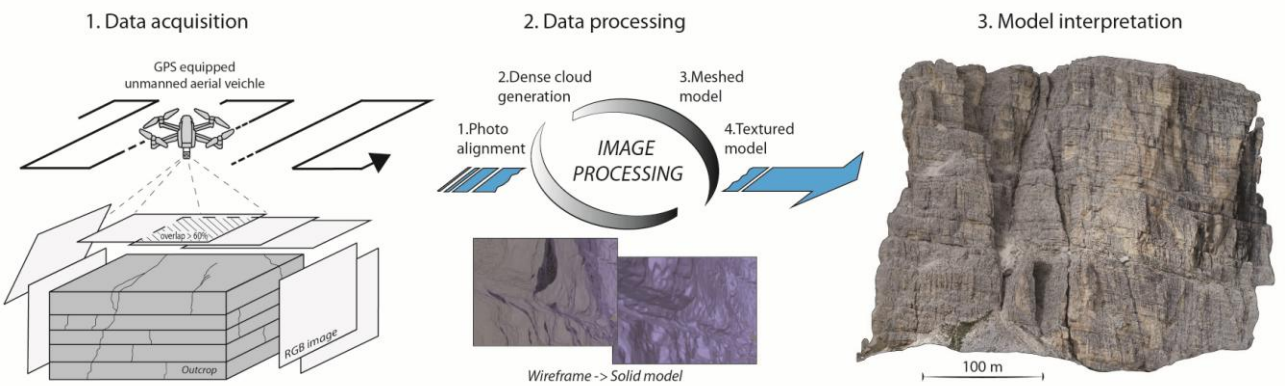

Fig. 4.3. Schematic workflow followed for the generation of the Digital Outcrop Model. The images were acquired by an Unmanned Aerial Vehicle (UAV), equipped with a 20 Megapixel camera and GNSS-IMU instrumentation (GPS, compass, gyroscope and accelerometer). The image processing was performed using the software Agisoft Photoscan (the main stages of processing are summarized in the image). The resulting textured Digital Outcrop Model (DOM) was then interpreted and sampled using CloudCompare software.

The DOM was georeferenced in WGS84 / UTM 33N coordinate system using both the position of the images registered by UAV on-board, and the position of the GCPs measured in the field with the differential RTK GPS. The absolute accuracy of the DOM was calculated as the difference between the real position of the GCPs and their position detected on the DOM (Fig.4.4). The mean absolute accuracy is about 120 cm and 72 cm for the planar and the vertical positioning, respectively. The relative accuracy of the DOM was determined by calculating the difference in orientation and length between the vectors that join all the 22 measured GCPs (231 pairs) and the corresponding points identified on the DOM (Chesley et al., 2017). The analysis of the relative accuracy reveals a mean error <1° in orientation and of 0.17% in length: these values are considered

acceptable with respect to the scale and the purpose of the work, as they fall within the range of error of the manual compass-clinometer measurements (~2°, Jordà Bordehore et al., 2017; Cawood et al., 2017; Menegoni et al., 2019).

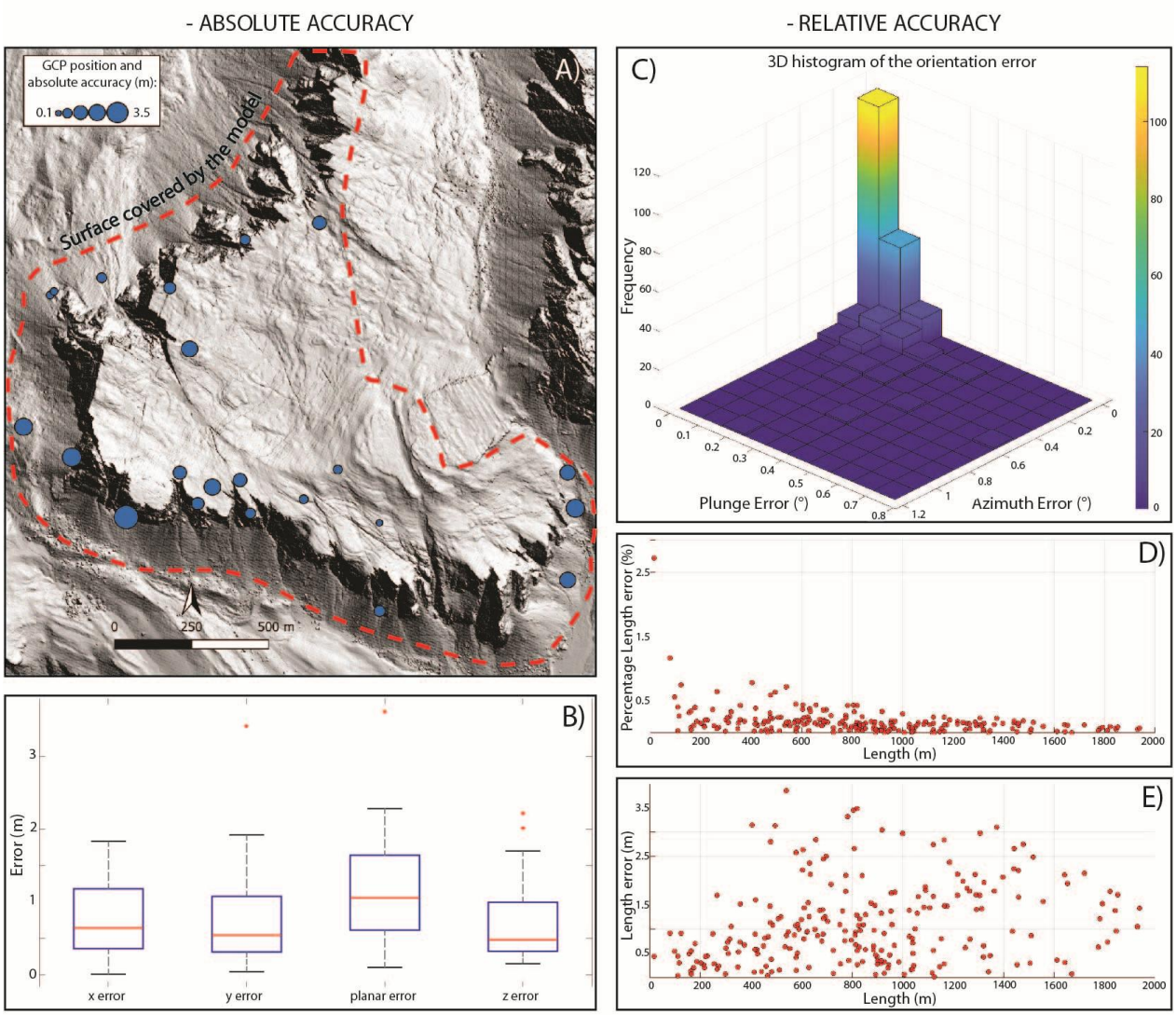

Fig.4.4. A) Position and absolute accuracy of the 22 Ground Control Points (GCPs) measured along the outcrop. B) Absolute error between the GCPs and the correspondent points of the model. C) Frequency distribution of the orientation errors (difference in azimuth and plunge between the vectors that join all the 22 measured GCPs and the corresponding points identified on the DOM). (D) Percentage and E) metric length errors (231 bins) of the same vectors.

4.3.3 Digital Outcrop Model analysis

The resulting point clouds and texturized models (Fig. 4.5A) were analyzed and interpreted in a 3D environment by the use of the CloudCompare software and a 3D Pluraview UHD stereoscopic hardware. The first steps of the DOM analysis and interpretation were the carbonate facies location

and the 3D line drawing. Both manual (by the Trace Polyline tool) and semi-automatic (by the qCompass plugin - Thiele et al., 2018) methods, that are embedded in the CloudCompare software, were used to trace the strata surfaces and measure the local bedding orientation and the real thickness of the strata (distance between two strata along the normal vector to the bedding best-fit plane). Successively, all the deformation structures (e.g. faults, joints and folds) were manually mapped and measured on the DOM, along the walls and the top of the plateau, and their mean orientation (dip direction and dip) was calculated as the best-fit plane. Curved faults and joints were measured in different sectors and their mean orientationwas evaluated. The most detailed sedimentological and structural analyses were carried out on the higher resolution DOMs. However, the general centimeter resolution of the models proved to be largely sufficient to ensure a good definition of the characteristics of the carbonate platform.

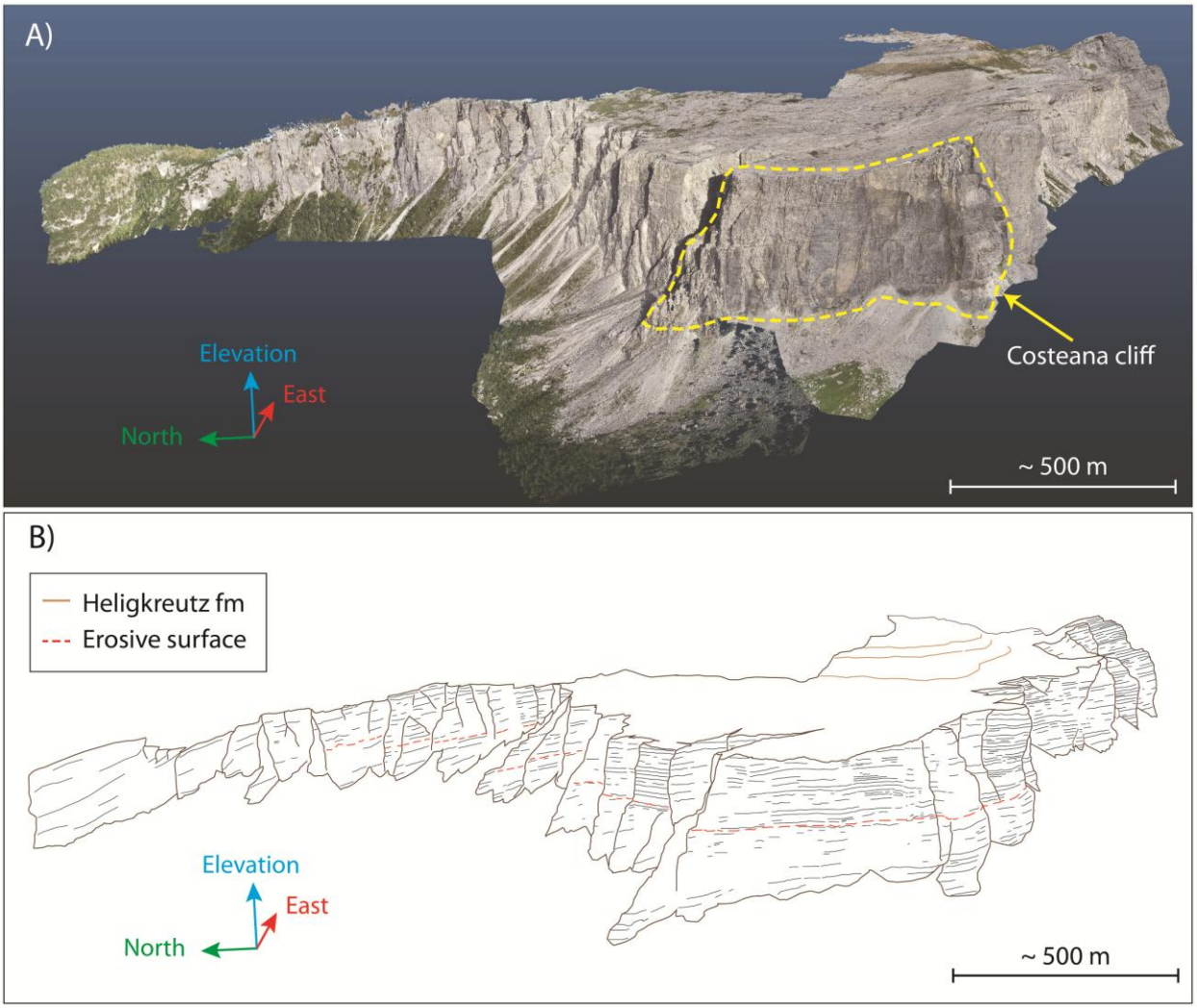

Fig.4.5. A) Overall perspective view of the final texturized Digital Outcrop Model (DOM), resulting from Photoscan image processing (DOM mean resolution ~ 5 cm/pixel along the vertical cliffs and ~ 7 cm/pixel in the summit plateau); B) line drawing obtained by the interpretation of the DOM: the 3D nature of the model

reduces the limitations of unfavorable exposures and perspective distortions and allows the correct measurements of the bedding. The image viewpoint is shown in Fig. 1.

4.4 Results

4.4.1 Platform facies distribution

The platform is subdivided into two overlapping parts by a marked morphological ledge that cross parallel to the bedding of the entire western and southern cliffs. The ledge is well exposed along the south-west edge of the outcrop (above Forcella Giau) where it is outlined by a ~ 3m thick layer of soil and detritus. The surface connected to this ledge presents slight but clear evidences of erosion observable from the DOM and is probably associated to a time gap in carbonate production during the platform growth (Fig.4.6). Based on this evidence, the carbonate body has been subdivided into an upper and a lower unit.

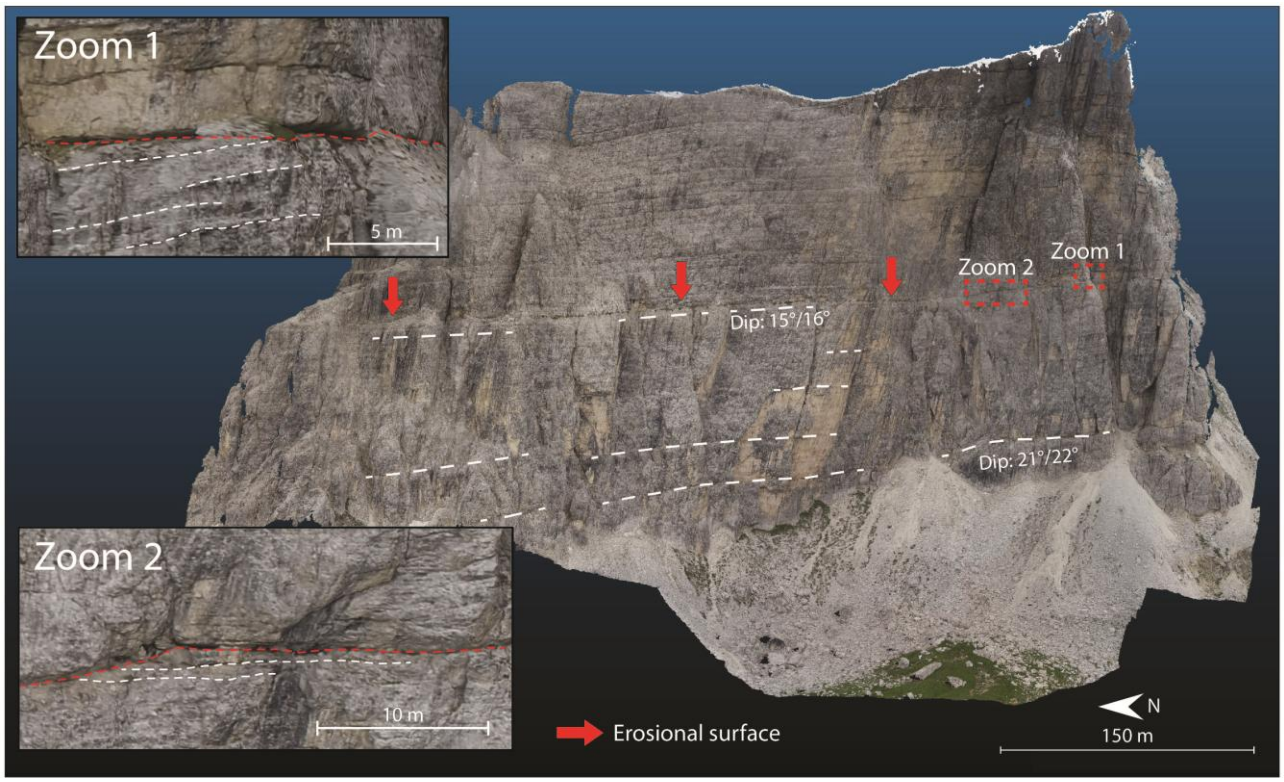

Fig.4.6. DOM image of the Costeana cliff (western portion of the outcrop): the ledge that crosses horizontally the carbonate body is indicated by the red arrows. Slight evidence of its erosive nature is shown in the Zoom 1 and Zoom 2 windows. The ledge divides the platform in two portions (Cassian I and II), with the upper part (Cassian II) that displays a more regular and marked cyclicity. This surface is probably connected to a time gap in carbonate production during the platform growth.

The upper unit is markedly stratified and displays a regular, plane-parallel layering with a spacing of ~ 7-9 m. The organization of this unit in peritidal cycles is clearly visible from the model, especially along the south wall (Fig.4.7). The field characterization of this unit has highlighted the extensive dolomitization that affects the platform, and often totally obliterates the original depositional fabric, the sedimentary structures and the fossil content. Samples of Cassian dolomite are mainly composed by fine grained greyish and whitish dolomite with sucrose texture.

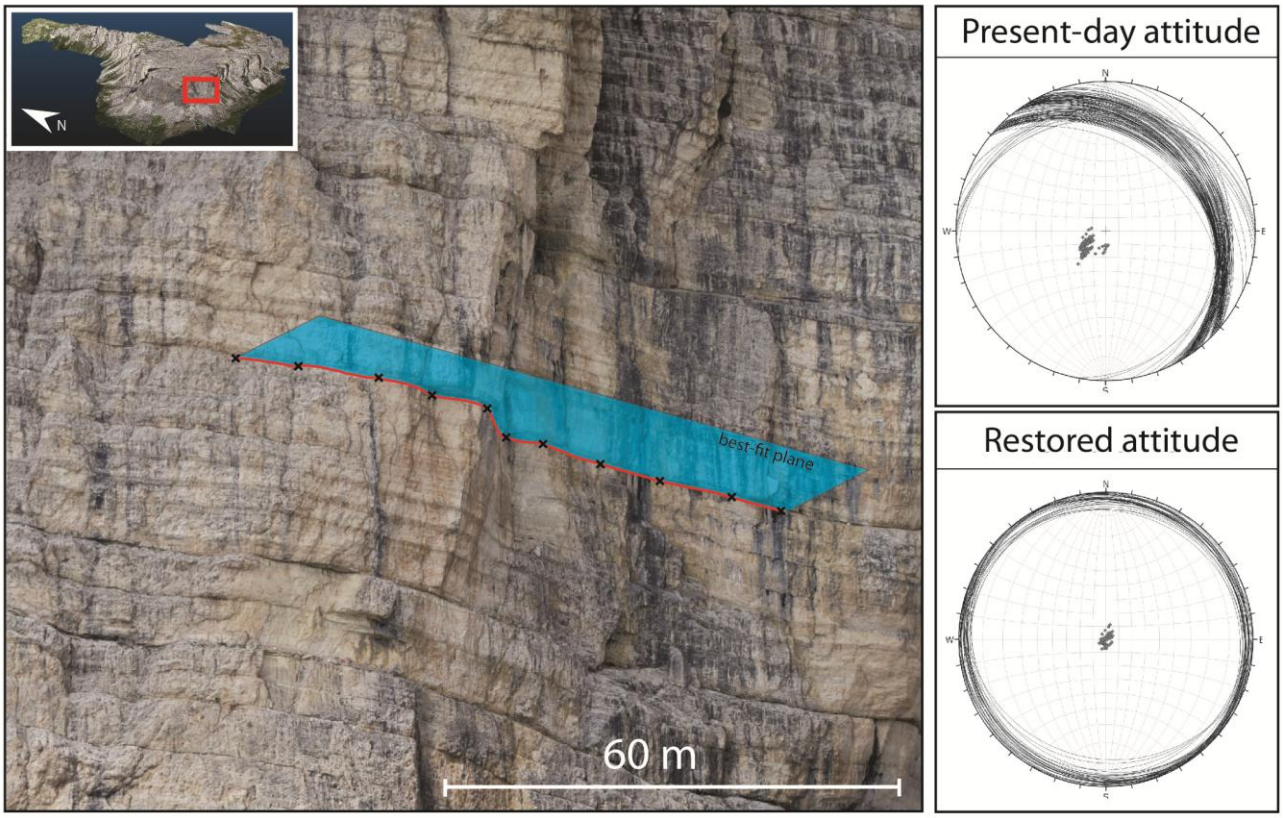

Fig.4.7. Details of the peritidal cycles visible in the upper unit (Cassian II) from the Digital Outcrop Model (southern part of the outcrop). The attitudes of the layers were collected by measuring the planes that best fit the 3D traces of the bedding.

The lower part of the unit presents multi-meters thick plane-parallel banks with rare ghosts of macrofossils (bivalves, gastropods). Toward the top, the layers thin and become sub-metric, and pisoids, stromatolites and occasional mud-mounds are visible; sedimentary structures are poorly preserved, but large tepee and locally cross-laminations are observable (Fig. 4.8 C). This unit corresponds to the inner platform facies of the Cassian platforms described by Neri et al. (2007), and formerly included in the Dürrenstein dolomite (sensu Bosellini, 1984). The sharp, upper limit with the overlying Heiligkreuz formation is characterized by an abrupt morphological and lithological change, that marks the demise of the carbonate platform and the onset of the

Heiligkreutz Fm (Neri et al., 2007; Breda et al., 2009; Gattolin et al., 2013). In the field, this surface is highlighted locally by pervasive paleokarst and paleosoil levels, that testify to subaerial exposure.

Fig.4.8. A, B) Dolomitized corals; C) metric-scale tepee structures at the platform top, testifying subaerial exposure episodes; D) massive clinoforms interdigitated with the basinal San Cassiano formation and visible at the base of the rock walls of the Forcella Giau (southern sector of the outcrop The low degree of dolomitization of the lower body allows the recognition of the original megabreccia fabric; E) detail of the bioclastic turbidites constituting the San Cassiano formation.

Thick clinoforms were mapped in the northern part (Val Formin and Muraglia di Giau sections, Fig. 4.9), where they are connected to the inner platform facies of the upper unit by a massive margin. Locally, the original texture of the clinoforms, ranging from breccia to megabreccia, (with individual blocks larger than 1 m), is preserved; here, the stratal joints are irregular and undulate, conversely to the sharp ones of the inner platform facies.

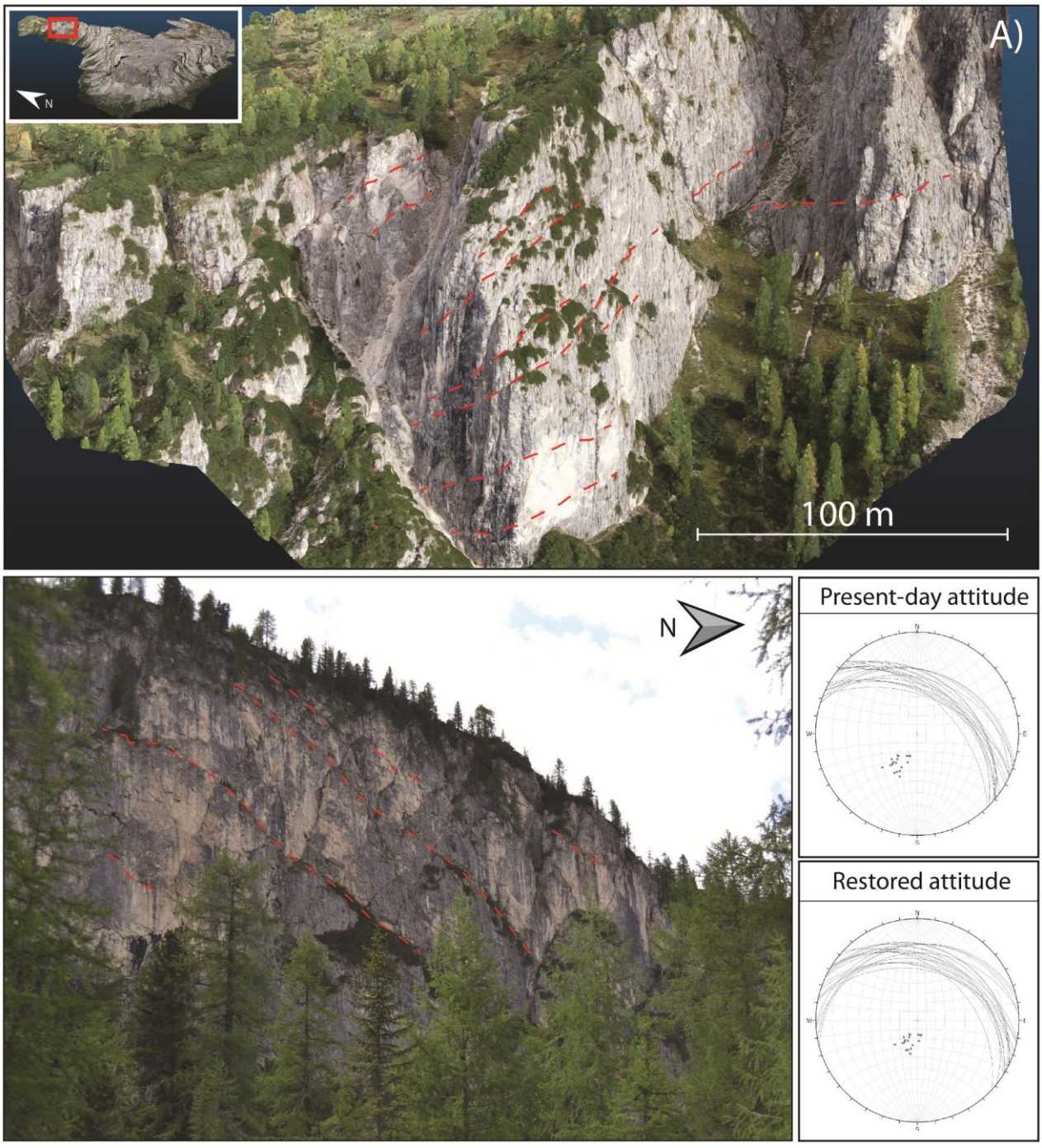

Fig.4.9. Massive clinoforms belonging to the upper unit (Cassian II) that are visible, in the 3D model (A) and in the field (B), near the northern part of the outcrop. The attitude measurements were restored at the original dipand indicate an average direction of progradation toward north/northeast.

The lower unit is mainly exposed along all the Western cliff of Lastoni. It has a generally less marked bedding, and at the base of the outcrop thick and massive strata, (partially buried by colluvial detritus) interpreted as clinoforms, have been mapped. The contact with the underlying basinal San Cassiano Fm. is visible at the south-west edge of the outcrop (Forcella Giau Section, Fig. 4.8D). The San Cassiano Fm. consists of an alternation of marls and pelites with swarms of oolitic/bioclastic calcarenites. Few decametric olistholites, embedded in fine grained basinal material, have partially escaped dolomitization, and exhibit a megabreccia fabric. The dip of the strata of the lower unit decreases upward (from 21°/22° at the base of the unit to 15°/16° at the top) and the topmost layers are nearly parallel to those of the upper unit (see Fig. 4.6). In the Val Formin both the upper and the lower units outcrop (Fig.10). The lower unit is dominated by clinoforms that reach an original dip of ~ 25/30°, and are topped by decimeter-thick planar stratified topset beds (Fig.4.11). In correspondence of the shelf break, few remnants of coral colonies have been found in life position (Fig.4.8 A and B): dolomitization does not allow the characterization of the entire facies belt of the margin, which appears massive. The topsets beds are surmounted by the thick banks of the upper unit.

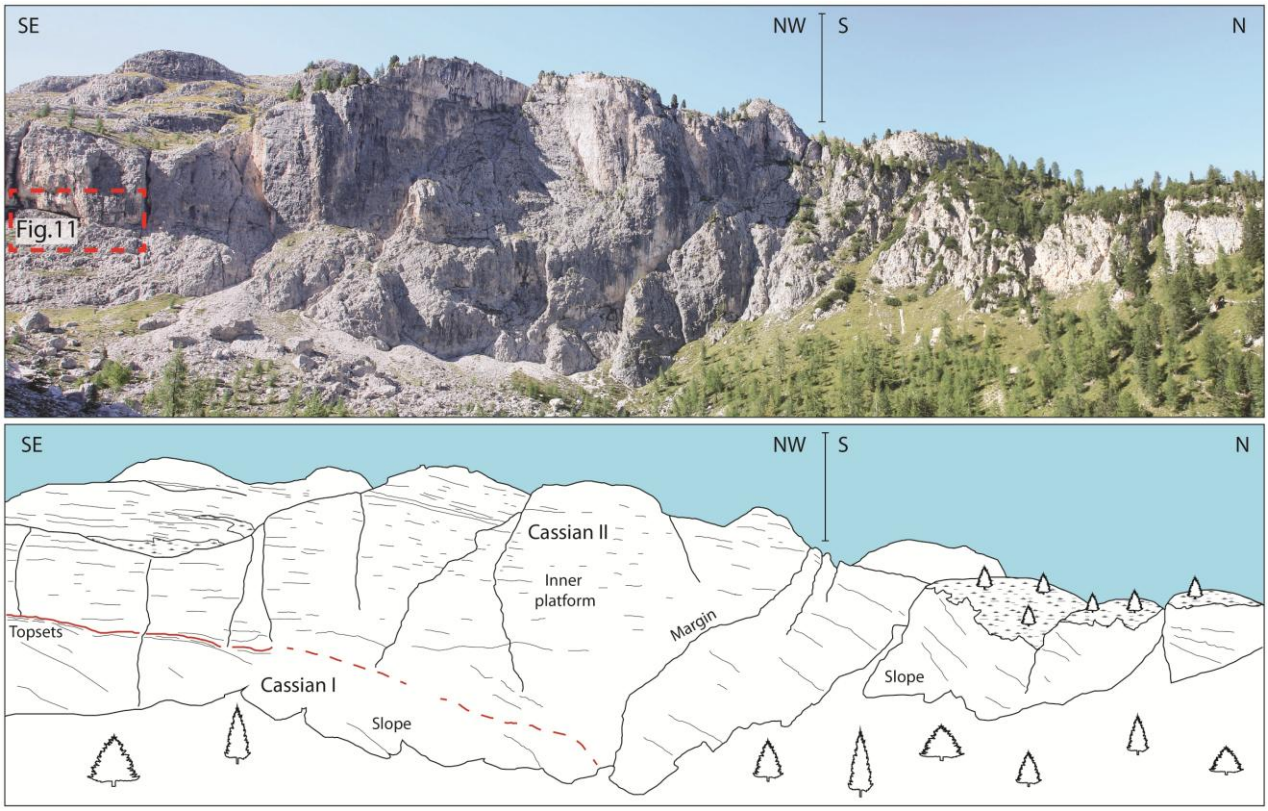

Fig.4.10. Interpretation of the Val Formin section, where the transition between inner platform and slope of the upper unit (Cassian I) is visible. Dolomitized coral colonies that may indicate the existence of a small,

bioconstructed reef rim have been found in proximity of the topset beds. The image viewpoint is shown in Fig. 4.1.

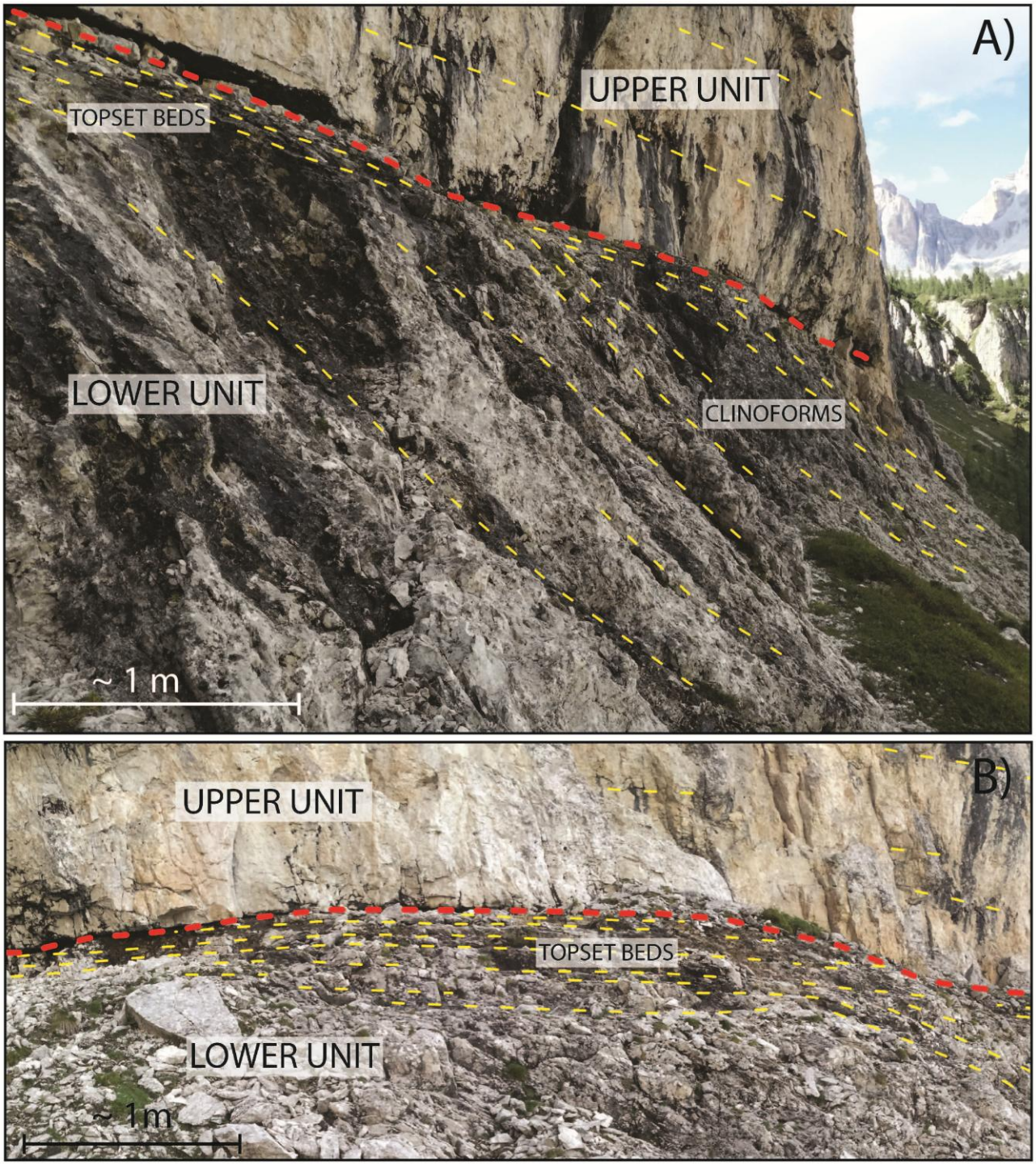

Fig. 4.11. Details of the transition between the lower and the upper unit visible in the field at the Val Formin section (Fig. 410). A) Steep clinoforms of the lower unit are topped by topset beds; B) the topset beds of the lower unit are cut by the erosional surface that marks the onset of the thick peritidal cycles of the upper unit.

4.4.2 Geometry of the platform

A line drawing was performed directly on the Digital Outcrop Model, and the geometries of the platform were interpreted in a 3D environment (Fig. 4.5B). The dimensions and the high resolution of the DOM allowed the correlation of single strata throughout all the perimeter of the outcrop. Furthermore, a detailed field mapping was carried out to support and integrate the DOM interpretation of the platform architecture. More than 150 beds of the upper unit were measured from the Digital Outcrop Model; presently, they dip on average towards north-east with an angle of about 15°; assuming the nearly horizontal deposition of peritidal cycles, this value can be considered the effect of tectonic tilting; possible variations within 5° are due to the adjustment of isolated blocks, or have been detected in proximity of the main faults: in any case, the presence of limited variation in the attitude of these strata does not affect the general interpretation of the buildup's architecture. The sharp, upper limit with the overlying Heiligkreuz formation was also traced on the model; it dips toward north-east of ~ 15/17° coherently with the general orientation of the platform. The measures obtained from the model, restored at the original attitude (dip equal to 0°) on the base of the present-day dip of the platform top, indicate a progradation toward NNE (see Figs. 4.7 and 4.9).

The dip of the inner platform beds of the upper unit were measured in five vertical sections, located at an increasing distance from the platform margin (Fig. 4.12A). The sections were selected to minimize tectonic geometric disturbance, such as tilting or block rotation induced by the presence of faults, and the measurements were corrected assuming that the uppermost layer of each section was horizontal at the time of deposition. The stratigraphic boundary between the Cassian platform and Heiligkreuz formation was assumed as reference horizontal layer. The results reported in the Fig. 4.12 show that in a vertical transect, in the innermost part of the platform, the bedding is essentially parallel; conversely, near the outer shelf, the strata display a flattening upward trend, with a relatively high difference in dip angle (Δ_{dip} ~ 8) from the lower to the upper layers. Moreover, the measurements of the thickness of the inner platform beds, along the western cliff of Lastoni outcrop (almost perpendicular to the direction of progradation), indicate a basinward thickening of the platform.

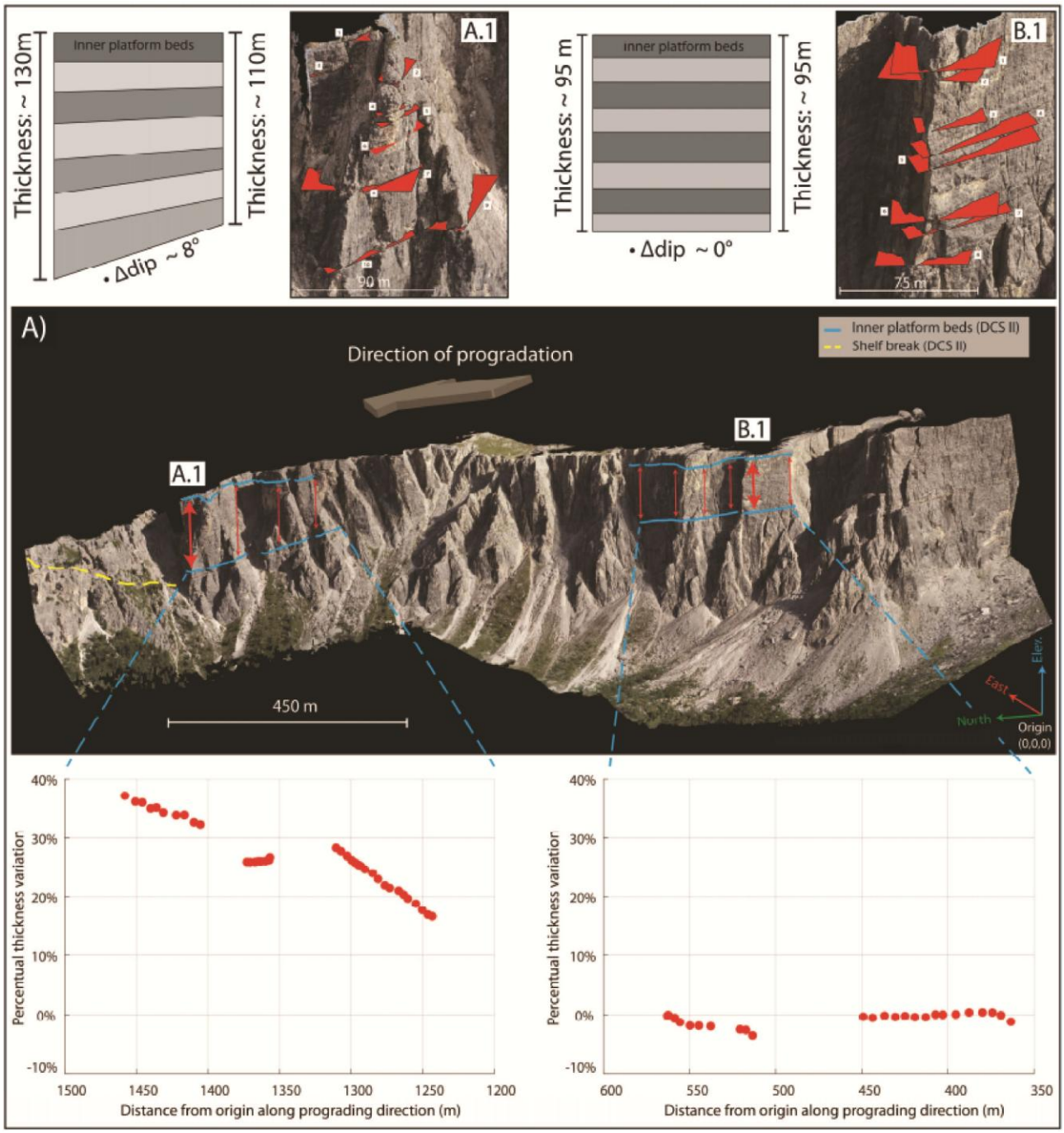

Fig.12. A) Digital Outcrop Model (DOM) of the western cliff of the Lastoni di Formin. The outcrop is nearly parallel to the direction of progradation of the platform. The windows A and B indicate the sections where thickness and dip of the inner platform beds of theupper unit have been measured. An upward flattening of the beds, with the older strata that are more inclined than the younger – and the thickening of the outermost part of the platform of about 20 % along a section of ~ 250 m have been ascertained. The possibility to gather 3D data was fundamental for the determination of the real stratigraphic thickness, because it can overcome bias due to unfavorable section exposures (apparent thickness).

4.4.3 Fractures (faults and joints)

Four main outcrop-scale fracture sets, formed by prevailing joints and some faults, were detected and measured both from orthoimages (Fig.4.13) and from the DOM (Fig. 4.14); they were grouped on the base of their mean directions: K1a - N110°, K1b - N125°, K2 - N160° and K3 - N15°. K1 includes both sub-vertical joints and normal faults. These faults are characterized by small, normal stratigraphic displacements and often present listric geometry, with branches and conjugate faults (synthetics and antithetic). The fractures of this set, that are sub-orthogonal to the bedding, extend for hundreds of meters and cut the entire outcrop: K1a and K1b intersect with a tight angle (<15°) and often show irregular or anastomosed geometry. K2 set represents ~ N160° trending normal and strike-slip faults and joints, dipping towards W generally with angles of about 80°. The main fault of this set dislocates both the Cassian platform and the overlying Heiligkreuz Fm (Fig.4.13). K3 is the less frequent set and it includes NNE-SSO trending sub-vertical joints and few probable strike-slip faults. The pervasive dolomitization and the weathering of the fault surfaces often mask any kinematic indicators: fault displacements were calculated from the digital model, measuring the orthogonal distance between correlated layers on the opposite side of the slip surface and generally are not greater than 1-2 meters.

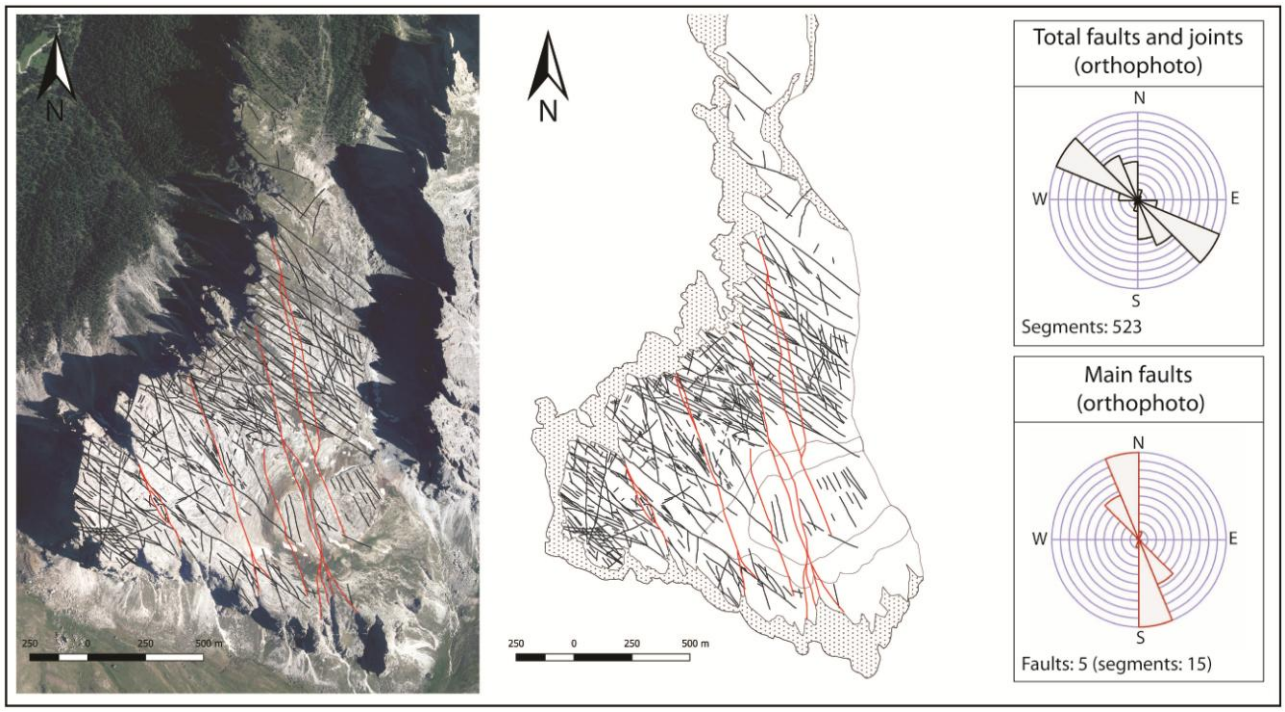

Fig.4.13. Direction of the main joints and faults of the Lastoni di Formin, mapped from the orthoimages.

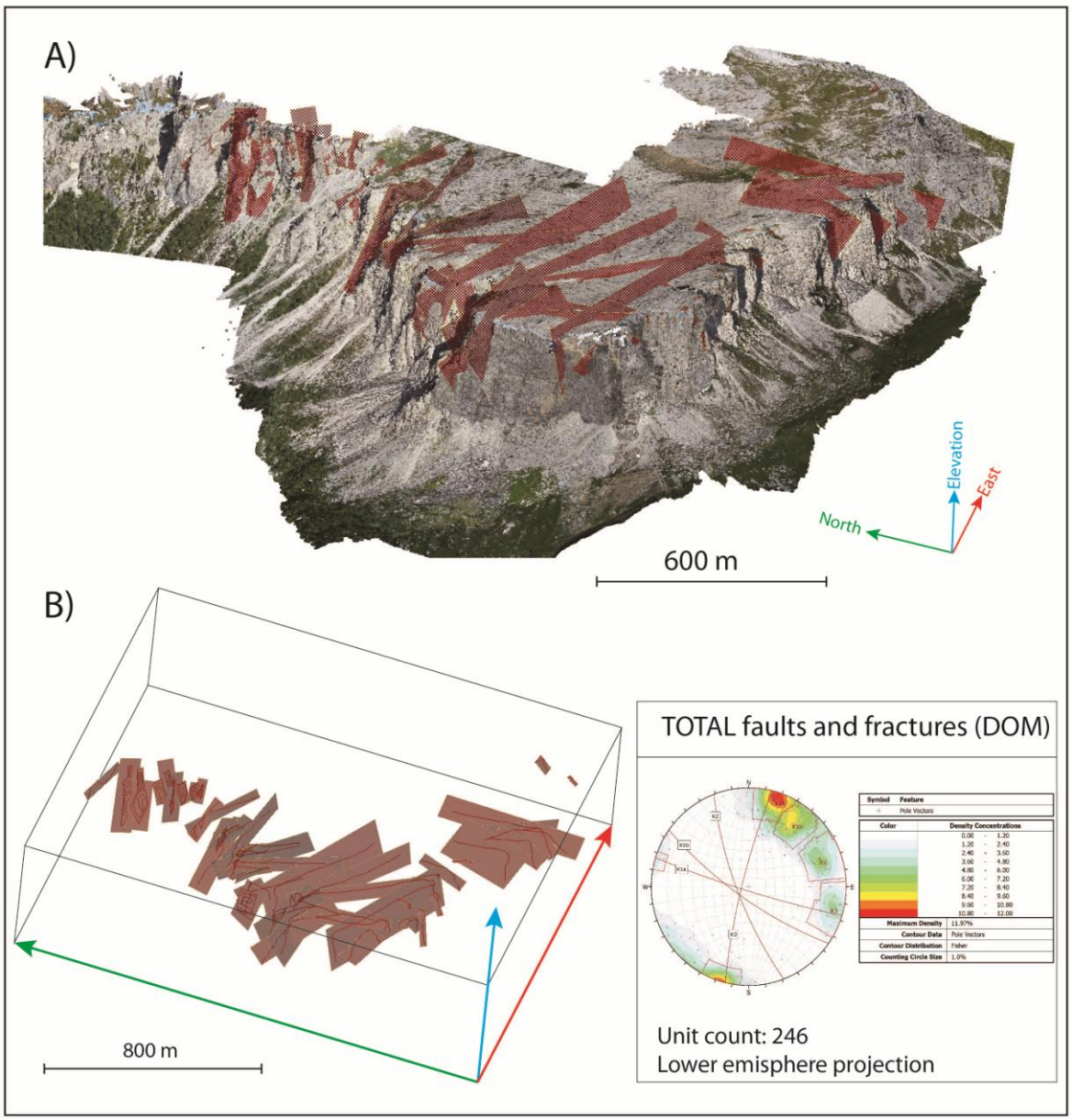

Fig.14. A) Principal faults and joints mapped in the Digital Outcrop Model. The 3D geometry of the outcrop, with a large plateau bordered by vertical walls, favored the collection of reliable measurements of the structures on the 3D model. B) The best fit planes of the polylines were automatically calculated and sampled in a 3D environment and allowed to define the mean dip and dip direction of each structure.

The analysis of the intersections between the different sets of fractures was performed essentially on the top of the platform, analyzing only the joint network and excluding the faults detected by the DOM analysis. The results are synthesized in Fig. 4.15 and indicate a certain predominance (59%) of the I terminations (isolated inside the rock matrix), while the X (crossing joints) and the Y (where a joint ends against another joint) intersections are the 22% and 19%, respectively. The study of the Y intersections shows that the set K1 is probably the oldest because both the largest part of the joints K2 and practically all the fractures K3 end against joints K1 (Fig.14 C,D).

However, these observations should be considered only as indicative because many joints show subsequent reactivations during the different tectonic phases that affected the study area.

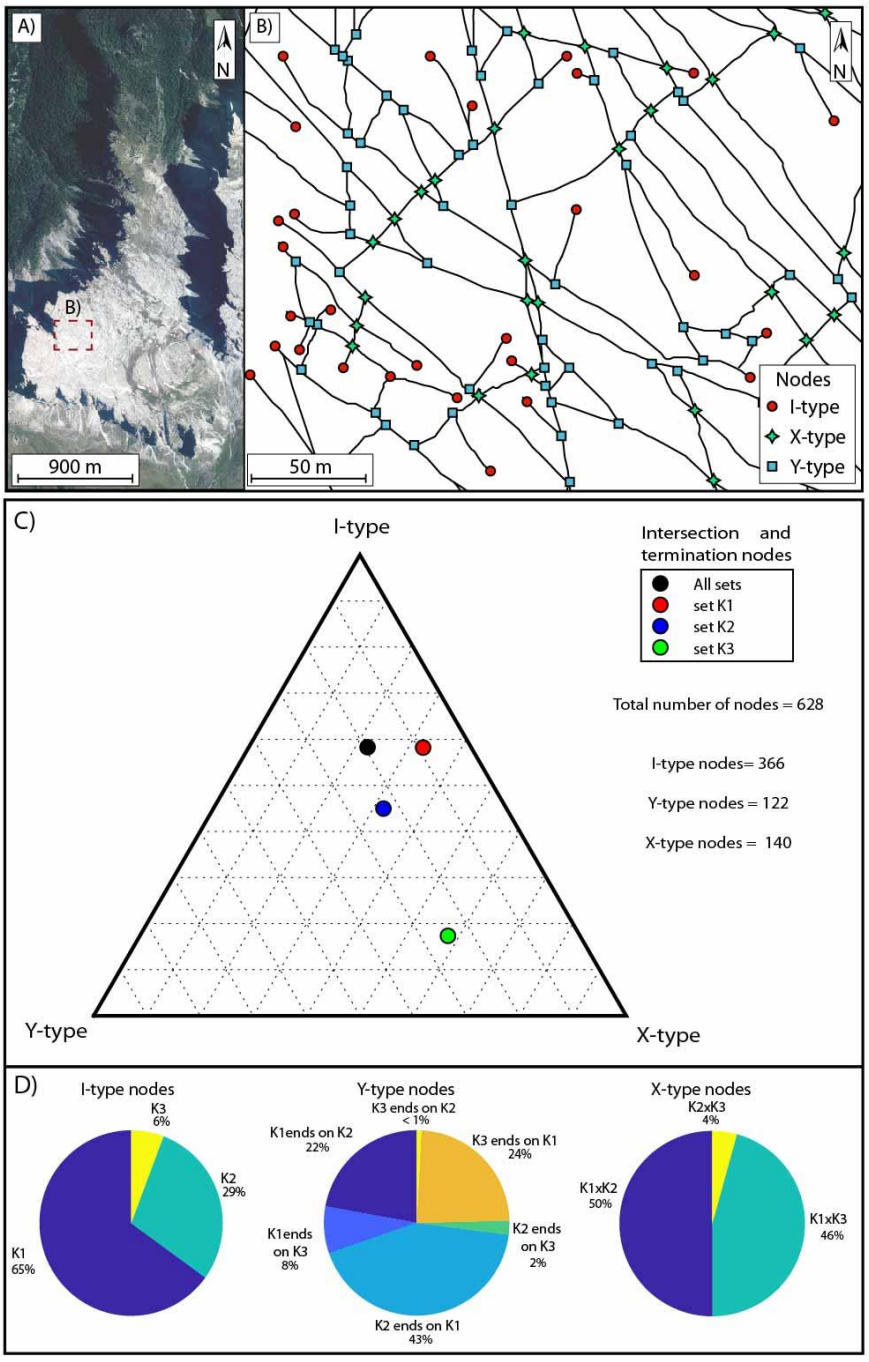

Fig. 4.15 A) Example of the analysis of the joint network relationships performed on DOMs. The square indicates the area of fig. B. B) Detail of the intersection and termination nodes locally detected. The joints of sets K1, K2 and K3 have a direction NW-SE, NNW-SSE and NNE-SSW, respectively. The nodes formed by joints belonging to the same set were not considered. C) Ternary plot of the proportion of node types of the three sets of joints and D) pie charts illustrating the classification of the different kinds of the intersection and termination nodes.

4.4.4 Early fractures

Some joints and faults belonging to set K1 display features that are typical for syndepositional deformation. The best evidences for their possible early origin are the disturbances that the bedding undergoes along some joints and faults that have been detected by the DOM analysis (Fig.4.16).

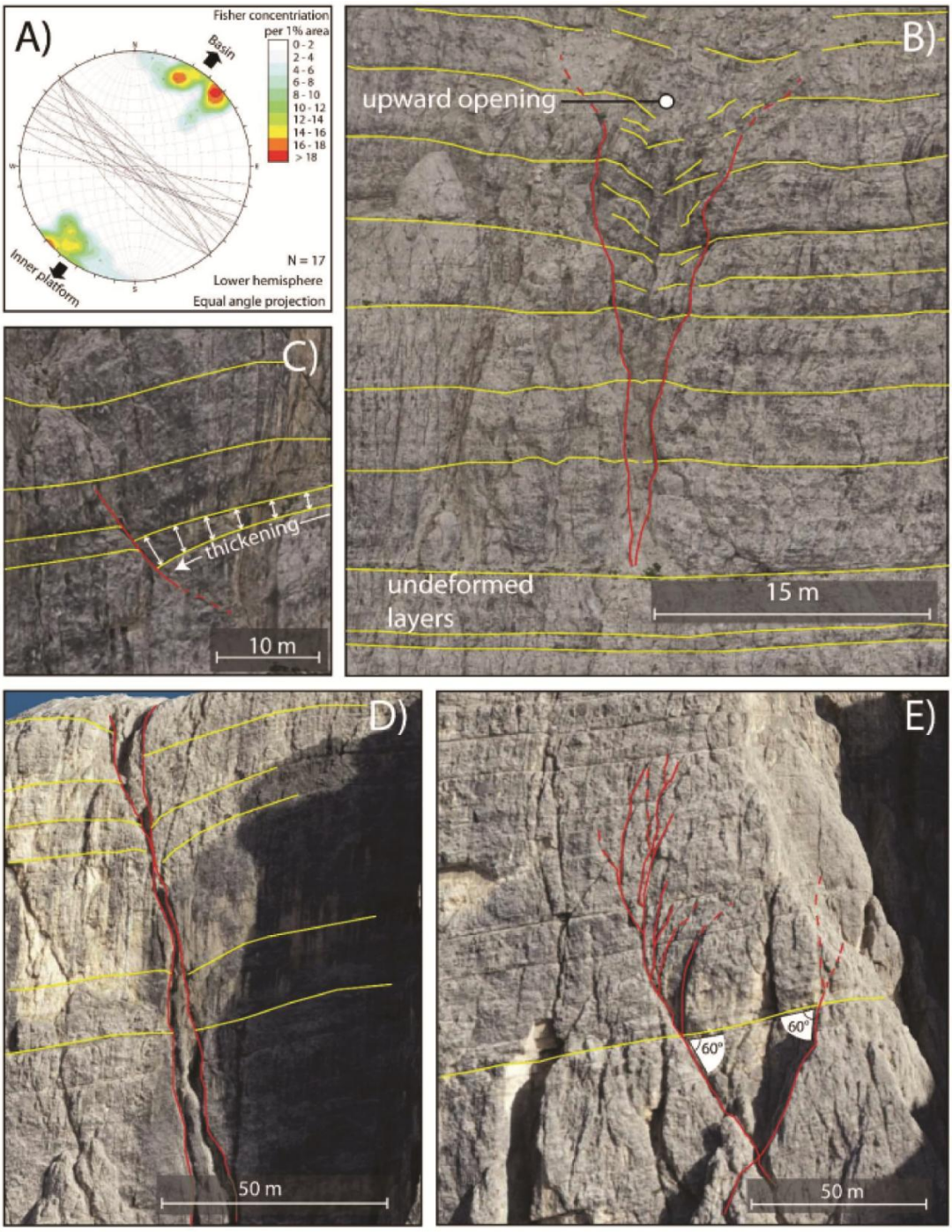

Fig.4.16. Examples of syndepositional extensional structures in the outcrop of Lastoni di Formin analyzed on the DOM. A) The azimuth of these structures is nearly orthogonal to the direction of progradation of the platform and they are also sub-orthogonal to the bedding. B) Upward-opening extensional fracture

developed in the inner platform that caused a perturbation of the tidal cycles. C) Small normal fault with synsedimentary thickening of the hanging-wall strata (grow fault); upwards the layers return undisturbed. D) Vertical extensional fracture with irregular geometry and non-matching walls. The strata on the right side display a progressive tilting toward the fracture. E) Incipient extensional structure, orthogonal to bedding (nearly Andersonian), with splays, that probably predate the tilting of the sequence.

In particular, the following structures have been identified: growth faults along which strata of the hanging wall show a clear thickening (Fig.16 C) and non-matching margins (Fig. 16D); opening upward joints that induced sinsedimentary deformations (tilting and folding of the bedding) (Fig. 4.16B); faults that clearly terminate upward against younger strata (Figs. 4.16C and E) or whose displacement progressively decreases upwards, moreover in some cases, fault tips are in correspondence with the perturbation of the overlying beds. These fault synsedimentary terminations are detectable only along the exposed walls by the DOM analysis. These early structures are small normal faults or opening mode joints with a sinuous to irregular geometry are sub-orthogonal to the bedding and generally display irregular and non-matching walls; some joints display downward tapering and opening at the top. In a few cases they break out the top of the platform, where can be observed at different scales, with an extension ranging from ten to hundreds of meters and aperture generally > 1 meter, to an extension from centimeters to a few meters, and apertures of about 5 - 10 cm. (Fig. 4. 17A and B).

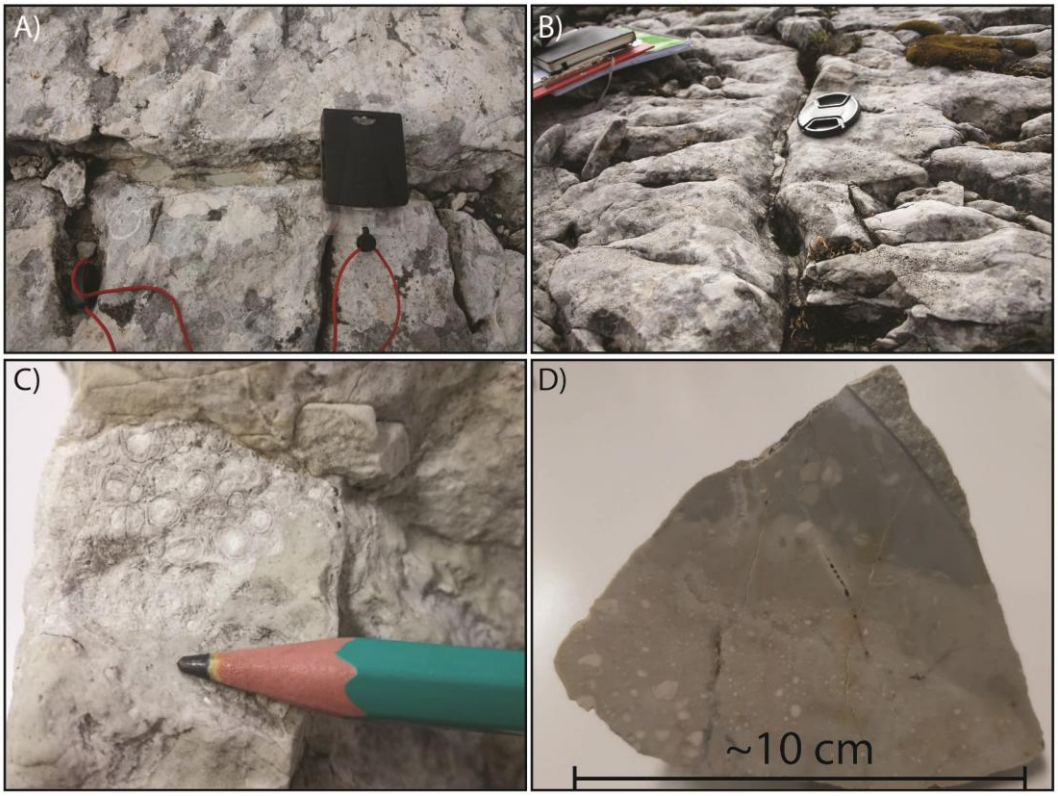

Fig.5.17. A and B) examples of neptunian dykes filledby platform derived materials visible on the top of the buildup. These fractures have a cm-scale opening and irregular and karsified margins. The sediment that infill these structures is mainly composed by a greenish marly limestone. C) Sample of the fracture fills The presence of undolomitized allochems (pisoids) of platform-derived origin in the fractures may indicate that these structures were already open during the platform growth, giving a good constrain on their early origin. D) Different generations of fillings that have been recognized in some fractures may suggest a progressive opening. E) Detail of the fracture fills with undolomitized breccia clasts (embedding a gastropod fossil) with karsified edges.

The sediments that infill many of these joints are of platform origin, are mainly composed of a greenish marly limestone, and embed small non-dolomitized carbonate intraclasts (Fig, 17C and D). The presence of rock fragments composed by aggregates of pisoids, that are typical of the platform interior of the Cassian carbonate banks, may give a further indication that the platform lithified early. Some outcrop scale K1 synsedimentary joints show irregular margins with signs of karstification at the top of the platform, probably caused by sea level fluctuations of unknown duration. Clear marine cements along these joints were not found, but field observations of the fracture filling were possible almost only at the top of the platform, where often the fractures are masked by recent debris deposits, while the sub-vertical walls of the platform, where the fractures are well exposed, are practically inaccessible.

The only fractures (joints and faults) that show an early synsedimentary origin belong to the set K1, while K2 and K3 fractures have different features, and are connected to successive tectonic deformations. However, it should be clearly emphasized that not all K1 fractures are early and that even the synsedimentary fractures show signs of subsequent reactivation. Moreover, the exact

quantification of the incidence of syndepositional fracturation is strongly limited by the current condition of the outcrop, pervasively dolomitized and strongly modified by subsequent deformational events.

To confirm the early age of some K1 fractures and to date the discontinuities affecting the Cassian platform, a field survey was conducted at the top of the outcrop and a comparison at the field scale with Heiligkreutz fractures was performed. 384 data were collected in 10 scan areas (1,5m x 1,5m and 2m x 2m) on the Cassian platform-top surface and 7 on Heiligkreutz Fm; the position of the scan areas were previously decided on the base of the photogrammetric model to obtain a uniform distribution along the outcrop and to avoid interference with the main fault zones. Field activity was preceded by the outcrop-wide fracture mapping performed on the high-resolution textured Digital Outcrop Model and aerial imagery. Comparison of field data orientation confirms the probable syndepositional age of many K1 structures showing that this set, widely present on the platform pavements, is much less present in the overlying Heiligkreutz Fm, deposited after the demise of the Lastoni buildup (Fig.4.18).

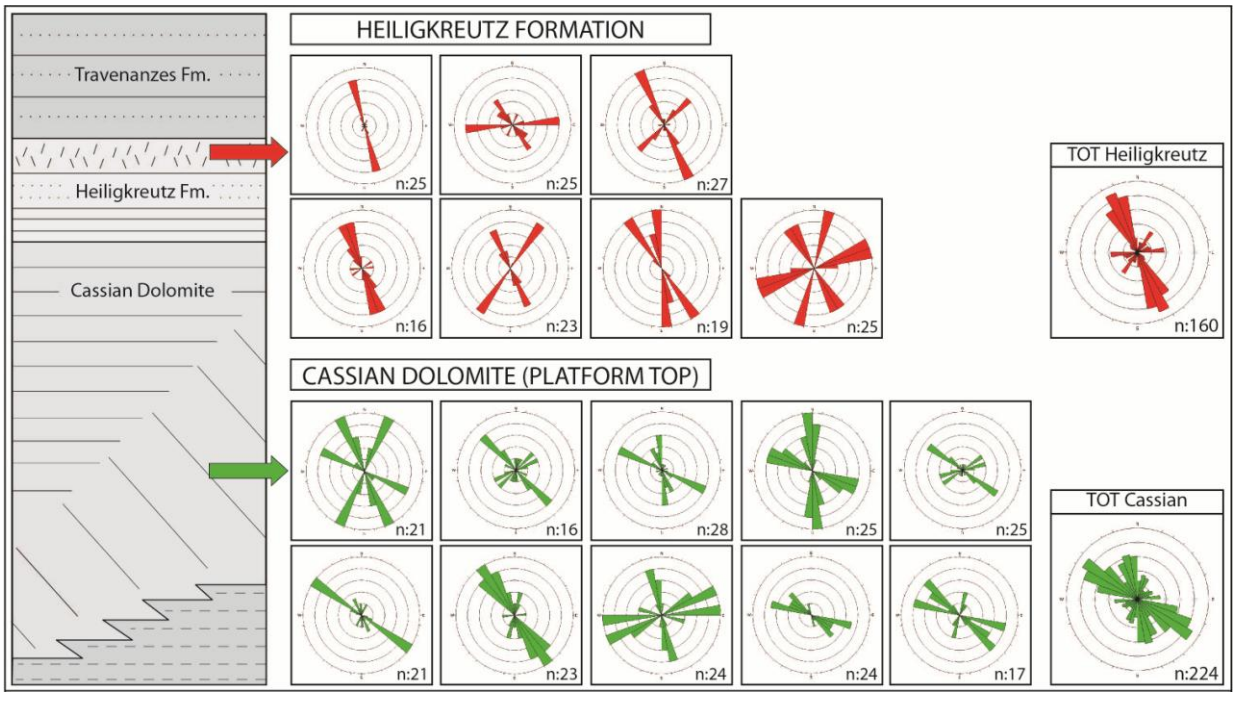

Fig.4.18. Comparison between fracture orientation on the top of the Lastoni di Formin platform and on top of the overlying Heiligkreutz formation. The fractures (SE-NW faults and joints) belonging to the set K1, widely present on the platform top, are nearly absent in the overlying Heiligkreutz fm. The data were collected in the field using the scan- area method:the locations of the scan-areas were previously selected in order to avoid the influence of the main faults.

4.4.5 Architecture and evolution of the platform

The interpretation of the outcrop's architecture is mainly based on the evidences and the quantitative measurements collected from the analysis of the Digital Outcrop Models realized using Unmanned Aerial Vehicles Digital Photogrammetry: the inaccessibility of the cliffs and the extensive dolomitization that affect the carbonate body were a strong limitation for an accurate field sedimentological characterization of the facies belt. The analysis highlighted some typical features of the Lastoni di Formin carbonate platform that can be synthetized as follows:

a) The platform can be subdivided into two overlapping units separated by an erosional surface (Figs. 4.5, 4.6 and 4.11) that can be considered as a maximum regressive surface representing a sequence boundary (probably the transition between Cassian I and II), that separates the two highstand phases of the platforms progradation;

b) The lower unit (Cassian I) is dominated by slope facies, strongly prograding toward N/NE with a low angle (< 6-8°). The clinoforms show a decreasing upward dip of the strata and become nearly horizontal at the top of the unit. In the northernmost section of the outcrop, the shelf break is exposed, and is characterized by the presence of coral heads in life position (Fig. 4.8A and 4.8B). Ahead of the shelf break, the clinoforms become abruptly steeper;

c) The upper unit (Cassian II) is constituted by peritidal cycles (Fig. 4.7) that are connected, in the northern part of the massif, to a second generation of clinoforms that dip to N/NE with an angle of 20°/25° (Fig. 4.9).

d) The thickness of the inner platform beds of the upper unit undergo a progressive general basinward thickening; this phenomenon is more accentuated in proximity of the shelf break than in the innermost part of the platform (Fig. 4.12);

e) A certain number of ESE-WNW trending joints and faults, belonging to set K1, are most likely synsedimentary and indicate an early deformation of the platform. Their extensional nature is confirmed by the opening-mode features of the joints and by the normal throw both down-to-the-south and down-to-the-north of the faults. All these synsedimentary fractures are sub-orthogonal to the bedding and are orthogonal to the prograding direction of the platform (Fig. 4.16).

All these features suggest a synsedimentary basinward tilting of the buildup of the upper unit that have influenced the platform architecture, and may be caused by differential compaction of the poorly consolidated basinal San Cassiano Fm. Comparable geometries have been observed in other

strongly prograding platforms (Capitan reef, Guadalupe mountains (USA): see Hunt et al., 2002; Sella platform, (Italian Dolomites): see Doglioni & Goldhammer (1988); Esino limestone (Italy), see Berra & Carminati, 2012)), where have been interpreted as the result of increased subsidence in basinward direction related the compaction of the basinal units. During the evolution and growth of high relief carbonate platforms, compaction-induced subsidence has been reported to exert an important control on the depositional trajectories and strata geometries (Doglioni & Goldhammer, 1988; Hunt et al., 1995; Hunt et al. 2002; Saller, 1996; Rusciadelli & Di Simone, 2007; Resor et al., 2010; Berra et. al., 2016). The presence of early fractures affecting the Lastoni di Formin platform and sub-orthogonal to its margin fits well with the described scenario. In fact, as pointed out by several authors (Daugherty et al., 1986; Whitaker & Smart 1997; Nooitgedacht et al., 2018) a generation of margin parallel (i.e. perpendicular to the progradation direction) opening-mode fractures and normal faults can develop during the platform growth (or soon after the deposition), driven by the local stress field confined within the carbonate body and generated by the progradation of the platform over a subsiding basin.

The extensional forces are controlled by the geometries and the architecture of the platform itself, and are independent from the regional stress field (Frost&Kerans, 2010; Nolting et al., 2018; Nooitgedacht et al., 2018). In the schematic representation of Fig. 4.19 the possible mechanism of formation of the syndepositional joints and faults related to the platform progradation and compaction-induced subsidence of the San Cassiano basin is illustrated.

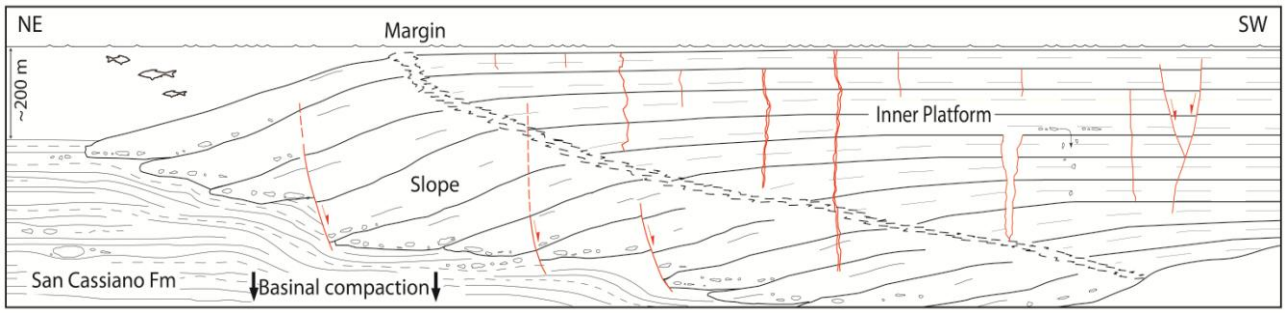

Fig.4.19. Schematic representation (not to scale) of the syndepositional joints and faults connected to a differential compaction, that affected the Lastoni di Formin platform. The fold deformations of the basinal deposits of the San Cassiano Formation at the base of the clinoforms are caused by differential compaction. These structures are clearly visible immediately to W of the study area, at the base of the Gusela del Nuvolau. The height of the water column must be considered indicative, and is deduced also from what can be observed at the Gusela del Nuvolau.

4.5 Discussion

4.5.1 Platform architecture

The transition between the two Cassian platforms (I and II) has been recognized elsewhere in Western Dolomites and in the Cortina area (monte Coldai, Richtofen riff, Lagazuoi, Gusela del Nuvolau), where it is marked, in the basins, by the onlap of the San Cassiano fm. on the Cassian slopes (Fois & Gaetani, 1982; De Zanche et al., 1993; Gianolla et al., 1998; Roghi et al., 2014). In the Lastoni outcrop, a complete section of the slope – basin transition is missing, preventing a direct correlation: the transition between the two platforms is only detectable on the shelf, where it is represented by an erosive surface at the top of the Cassian I.

A different interpretation of the carbonate banks of Lastoni di Formin was given by Blendiger & Blendinger (1989), according to which the outcrop shows the superposition of the low-energy tepee-pisolite facies directly on clinoforms (dipping ~ 3° toward North), with a sharp contact. This low angle of progradation and the facies distribution would be controlled by the leeward position of the bank margin, protected from high energy fluxes (wind and storm) coming from the south/southwest.The hypotesis of Blendiger & Blendinger (1989) partially fit with our observations, and represent a reasonable explanation of the low angles of clinoforms in the first stages of the Cassian I platform growth. However, this interpretation is probably based only on an outcrop window that is not representative of the totality of the buildup: in fact, in the northern part of the west cliff, clinoforms unequivocally steeper (with an average inclination of about 25°) than those described by Blendiger & Blendinger (1989) are visible. Moreover, also in the Val Formin section, the clinoforms associated with Cassian I and observable ahead of the shelf break show much higher angles than in the south and south-west sectors.

Although a complete paleogeographic reconstruction is not possible (parts of the outcrop are eroded or covered by several meters of loose debris), these new data suggest that, despite the general validity of the interpretation of Blendiger & Blendinger (1989), other factors can contribute to modulate the geometries of the platform. In particular, the distal steepening of the clinoforms could indicate an inherited deepening of the sea bottom topography.

4.5.2 Early fractures

Quantitative determinations on the incidence of the synsedimentary fractures, as well as any correlation with the main facies of the platform, is strongly inhibited by the condition of the

outcrop, pervasively dolomitized and strongly modified by several deformational events occurred over times. In particular, the WNW-ESE synsedimentary K1 fractures were surely reactivated and other parallel new fractures generated, during the Alpine compressional phases and for this reason their distinction is very difficult. The development of early fractures in carbonate environment is controlled by the early lithification of the platform, that allows the occurrence of brittle deformation shortly after deposition (Bathurst, 1982; Kerans et al., 1986; Grammer et al., 1993; 1999). The occurrence of early lithification was a predominant process affecting the carbonate platforms of the Dolomites, including the Cassian platforms (Keim, 1999; Keim and Schlaeger, 2001, Schlager, 2003; Reitner et al., 1995; Neuweiler et al., 1999; Guido et al., 2016; 2018). It has been related to the production of automicrite (in-situ produced micrite) and the abundance of marine cements in all the major zones of the platform.

4.5.3 Advantages of digital outcrop modeling

The Digital Outcrop Model developed by UAV-based digital photogrammetric survey allowed the detailed study and measurement of the sedimentological and structural features of the *Lastoni di Formin* carbonate platform that largely outcrop along sub-vertical and inaccessible cliffs. The photogrammetric reconstruction of the outcropping platform gives the possibility to collect a great amount of data, which can be checked and corrected at any time, quickly and effectively. The substantial advantages respect to traditional field surveys consist in the possibility of measuring strata and fractures orientations, thicknesses and other features that cannot be detected in the field because of their huge dimensions and/or their inaccessible location or unfavorable exposure. Moreover, large structures and complex geometries can be directly analyzed and interpreted at the outcrop scale on the point cloud, in a stereo 3D environment and with great resolutions. The availability of a 3D dataset overcomes the limitation of the unfavorable exposure of the outcrop cliffs (i.e. the absence of outcrops exactly perpendicular to the direction of progradation), that can lead to significant errors in the interpretation of the outcrop geometries (i.e. apparent thickness vs real thickness). The use of a drone allowed the detection of large surfaces in a short time, and the acquisition of high resolution data of the most remote and inaccessible portions of the carbonate body (i.e. vertical cliffs). At the same time, the UAV photogrammetry overcomes some of the limitations of other types of investigations (e.g. terrestrial laser scanning or digital photogrammetry), such as occlusions and unfavorable exposures.

4.6 Conclusion

In this study, advanced Unmanned Aerial Veichles Digital Photogrammetry techniques have been successfully applied to the reconstruction of the outcrop-scale architecture and depositional geometries of the Cassian carbonate platform ofthe *Lastoni di Formin* (Italian Dolomites). The integration of remote sensingand field data revealed that this buildup is formed by two superimposed carbonate bodies (Cassian I and II), that represents two highstand phases of the platform progradation toward NNE. The strata measurements obtained from the 3D model highlight the lateral thickening of the inner platform beds of the upper unit (Cassian II), and the tilting toward the basin of the outermost part of the platform, that was possibly induced by the differential subsidence affecting the Lastoni di Formin system. The strongly prograding platform, and the presence of a basinal, poorly consolidated San Cassiano Fm. that underlies the carbonate body are the principal factors that favored the occurrence of compaction-induced subsidence, especially of the external sectors of the platform. Furthermore, despite the dolomitization of the outcrop and the superimposition of several subsequent deformational events, the presence of an early generation of extensional faults and joints has been detected: these synsedimentary fractures developed nearly parallel to the platform margin. Their features and the presence of platform-derived materials (pisoids) in the fills of the fractures, allow to constraint the syndepositional age of these structures. Basing on their morphological expression and their orientation, a correlation of these early faults and joints with the instability of the buildup that was generated by the differential subsidence is strongly probable.

Acknowledgements

We would like to thank Luca Pizzimenti (INGV-Rome) for the precious advices in the use of the LiDAR data.

References

References are reported at the end of the thesis.

5. Manuscript B: Structural analysis of the Lastoni di Formin carbonate platform (Italian Dolomites) from UAV digital photogrammetry and Digital Outcrop Modeling

Manuscript in preparation

Riccardo Inama[1], Niccolò Menegoni[1], Cesare Perotti[1]

[1] Università di Pavia

Abstract

The recent advances in Digital Photogrammetry, together with the implementation of new algorithms and methodologies for the image processing (e.g. Structure from Motion, SfM) have enhanced the role of Digital Outcrop Modeling as a powerful tool for many geological investigations, including structural geology. In particular, these techniques allow the fracture characterization and the extraction of georeferenced structural data from large and inaccessible outcrops. However, they cannot completely substitute the classical fieldwork activity, which remains complementary and allow observations and interpretation at the small scale. In this work, we integrated Digital Outcrop Modeling techniques and field studies in order to unravel and characterize the complex fracture network observed along the middle - Triassic carbonate platform of Lastoni di Formin, located in the Italian Dolomites. The huge dimensions of the carbonate body and the superb exposure of its vertical cliffs, make the Lastoni platform an ideal outcrop to demonstrate the effectiveness of Unmanned Aerial Vehicles Digital Photogrammetry (UAVDP) and DOM reconstruction. The results of the structural analysis show that the present - day fracture pattern is the result of several deformational events that can be summarized as follows:

- Compaction – induced deformation that generated WNW-ESE trending K1 extensional joints and normal faults perpendicular to the direction of progradation of the platform;

- Extensional tectonics, likely related to the Jurassic rifting phase, that led to the formation of NNW- SSE striking fractures and westward dipping normal faults;

- Neogene compressional tectonics, characterized by a N-S to NW-SE crustal shortening that deformed the platform essentially with strike-slip structures.

5.1 Introduction

5.1.1 Scope of the work

The Lastoni di Formin Massif is a dolomitized carbonate complex located in the central - eastern Dolomites. Since most of the strain developed during the Alpine orogeny was accommodated by intensive thrusting at the southern margin of the Alps, the central part of the chain remained fairly undisturbed (Bosellini and Neri, 1991; Cadrobbi et al., 1995; Mollema & Antonellini, 1999). Despite the relatively mild tectonic deformation that preserved most of the original depositional geometries, the carbonate rocks of the Lastoni registered several subsequent tectonic events, which form an extensive network of faults and joints. Fractures occur at multiple scales, particularly at sub-seismic resolution where the joint density is extremely high; in reservoir modeling, heterogeneities of this dimension are often included into the matrix properties (La Bruna et al., 2019). For this reasons, studies performed on outcrop analogue are particularly important to cover the gap of resolution between core samples and geophysical observations, because they allow the acquisition of very large fracture datasets at multiple scales (McCaffrey et al.,2005; Bistacchi et al., 2015; Bertrand et al., 2015; Martinelli et al., 2020). This work is an attempt to disentangle the structural complexity that characterizes the outcrop and discuss the origin and timing of the tectonic feature that led to the formation of the present – day fracture pattern.
The results are obtained from a combined approach of field and remote sensing observations. Photogrammetry – based Digital Outcrop Modeling supports the collection of large dataset and enables the acquisition of reliable georeferenced fracture orientation on remote and inaccessible parts of the outcrop (e.g. vertical cliffs). Field investigations and high – detailed models of selected *areas of interest* provide a focus on centimeter scale joint arrays.

5.1.2 Digital survey technique

The use of Digital Outcrop Modelling for the study of outcrop analogues has raised in the last two decades (Hodgetts, 2013; Seers et al., 2013; Franceschi et al., 2015; Pless et al., 2015;) The digital data required for the DOM generation may be obtained from high – resolution laser scanning or, from photogrammetric techniques (Casini, et al., 2016; Corradetti et al., 2017; Westoby et al., 2012, Martinelli et al., 2020). Whereas Laser Scanner can be very expensive, and its usage can be difficult in some operative contexts (i.e. heavy and bulky equipment, longer acquisition time from multiple positions), the use of Digital Photogrammetry is flexible, yields to extremely high resolution data

with a lower cost and a more user-friendly survey planning (Remondino and El-Hakim 2006; Westoby et al. 2012; Bemis et al., 2014).
Moreover, the development of new algorithms for the image processing, such as Structure from Motion (SfM), as well as the technological advances of computer processors and sensors, has made Digital photogrammetry even easier and more accurate, enhancing the quality of structural and sedimentological data that can be collected from photogrammetric outcrop models. In this work, the acquisition was performed by Aerial Digital Photogrammetry, using a camera – equipped Unmanned Aerial Vehicle (UAV, or drone).

5.1.3 Terminology

In the following paragraph we give a summary of the terminology used in this paper to describe individual structural features or their associated organization in sets. We used the term *fracture* as a general term to indicate any surface of discontinuity within the rock mass that forms as a result of stress. *Faults* are instead fractures showing offsets or evidences of movements on the fault surface (mode II and III fractures sensu Pollard and Segall, 1987). The term *joint* was used to indicate cracks that have little or non-discernible offsets; depending their nature, they have been classified as extensional (mode I fractures sensu Pollard and Segall, 1987) joints or shear joints.
Eventually, analogue modeling performed on the DOM and improved with field data support observations covering a range of scales from kilometric to sub - metric levels. In this paper the terms *Seismic scale* or *Outcrop scale* are used for large features > 60/80 m in length (i.e. detectable with the resolution of seismic data). This type of data is mainly measured from the DOM. *Field scale* data are instead elements with sub – seismic resolution size, and are obtained from higher – resolution models or traditional field survey. However, this separation is only qualitative, since the two definitions potentially overlap when describing medium-scale structures.

5.2 Geological and structural Setting

The *Lastoni di Formin* massif is located nearby passo di Giau (Belluno province, Italy) in the eastern Dolomites, a portion of the Italian Southern Alps. The Dolomites are bounded to the north by the Funes-Passo delle Erbe line and to the south by the south verging Valsugana thrust (Doglioni, 1987) (fig.5.1). The domain includes terrains only mildly deformed by tectonics, which cover a period of time from Permian to Jurassic; the landscape is dominated by Middle Triassic spectacular carbonate edifices. The relief of *Lastoni di Formin* represents the remnants of an

exhumed carbonate platform (so - called Cassian Dolomite) of Upper Ladinian – Lower Carnian age, and appears as a vast isolated plateau, gently tilted toward North-East of about 15° and extended for over 2 km^2. It is bordered on the western and southern side by vertical cliffs up to 250-300 m high. To the east, it is closed by the Pinnacles of the Croda da Lago, carved into the Norian Dolomia Principale.

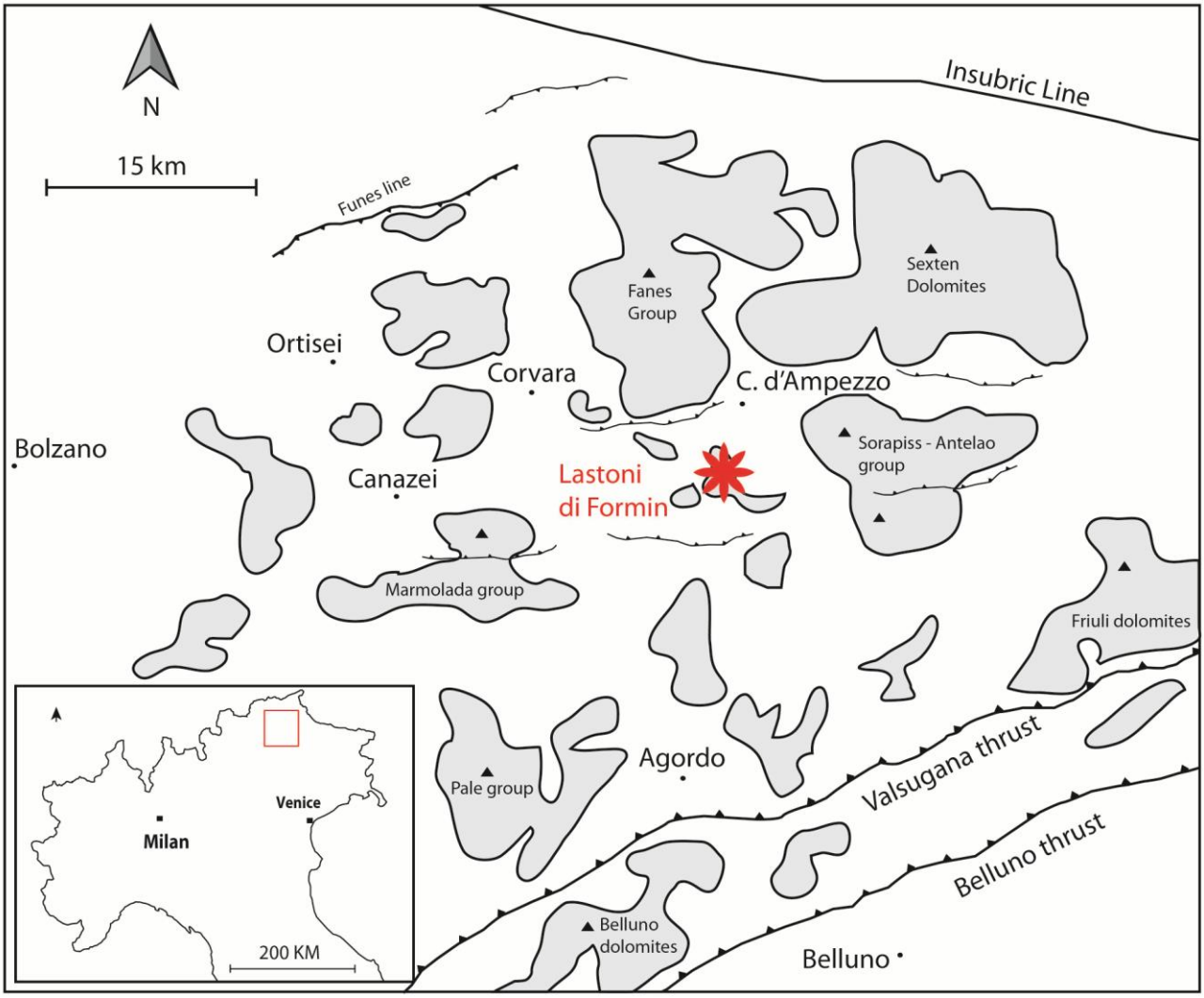

Fig.5.1 Simplified map of the central Dolomite region showing its northern and southern tectonic boundaries. The red star indicates the location of the study area.

The outcrop is formed by two superimposed carbonate complexes, separated by a horizontal unconformity (fig. 5.2): i) the lower body is dominated by 10-15 m thick, low angle northward-dipping clinoforms; ii) the upper unit is organized in well-developed regular cycles of peritidal deposits, outcropping in the central and southern part of the massif, connected to margin and slope facies (dipping 20°/25° to N/NE) in the northernmost sector. Individual cycles have a thickness of

7-9 m to metric in the uppermost complex. However, the internal organization of the cycles and bed - parallel structures such as stylolites, enhanced by weathering (especially in the upper layers), create an apparent sub-metric stratification with a thickness of 20-50 cm. The lithology of the Cassian Dolomite consists of fine grained greyish and whitish dolostone with sucrose texture. The extensive dolomitization almost totally obliterates the original depositional fabric and the sedimentary structures that are only locally visible. The outcrop of Lastoni represents the easternmost part of a larger carbonate platform that included, from West to East, the outcrops of Sass de Stria, Col Gallina and Nuvolau-Averau (Leonardi, 1968; Bosellini et al., 1982; Blendinger & Blendinger, 1989).

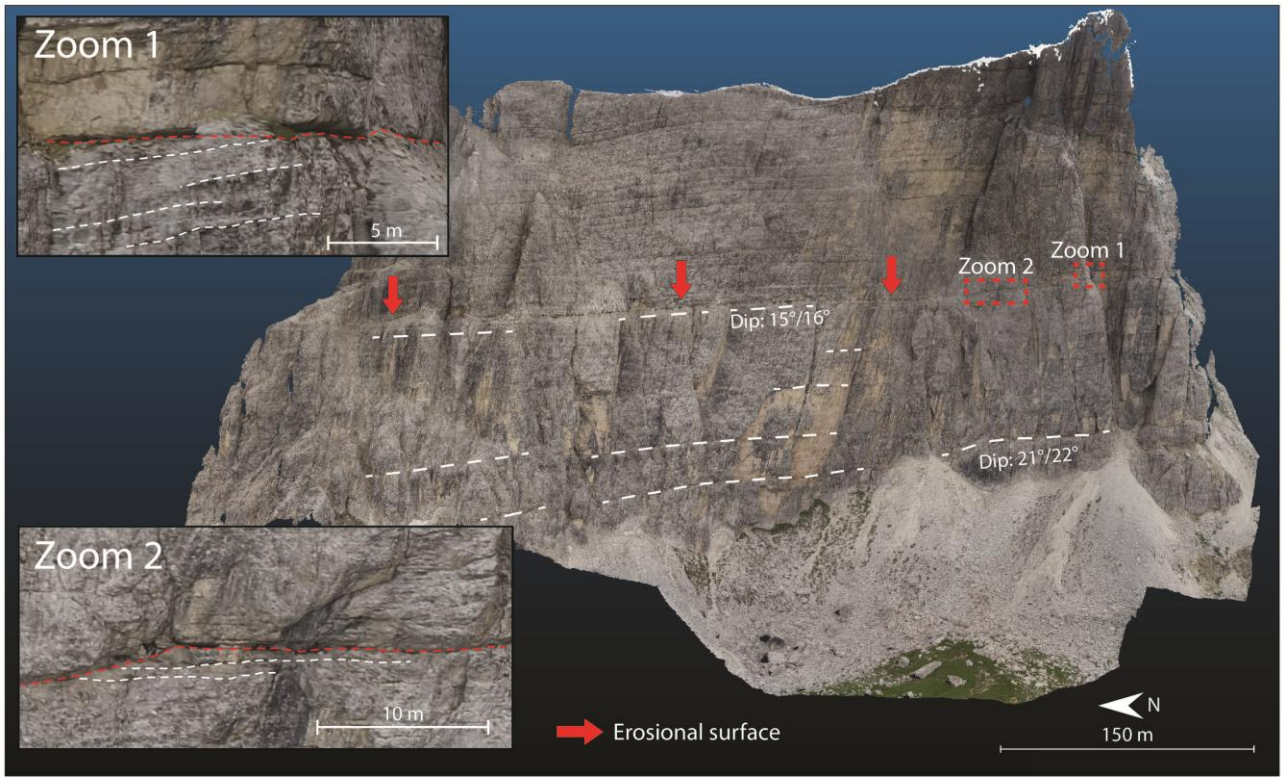

Fig.5.2. DOM image of the Costeana cliff (western portion of the outcrop): the horizontal unconformity indicated by the red arrows separates two superimposed carbonate bodies. Slight evidence of its erosive nature is shown in the Zoom 1 and Zoom 2 windows (after Inama et al, 2020).

Faults and joints lack of chemical alteration halos that may indicate their role in driving dolomitizing fluids. The summit plateau is surmounted, in its southern sector, by the mixed carbonate-terrigenous deposits of the Heiligkreuz formation (sensu Keim and Brandner, 2001; Neri et al., 2007). The onset of the Heiligkreutz formation marks the demise of the high - rimmed carbonate platforms, corresponding to a Tethys-scale crisis of the carbonate factories and a significant increase of siliciclastic input (De Zanche et al., 1993; Stefani et. al., 2004; Stefani et al.,

2010). According to several authors, this crisis is caused by a global episode of climate change, the "Carnian Pluvial Event" (CPE, Simms and Ruffell, 1989, 1990), which consist in a switch to humid condition and increase rainfall and runoff at low latitudes, triggered by a major perturbation of the global carbon cycle (Gattolin et al., 2013; 2015; Roghi, 2004; Preto et al., 2010; Dal Corso et al., 2012; 2020). The Heiligreuz was deposited in a ramp environment that progressively filled the intraplatform basins, onlapping the platform slopes and leveling the paleotopography. In the study area, this formation corresponds to a ~ 50/60 m thick sequence consisting of a densely stratified carbonate basal unit (upper part of the Borca member), an intermediate unit mainly composed by marls and marly limestones with evident cross lamination (Dibona mb.), and a topmost unit represented by a 10-15 m thick massive oolitic bank, almost totally dolomitized (Lagazuoi mb.). The Dolomites recorded a complex tectonic evolution from the Late Permian and Early Triassic that is strictly connected with the depositional history and the stratigraphic framework of the domain. During Late Permian and Early Triassic, a rifting phase produced N-S trending structural highs and lows (Bosellini et al., 2003). The structural highs became the nucleus of shallow water carbonate production, which evolved to the development of build-ups, while in the subsiding areas the deposition of basinal units took place. During the Ladinian, sinistral transpressive tectonics occurred in the central Dolomites (Doglioni, 1984; 1987), developing flower structures and high angle strike slip faults concentrated along the alignment of the Strava fault and Cima Bocche anticline, characterized by a N70° strike. These structures are reported to cut the entire basement and sedimentary cover up to Early Ladinian rock (Doglioni, 2007). Subsequently, these structures are cross-cut by the Late Ladinian - Early Carnian intrusive complexes of Predazzo and Monzoni associated also with subaerial events (Sciliar, Monte Agnello) that occurred in the area (Castellarin., 1988; Abbas et al., 2018).

From the Late Trassic to Jurassic times the dolomites were subjected to a rifting and progressively became part of the passive continental margin of the Adria plate (Bertotti, 2001; Berra and Carminati, 2010), associated with the opening of the western Alpine Tethys (Piedmont-Ligurian Ocean). This rifting led to the fragmentation of the large Dolomia Principale platform in structural highs and lows (Lombard Basin, the Trento Platform, the Belluno basin and Friuli Platform) and was controlled by the presence of N-S striking normal faults. During Paleogene and Neogene times the Southern Alpine domain was involved in the Alpine Orogeny, and the Dolomites became the innermost part of a south-vergent thrust belt (Doglioni, 1987; Berra & Carminati, 2010). The compressional tectonics started with the subduction of the Alpine Tethys ocean during the Cretaceous (Polino et al., 1990; Schmid et al., 1996), and extensive investigations have highlighted the presence of several distinct tectonic phases (Caputo, 1996; Caputo et al., 1999). During the

Dinaric phase (Chattian-Burdigalian) the maximum compressive axis was oriented ENE-WSW (Caputo, 1996, 2008). Between Serravallian and Tortonian (Alpine - Valsuganense phase) N-S to NW-SE compression was recorded by the orientation of the major overthrusts (i.e., Valsugana and Belluno overthrusts, Doglioni, 1987; Caputo, 1996; Schönborn, 1999; Antonellini & Mollema, 2000). In the Late Messinian–Pliocene times, the last Alpine phase (Schledrense phase) was characterized by the reorientation of the σ_1 axis to NW-SE (Castellarin et al., 1992; Caputo, 1996), depicting an anticlockwise rotation of the main compressive direction from NE-SW to NW-SE (Caputo, 1996; Mazzoli & Helman, 1994).

5.3 Data and Methodology

The huge dimension of the massif and the inaccessibility of its vertical cliffs represented a potential disadvantage for an effective structural data collection and interpretation. Traditional field structural measurements result to be very time consuming and have been necessarily limited to a weighted number of sampling windows, mostly located on the topmost plateau.

The 3D nature of Digital Outcrop Models represents a valuable option to resolve the issue, allowing to acquire, in a fast manner, large volumes of three-dimensional, georeferenced digital measures at multiple scale and distributed around the outcrop. According to the scope of the work and the nature of the outcrop, DOMs can be rendered as a point cloud, a textured mesh, a Digital Elevation Model (DEM) or an orthophoto (Martinelli et al., 2020). The DOM of Lastoni di Formin was obtained from photogrammetric data that were processed applying the principles of the Structure from Motion (SfM) technique (Westoby et al., 2012). The close-range photogrammetric acquisition was performed by means of an Unmanned Aerial Vehicle (UAV, or "drone"), that allowed to scan the wide cliffs of the massifs along a pre-planned flight pathway. With respect to ground-based photogrammetric acquisition, the use of a drone has also the advantage to minimize truncation and occlusion effects. The orientation of the camera was maintained orthogonal to the outcrop surface, and more than 12000 images were captured along the vertical cliffs and on top of the outcrop, with an overlap and a sidelap greater than 90%. The position and orientation of the cameras were recorded by the on-board GNSS-IMU instrumentation. However, a topographic survey was conducted in the field, by the use of a differential Real Time Kinematic (RTK) GPS (type Topcon Hiper Pro), to measure 22 Ground Control Points (GCPs), to improve the processing (alignment, scaling and orientation) of the DOM. The workflow employed for the generation of the DOM of the study outcrop has been addressed in the preceding work (Inama et.al, 2020, and reference

therein). The image processing was carried out by the *Photoscan* software (Agisoft), through main steps that can be summarized as following: i) Pre-processing: removing of unwanted, blurry or defective images; ii) Image matching, bundle block adjustment, and generation of sparse Point Cloud; iii) Reconstruction of the dense point cloud using the high-quality setting of Photoscan; iiii) Mesh and texture generation and developing of georeferenced orthophoto mosaic, based on the dense cloud reconstruction.

The resulting point clouds (fig.5.3) and texturized models (img were georeferenced in WGS84 / UTM 33N coordinate system using the combination of on-board registered coordinates and GCPs position measured in the field. The image resolution of the final texturized models were comprised within 2.7 to 7.9 cm/pixel. However, few models with higher resolution (0.7 cm/pixel) were realized along some specific transects by acquisition flights very close to the rock walls. To assess the accuracy of the model and quantify the effect of errors on the measurements, the absolute and relative accuracy (sensu Chesley et al, 2017) of the models were calculated.

The mean *absolute accuracy* (difference between real positions of the GCPs in space and "virtual" positions detected on the DOM) resulted 120 cm and 72 cm for the planar and the vertical positioning, largely sufficient for the analysis of seismic scale features.

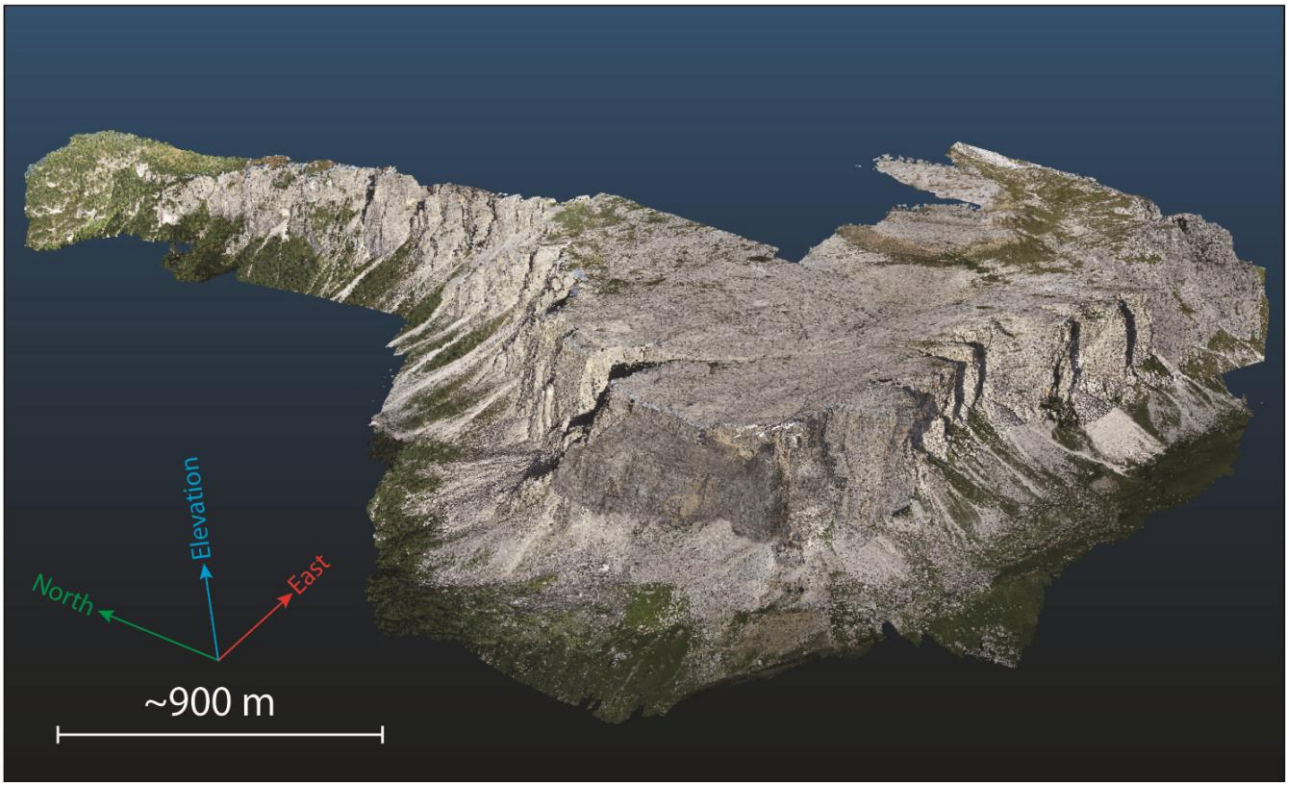

Fig.5.3 Overall DOM of the Lastoni di Formin outcrop.The sequence is gently tilted towards north/east of ~ 15° (Inama et al, 2020).

More importantly, the *relative accuracy* (difference in orientation and length between the vectors joining the 231 pairs of GCPs and the corresponding points identified on the DOM) revealed mean error <1° in orientation and of 0.17% in length, compatible with the range of error of the manual compass-clinometer measurements (~2°, Jordà Bordehore et al.; 2017; Cawood et al., 2017; Menegoni et al., 2019).

The DOM was imported and sampled in the software *CloudCompare stereo* (combined with a stereoscopic screen) for the structural data interpretation and extraction; faults, joints and bedding attitudes were collected using manual (fig.5.4) and semi-automatic (qCompass plugin - Thiele et al., 2018) tools.

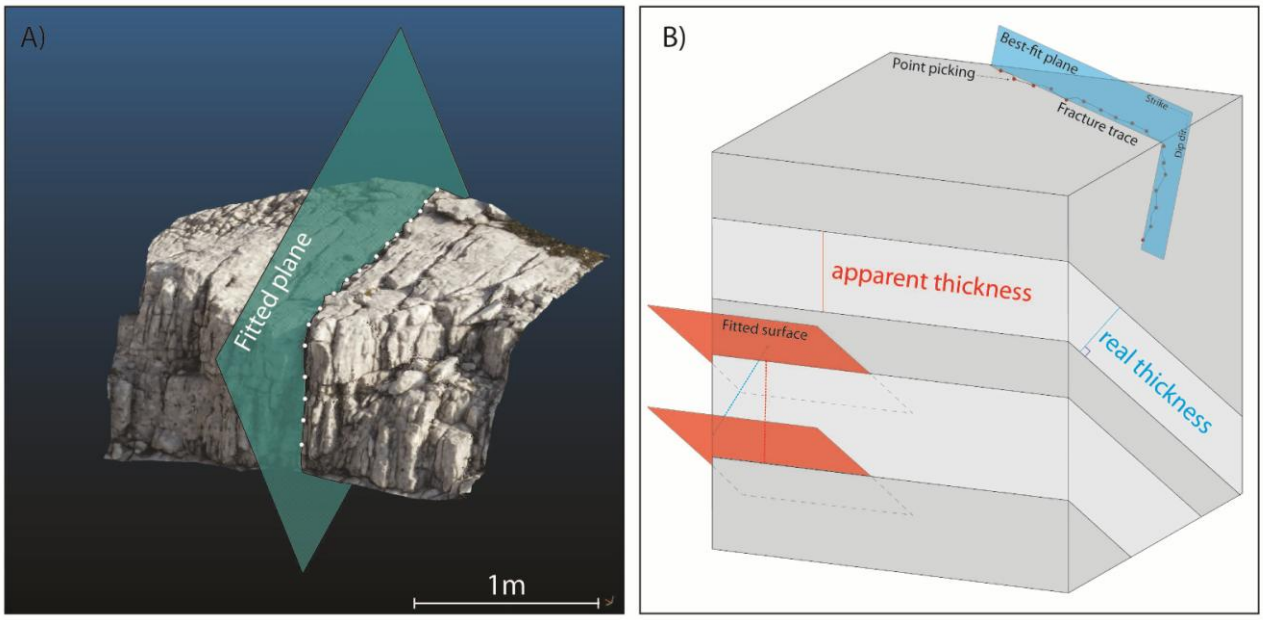

Fig.5.4 Example of the manual procedure for 3D data collection (A): the fracture is sampled by picking several points along its trace on the DOM. Then, the best - fit plane is calculated. The 3D nature of the DOM allow to reduce some of the biases of the bi - dimensional interpretation, such as apparent thicknesses and orientations of the features (B).

More detailed structural analyses were carried out selecting several sampling windows on the higher resolution DOMs. Field measurements were carried out at the outcrop scale, limitedly to the accessible part of the massif, consisting in the upper plateau and few spots at the base of the cliffs. Some of these sampling windows are included in the high resolution models, allowing the comparison between digital and field data.

5.4 Results

5.4.1 Distribution and description of the structures

Seismic - scale fractures and faults have been mapped manually on the DOM. Orientation and position of the structures were obtained picking points along the fracture trace and/or surface and calculating their best-fit plane (fig.5.5A).The geometry of Lastoni is particularly suitable for this method, since large scale features can be traced seamlessly on three sides of the outcrop. The faults displacements were calculated from the digital model, measuring the orthogonal distance between correlated layers on the opposite side of the slip surface. The analysis highlighted the presence of two main sets of extensional faults extended for hundreds of meters that cross the entire volume of the outcrop with an attitude of N210 °/64 ° (K1) and N250 °/75 ° (K2). K1 faults are particularly well exposed in the central part of the western cliff of Lastoni, displaying listric geometry and small normal stratigraphic lowering towards SW. They present branches and conjugate faults, and are arranged in regularly spaced domino array (fig. 5.5B).

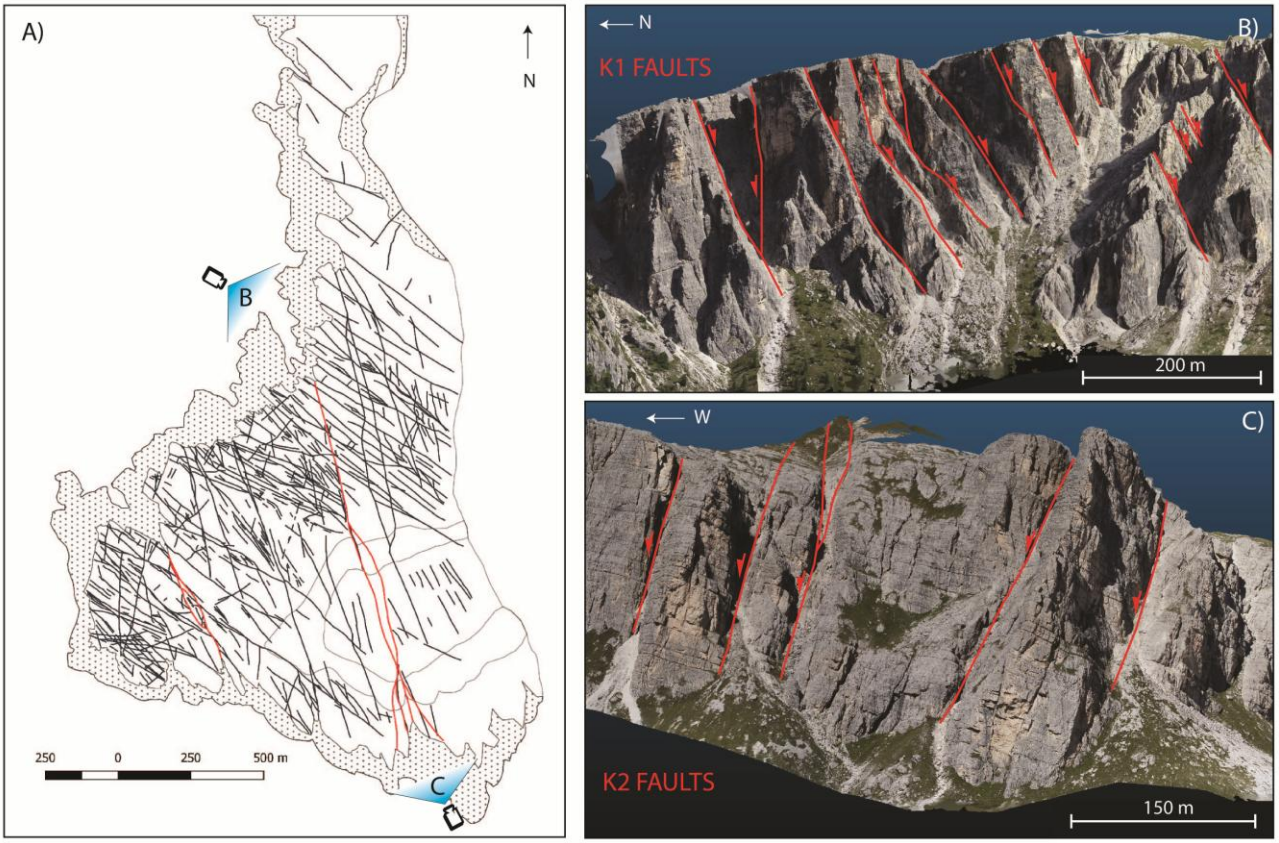

Fig 5.5. A) Seismic scale fractures and faults mapped from the top view of Lastoni di Formin outcrop from DOM derived orthoimages. B) K1 and C) K2 normal faults detected on the DOM; the points of view are indicated in the fig.5.4A.

The same set is also detectable on the southeastern section of the outcrop, where the main faults and associated splays form horsetail geometry. The K2 faults show a higher inclination (about 75°) and immersion towards W. A main K2 fault dissects both the Cassian dolomite and the overlying Heiligkreutz formation (fig. 5.5.C). The stereoplots showing the orientation of the faults are shown in fig.5.6.

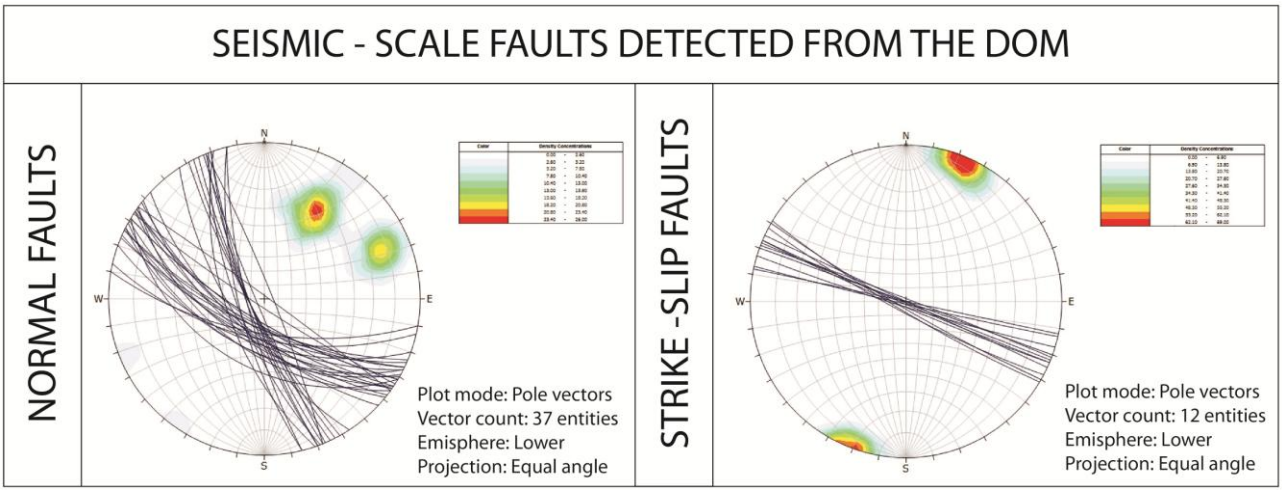

Fig. 5.6 Stereoplot of the seismic- scale K1 and K2 normal and the strike slip faults detected from the DOM.

This fault splits in three branches in correspondence of the south wall of the outcrop, where it is possible to measure a displacement of more than 20 meters on the main branch. In the field, the fault surfaces are strongly altered by pervasive dolomitization and weathering, preventing the recognition of kinematic indicators, as slickenlines and calcite slickenfibers. Both K1 and K2 form large trenches at the fault core (1 m ca. Fig.5.7), sealed by soils and loose carbonate material. Moreover, the DOM inspection outlines the presence of seismic scale fractures with no offset observed and typically oriented parallel to the main faults trends. Some large fractures are also oriented parallel to the bisector of the faults.

A third, significantly less frequent set of outcrop scales fractures, oriented with a NNE - SSW strike (K3) were detected from the DOM. Despite their extension, no signs of slip are visible from the top view of the platform, nor appreciable stratigraphic displacements were detected along the cliffs: for these reasons K3 fractures were classified as joints. Some of these stop at the horizontal interval between the two Cassian bodies.

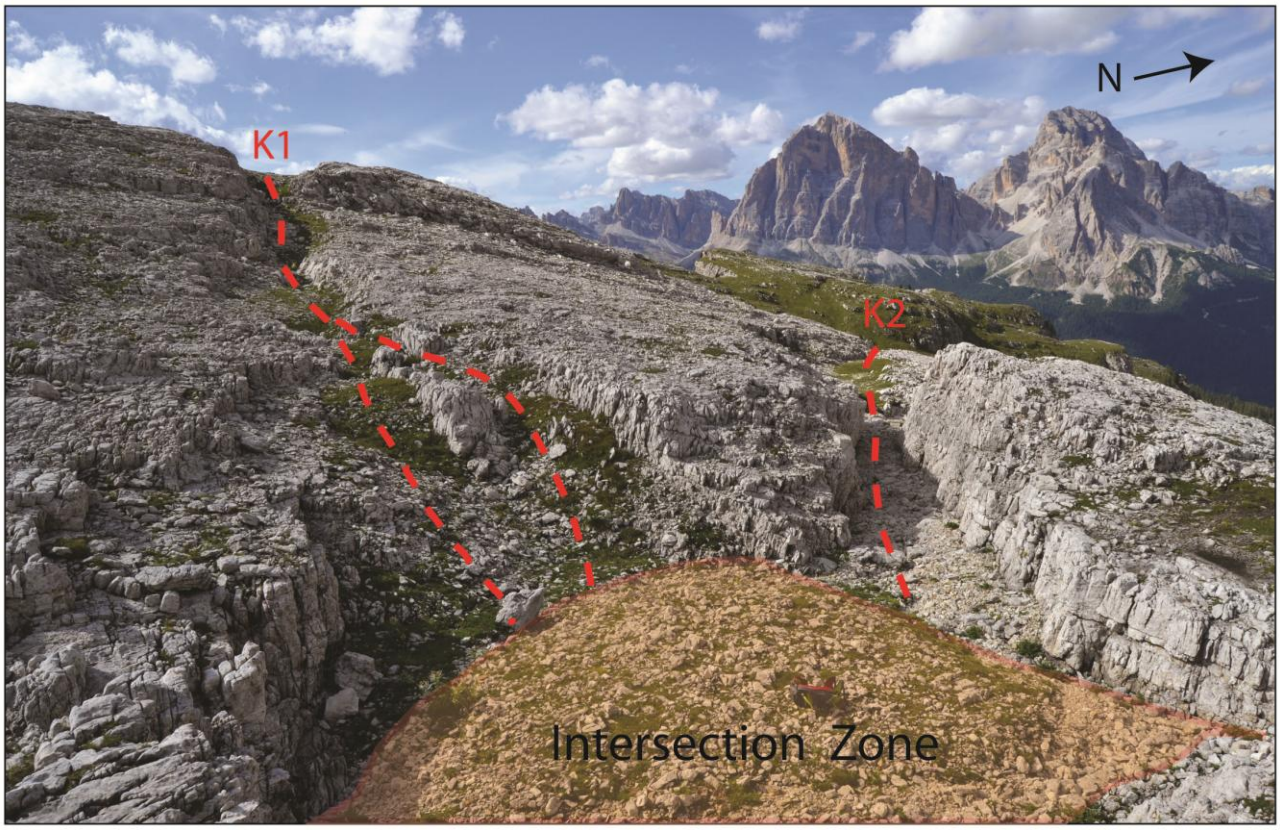

Fig.5.7. Intersection of K1 and K2 faults on the top of the Lastoni di Formin platform. Note the large trenches that characterize the fault core and the depression zone formed at the intersection between the two fractures.

Field scale joints are the most common deformational structures occurring in the Lastoni group; the summit pavements provide good examples for the study of their distribution and geometrical arrangement. The analysis has been performed on the highest – resolution (2 cm) DOM and integrated by field measurements from several scan – areas. However, the extremely pervasive fracturing and the strong alteration of the rock that "smooth" the features, do not allow to detect small offsets. These structures display straight trends and plane parallel matching walls. The principal fracture pattern is extensive all over the platform top, and it is formed by two main sets of conjugate systematic joints that resemble the orientation of the major faults, and intersect with an angle of ~ 35 - 50 ° Locally, abutting cross joints are found at high angle (nearly orthogonal) to the two main sets. A third, less present set of joints NNE – SSW oriented (K3) cross-cuts the conjugate array. The damage zones of the main faults show joint zones with narrowly spaced fractures oriented parallel to the fault trend.

5.4.2 Compaction induced fractures

The existence of synsedimentary fractures affecting the Lastoni di Formin has been demonstrated by Inama et.al (2020). Some of these have been classified as "early fractures" (sensu Kosa & Hunt, 2005; Frost & Kerans, 2009; Berra & Carminati, 2012), the development of which may be driven by the instability of the buildup generated by the differential compaction - induced subsidence. The occurrence of early fractures in carbonate platforms is controlled by the early lithification of the platform, responsible for brittle deformation shortly after deposition, a widespread condition in the carbonate platforms of the Mesozoic (Keim, 1999; Keim and Schlaeger, 2001, Schlager, 2003; Neuweiler et al., 1999, 2001; Reitner et al., 2000; Guido et al., 2016, 2018). Several joints and few faults, with an extension from ten to hundreds of meters, display characteristics that are typical of this kind of deformation (fig. 5.8) : i) they develop perpendicularly to the direction of progradation of the platform (i.e. parallel to the margin); ii) fractures are opening - mode, with a sinuous to irregular geometry, sub-orthogonal to the bedding and display non-matching walls; iii) they pre-date the other structures and the tilting of the carbonate platform; some fault terminations are visible along the exposed walls; iiii) fractures are associated with thickness variations perturbation of the overlying strata geometries. At the field scale, neptunian dykes with an extension of few meters and apertures of about 5 - 10 cm have been found on pavements. The margins of these fractures are irregular and karstified and the filling is composed by siltstone, embedding clasts clearly of platform origin. The ENW - WSW orientation of these fractures largely overlaps with that of the set K1, strongly inhibiting the discrimination and quantification of their occurrence.

5.4.3 Strike slip deformation

Despite the general lack of direct kinematic indicators (slickenlines), it was possible to detect evidences of strike slip deformation affecting the platform, that lead to the strike-slip reactivation of older structures and the possible creation of new faults. Several nearly vertical faults, with a mean orientation of N202°/87° are clearly visible along the west cliff; they cross cut and displace the older K1 fault planes (fig.5.9 A, B). Since strike slip tectonic typically develop vertical or sub – vertical fault planes, probably these structures post – date the northeastward tilting of the stratigraphic succession. Near Forcella Giau a positive flower structure, which is characterized by narrow straight branches with reverse separation, generates an uplifted antiformal area on the top surface, and indicates the presence of combined compressional and strike - slip displacement (fig.5.9A).

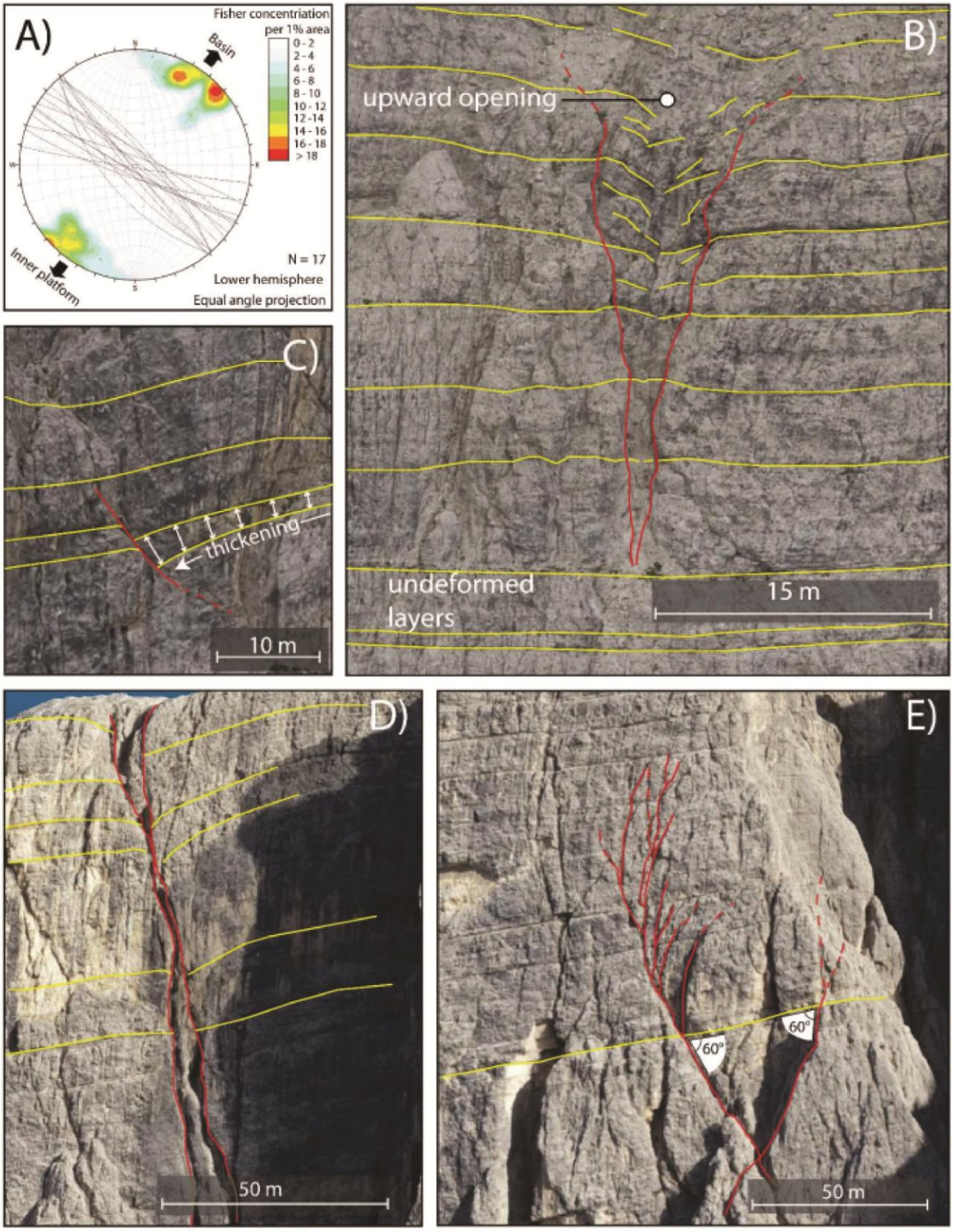

Fig.5.8. Examples of syndepositional extensional structures in the outcrop of Lastoni di Formin analyzed on the DOM (from Inama et al. 2020) . A) The azimuth of these structures is nearly orthogonal to the direction of progradation of the platform and they are also sub-orthogonal to the bedding. B) Upward-opening extensional fracture developed in the inner platform that caused a perturbation of the tidal cycles.

C) Small normal fault with synsedimentary thickening of the hanging-wall strata (grow fault); upwards the layers return undisturbed. D) Vertical extensional fracture with irregular geometry and non-matching walls. The strata on the right side display a progressive tilting toward the fracture. E) Incipient extensional structure, orthogonal to bedding (nearly Andersonian), with splays, that probably predate the tilting of the sequence.

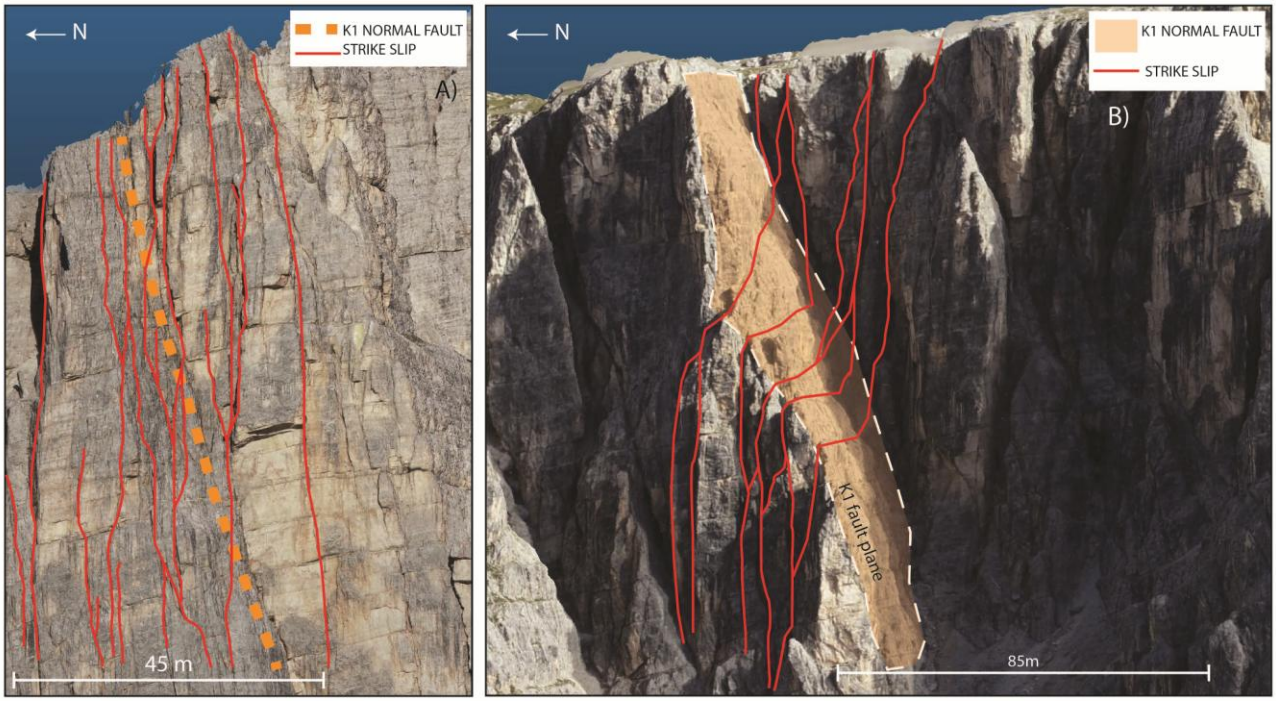

Fig.5.9 A) Sub-vertical strike - slip faults that cross - cut a K1 fault near forcella Giau. The combination of strike-slip and compression generates an uplifted antiformal "dome" that forms the peak of Lastoni. B) Detail of sub-vertical faults that cross cut a K1 fault plane along the western cliff of the outcrop.

Further indications of strike slip movements can be deduced from the analysis of the structures intersecting the top of the platform. Typical stepover zones were found at the bridge between the beginning and the end of parallel shear faults. The sense of shear of the faults was inferred by the geometries of these structures: extensional releasing stepovers form small local zone of depression, often partially filled by detric materials or soil. Restraining compressional stepovers, on the contrary, produce local shortening that generates uplifted areas that are usually partially eroded and, therefore, more difficult to recognize. The linkage of the parallel fault segments occurs generally through the development of R and P fractures. These observations revealed a dextral cinematic for the subvertical, nearly –E-W trending faults (parallel to K1 joints), and sinistral stike - slip reactivation for the inherited K2 faults (fig.5.10).

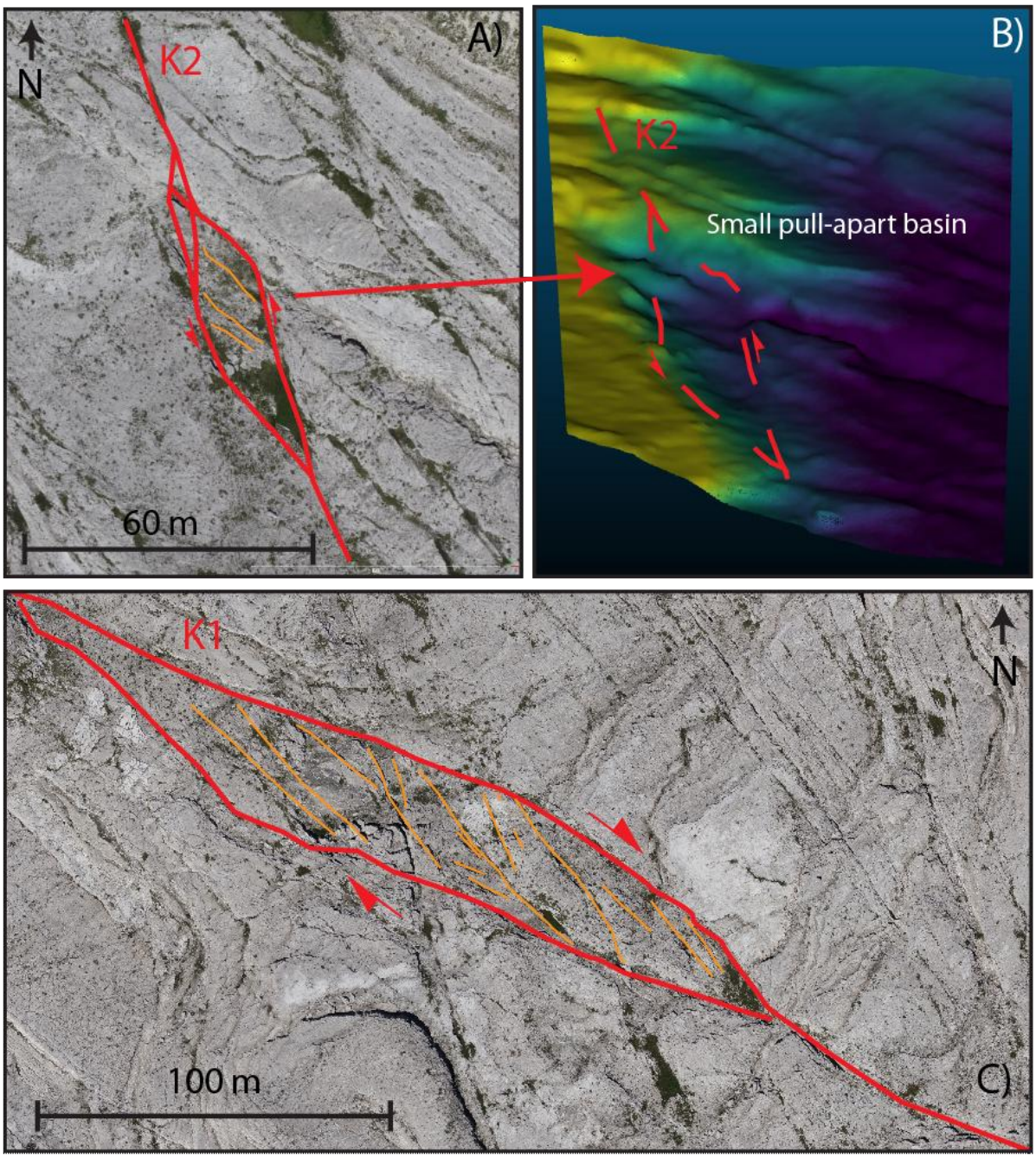

Fig.5.10. Strike slip structures visible at the top of the platform. A) top view and B)3D model of a releasing step-over structure that form a sort of small pull - apart basins in correspondence of the K2 fault.C) Releasing stepover on a K1 fault. The inferred kinematics is dextral for the K1 and sinistral for the K2 faults, respectively.

However, the presence of some indicators such as releasing bands suggest that also some K1 faults were subjected to dextral reactivation. The two sets of strike-slip faults form a conjugate geometry, intersecting with an angle of ~ 40°(fig.5.11). In some cases, several mode - I joints are oriented parallel to the bisector of these faults. This relationship between conjugate faults and tensional

joints is coherent with a mechanical model that presupposes a horizontal maximum compressive stress oriented NW-SE that is parallel to the extensional joints and bisects the faults.

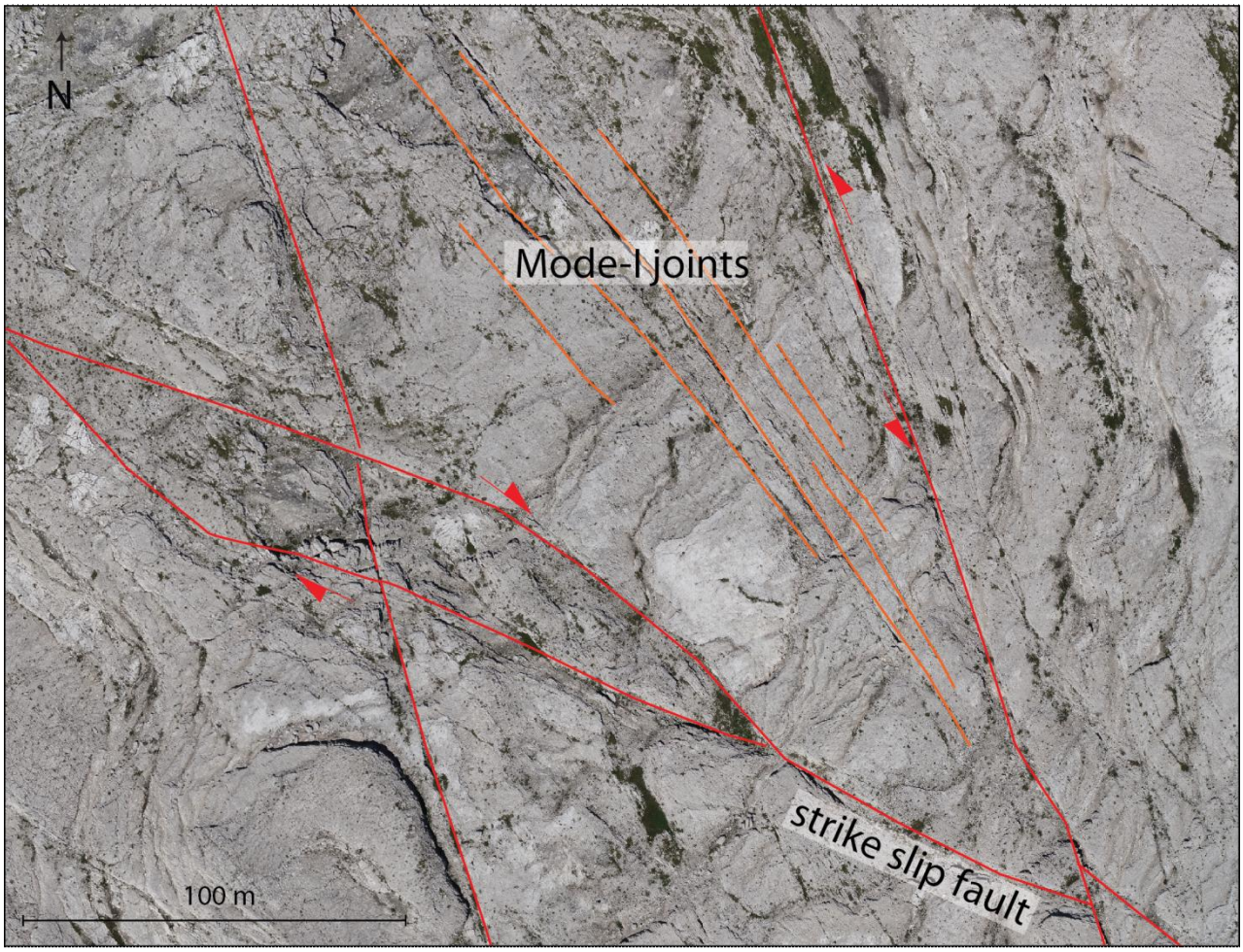

Fig.5.11. Seismic scale Mode I (tensional) joints that are oriented parallel to the bisector of the conjugate strike slip faults.

5.4.4 Comparison between the structures affecting the top of the platform and the Heiligkreutz formation

To constrain the timing of the different generations of fractures, a study was conducted at the top of the Heiligkreutz formation (Lagazuoi member). The host rock is a massive ~ 10 m thick carbonate body, heavily karstified, with a poorly visible stratification. This competent unit overlies the more erodible Dibona member (brownish, yellowish sandstones, marls and hybrid calcarenites, with a characteristic cross lamination), that makes the succession easy recognizable and prominent in the field. The fracture mapping conducted on orthoimages shows that seismic scale K1 fractures are pervasive on the top of the Cassian platform, and nearly absent on the top of the Heiligkreutz fm. A

detailed mapping of field - scale discontinuities was performed using 9m x 10 m scan areas on the highest portion of the DOM. 2685 and 818 fracture traces were collected on top of the Cassian platform and the Heiligkreutz fm respectively (fig.5.12).

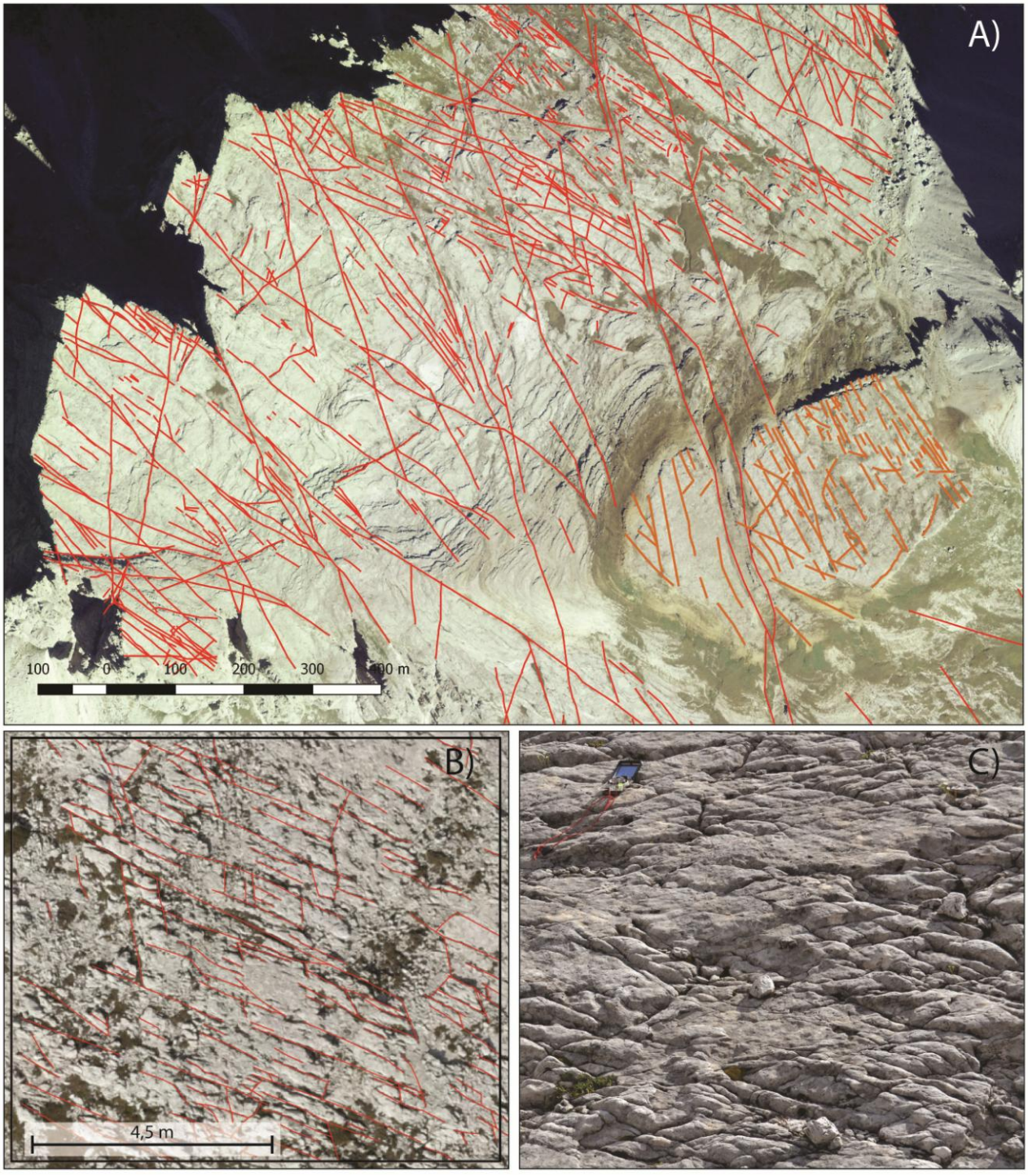

Fig.5.12 A) Seismic scale fractures and faults mapped from orthoimages. B) Example of scan - area and field - scale fracture tracing performed on the high resolution DOM surface. C) Discontinuities as they appear in the field.

Moreover, 244 data were collected on the field in 10 scan areas (1,5m x 1,5m and 2m x 2m) on the Cassian platform-top surface and 205 on Heiligkreutz Fm; the position of the scan areas was previously decided on the base of the photogrammetric model to avoid interference with the main fault zones.

The comparison revealed a strong prevalence of K2 structures at the top of the Heiligkreutz formation at both the outcrop and field scale (fig.5.13), with respect of K1 structures. These latter, widely present on the platform pavements, are much less frequent in the overlying Heiligkreutz Fm, deposited after the demise of the Lastoni buildup. The comparison of field and DOM data orientations constrain the genesis of most of the K1 structures before the deposition of the Heiligkreutz and the demise of the cassian buildups.

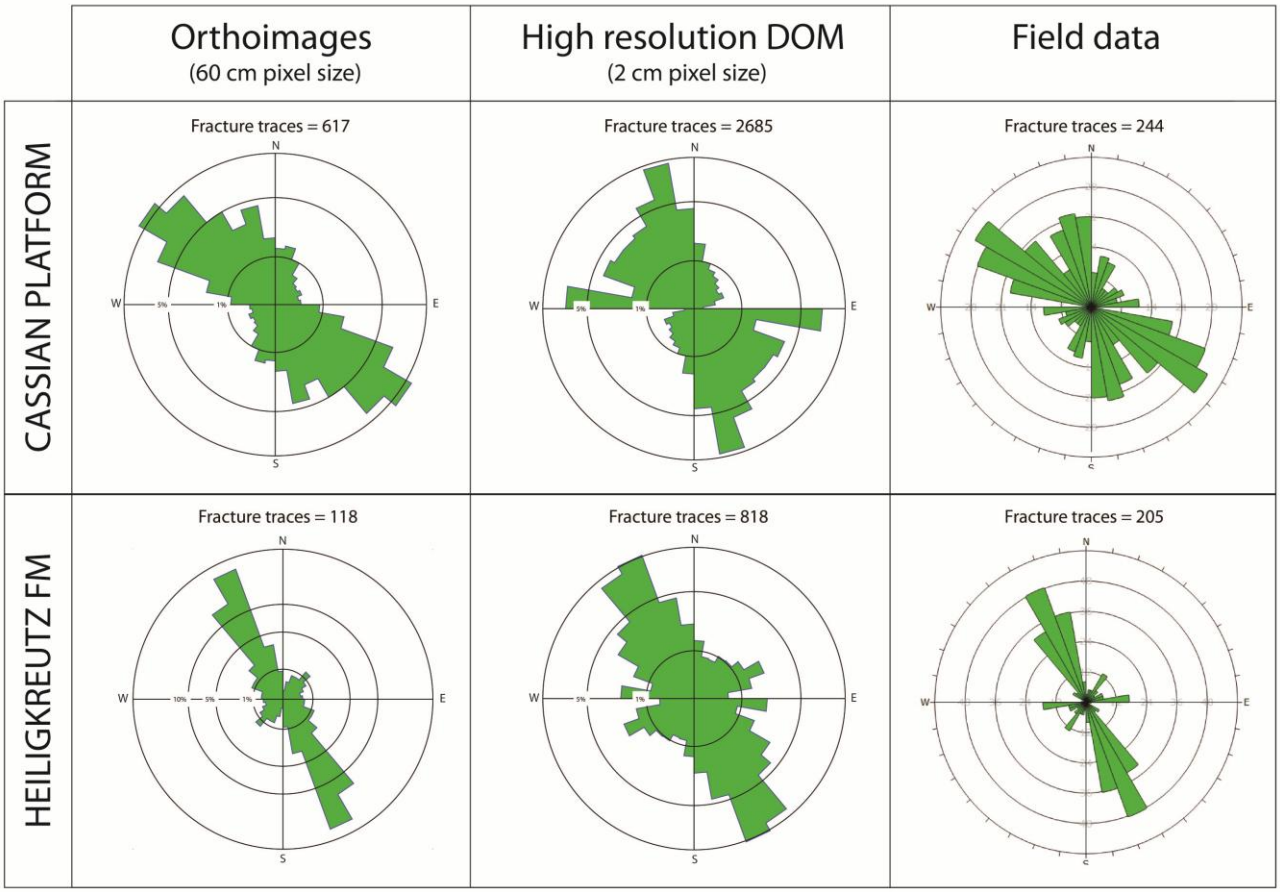

Fig 5.13. Comparison between the fractures traces mapped in 2D on the top surface of platform and on the overlying Heiligkreutz fm. Seismic scale fractures and faults were detected from orthoimages, while field scale discontinuities were mapped from the high - resolution DOM surface and in the field.

5.5 Discussion

5.5.1 Relative timing and implication for regional tectonics

The analysis of the DOM and high-resolution orthophotos, together with the results of field observations provided valuable information on the relative timing of the different sets of fractures affecting the carbonate platform. The first generation of fractures oriented in ESE – WNW direction occurred during or shortly after the platform growth and therefore pre-date the tilting of the platform and the other tectonic events. These fractures are made up of extensional joints and normal faults. As discussed in chapter 4.2, the main evidences of their early origin are the following: - thickening of hanging wall strata along normal growth faults; - opening upward joints that induced tilting and folding of the overlying beds; - incipient extensional structures that terminate upward against younger strata and are orthogonal to bedding (nearly Andersonian) and reasonably pre-date the tilting of the succession. K1 normal faults that show metric offsets toward the platform interior are generated by the same mechanism. Outcrop scale K1 normal faults affect extensively the Lastoni platform, but are substantially absent in the overlying Heligkreutz fm, constraining their origin before the deposition of this unit: these fractures were likely formed during or shortly after the platform growth (Late Ladinian, Early Carnian).

On the contrary, NNW-SSE K2 joints and faults are widespread in both the lithologies and post - date K1 structures. Taking into account their orientation and kinematic, we suggest that possibly this system is related to the East – West phase of extension and rifting occurred in the Dolomites during Jurassic times.

Strike slip tectonics was probably the manifestation of the last phase of deformation that affected the area. Dextral, nearly E – W trending (N100°-120°) structures of new formation cross cut extensional K1 faults NNW-SSE, westward dipping K2 normal faults were also reactivated as strike-slip faults with mainly a sinistral displacement. These features are consistent with a NW - SE direction of the maximum compressive stress during the last phases of the Alpine compressions, and with the consequent kinematic inversion of the pre-existent structures inherited from the earlier tectonic phases. Lastly, fractures of the set K3 are too scarce to establish cross cutting relationship with other fracture groups and therefore constrain their origin. However, their orientation suggest that they could have formed during one of the N-S to NNW-SSE compressive phase typical of the Alpine orogeny and that probably preceded the Neogene anticlockwise reorientation of the σ_1 axis from N-S (or NNE-SSW) to NW-SE direction.

The sketch of fig.5.14 summarizes the mayor deformational phases that affected the platform and the resulting structural features.

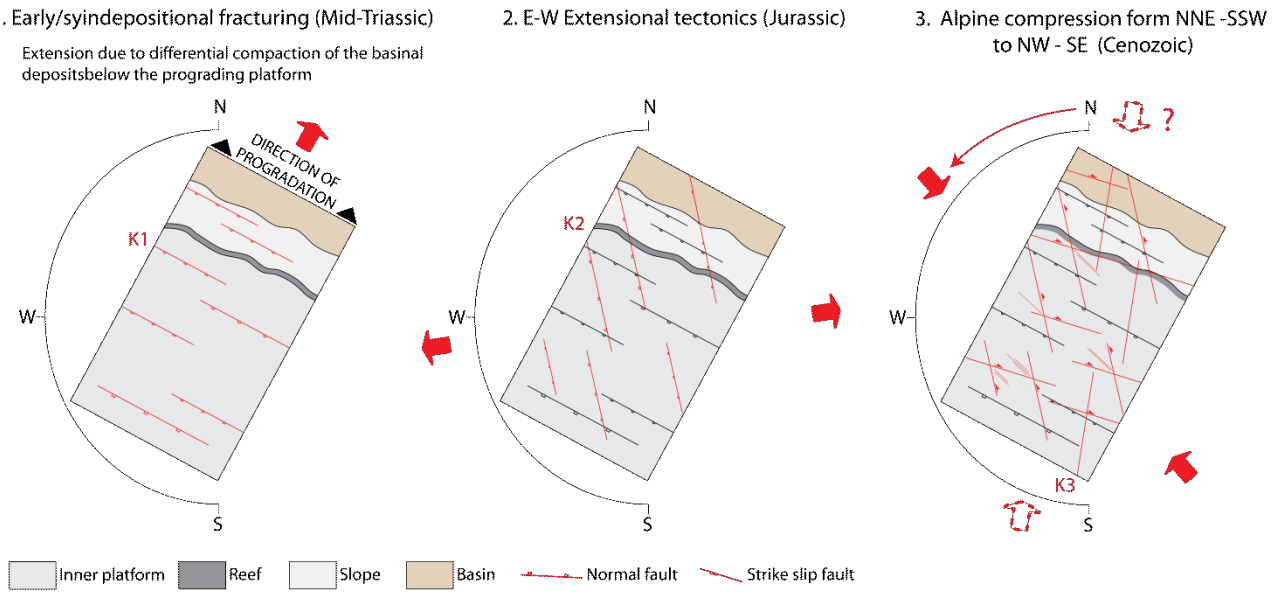

Fig.5.14. Sketch of the main deformational phases that affected the platform of Lastoni di Formin.

5.6 Conclusions

The complex fracture and fault network that affects the Lastoni di Formin platform is the result of several overlapping deformational events that occurred essentially in a brittle regime. Most of the mapped structures correspond to joints, and the faults detected along the platform seem to accommodate little strain, showing relatively small metric displacements (with the only exception of the main K2 fault that displays a normal stratigraphic offset of ~ 20 m, clearly dissecting the Heiligkreutz formation). The principal deformational events that affected the platform can be summarized as follows:

- Compaction – induced deformation that generated WNW-ESE trending K1 extensional joints and normal faults perpendicular to the direction of progradation of the platform, likely active during or shortly after the platform growth (Late Ladinian, Early Carnian);

- Extensional tectonics, likely related to the Jurassic rifting phase, that led to the formation of NNW- SSE striking fractures and westward dipping normal faults;

- Neogene compressional tectonics, characterized by a N-S to NW-SE crustal shortening that deformed the platform essentially with joints and strike-slip structures: the better documented indicate a NW-SE trending compressional axis and are made up by typical ~ N120° trending sub - vertical right strike slip faults, reactivated K2 normal faults with a dextral kinematic and NNW-SSE left strike-slip faults that are partially represented also by westward dipping K2 normal faults reactivated as strike-slip faults with a sinistral displacement.

5.7 References

The references are listed at the end of this thesis.

6. General conclusion

This research highlighted how the application of Digital Outcrop Modeling and Unmanned Aerial Vehicle (UAV)-based DP (UAVDP) can be a powerful tool for the study of Outcrop Analogues, since it can significantly improve the quality of the structural analysis providing a larger amount of quantitative data, from both accessible and inaccessible outcrop positions, and overcome some of the limitation of traditional filed surveys such as the scarce representativeness of the data sampled and the interpretation biases due to the unfavorable point of view. The sampling of the high - quality 3D model of the outcrop drastically increases the amount of data that can be collected at multiple scales from cm to hundreds of meters, providing a solid base for the interpretation of the geological problems.

Nevertheless, the development of an accurate DOM can be a relatively time consuming process, due to the technical difficulties to perform the photogrammetric survey (acquisition and ground control points measurements) and the processing time during the model development (Structure from Motion process and images georeferentiation); This amount of time can be reduced with an accurate survey planning and the use of performing workstations or, in the case of an RTK - equipped UAV, avoiding the use of Ground Control Points (GCPs) directly georeferencing the 3D model using the image position and orientation recorded by the GNSS/IMU of the drone. However, the disadvantages are largely counterbalanced by the benefits of having the outcrop at hand, allowing to sample it at any time and in every momentand significantly reducing the time required for the measurements if compared with the field activities (quicker sampling of a single feature, measures automatically digitalized, applications of semi-automatic methods).

In this study, Digital Outcrop Modeling and Digital Photogrammetry were successfully and effectively applied to the case of study of a Triassic isolated platform (Lastoni di Formin, Dolomites, Italy),

In particular, the first part of the research was dedicated to the reconstruction of the architecture and depositional geometries of the platform. The outcomes of the first part of this three - years project have been reported in the chapter 4 of this thesis, and were published as a research paper on *Marine and Petroleum geology* Journal.

The research highlighted that the platform is formed by two superimposed carbonate bodies (corresponding to the Cassian I and II platforms in De Zanche, 1993; Neri et al., 2007), that represents two highstand phases of the platform progradation toward NNE. Cassian I is dominated by low-angle clinoforms dipping north-northeastward and prograding over the basinal San Cassiano

Fm. Cassian II is characterized by a thick sequence of peritidal cycles connected northward to another generation of clinoforms. The carbonate system is affected by syndepositional deformation due to compaction - induced subsidence that control the depositional geometries and generate early fractures and faults. This was caused by the strong progradation of the platform over the basinal, poorly consolidated San Cassiano Fm. that underlies the carbonate body. The strata measurements obtained from the 3D model highlighted the lateral thickening of the inner platform beds of the upper unit (Cassian II), and the tilting toward the basin of the outermost part of the platform. Moreover, the presence of an early generation of sub-vertical extensional faults and joints that developed nearly orthogonal to the direction of progradation of the platform was detected.

The second part of the study was focused on the structural analysis of the Lastoni platform and on the characterization of the tectonic fracture network that affects the outcrop. The results were summarized in the chapter 5 of this manuscript.

The study shows that the present - day fracture and fault network that affects the outcrop is the result of several overlapping deformational events:

- Synsedimentary compaction – induced deformation (Late Ladinian - Early Carnian);

- Extensional tectonics, likely related to the Jurassic rifting phase;

- Alpine compressional tectonics, characterized by a N-S to NW-SE crustal shortening.

Moreover, in both the cases the advantages of the approach adopted for this study have been highlighted and the centimeter-scale resolution of the DOM satisfys the aims of the study and revealed to be appropriate for the definition of bedding, fractures and faults.

7. References

Abbas, H., Michail, M., Cifelli, F., Mattei, M., Gianolla, P., Lustrino, M., Carminati, E., (2018). Emplacement modes of the Ladinian plutonic rocks of the Dolomites: Insights from anisotropy of magnetic susceptibility. Journal of Structural Geology, 113: 42 - 61.

Akbar, M., Vissapragada, B., Alghamdi, A.H., Allen, D., Herron, M., Carnegie, A., Dutta, D., Olesen, J.R., Chourasiya, R.D., Logan, D., Stief, D., Netherwood, R., Russell, S.D., Saxena, K., (2000). A snapshot of carbonate reservoir evaluation. Oilfeld Review, 12: 20 - 40.

Antonellini, M., Mollema, P., (2000). A Natural Analog for a Fractured and Faulted Reservoir in Dolomite: Triassic Sella Group, Northern Italy. AAPG Bulletin, V. 84, No. 3: 314–344.

Assereto, R., Brusca, C., Gaetani, M., Jadoul, F., (1977). Le mineralizzazioni Pb-Zn nel Triassico delle Dolomiti. Quadro geologico ed interpretazione genetica. L'ind. Miner., 28: 367-402.

Bathurst, R.G.C., (1982). Genesis of stromatactis cavities between submarine crusts in Paleozoic carbonate mud buildups. Journal of the Geological Society of London, 139: 165-181.

Bemis, S.P., Micklethwaite, S., Turner, D., James, M.R., Akciz, S., Thiele, S.T., & Bangash, H.A. (2014). Ground-based and UAV-based photogrammetry: A multi-scale, highresolution mapping tool for structural geology and paleoseismology. Journal of Structural Geology, 69, 163-178.

Bernoulli, D., Kälin, O., and Patacca, E., (1979). A sunken continental margin of the Mesozoic Tethys: The Northern and Central Apennines: Symposium "Sédimentation jurassique W Européen": Association Sedimentologistes Français Publication Spéciale 1, p. 197–210.

Berra, F. and Carminati, E., (2010). Subsidence history from a backstripping analysis of the Permo-Mesozoic succession of the Central Southern Alps (Northern Italy). Basin Research, 22: 952–975.

Berra, F. and Carminati, E., (2012). Differential compaction and early rock fracturing in high-relief carbonate platforms: numerical modelling of a Triassic case study (Esino Limestone, Central Southern Alps, Italy). Basin Research, 24: 598-614.

Berra, F., Carminati, E., Jadoul, F., Binda, M., (2016). Does compaction-induced subsidence control accommodation space at the top of prograding carbonate platforms? Constraints from the

numerical modelling of the Triassic Esino Limestone (Southern Alps, Italy) Marine and Petroleum Geology 78: 621-635.

Bertotti, G., Picotti, V., Bernoulli, D., and Castellarin, A., (1993). From rifting to drifting: Tectonic evolution of the South Alpine upper crust from the Triassic to the Early Cretaceous: Sedimentary Geology, v. 86:53–76,

Bertotti, G., (2001).Subsidence, deformation, thermal and mechanical evolution of the Mesozoic South Alpine rifted margin: an analogue for Atlantic-type margins. Geological Society London Special Publications 187(1):125-141.

Bertrand, L., Geraud, Y., Le Garzic, E., Place, J., Diraison, M., Walter, B., Haffen, S., (2015). A multiscale analysis of a fracture pattern in granite: a case study ofthe Tamariu granite, Catalunya, Spain. Journal of Structural Geology, 78 : 52 - 66.

Bistacchi, A., Balsamo, F., Storti, F., Mozafari, M., Rudy, S., Solum, J., Tueckmantel, C., Taberner, C., (2015). Photogrammetric digital outcrop reconstruction, visualization with textured surfaces, and three-dimensional structural analysis and modeling: Innovative methodologies applied to fault-related dolomitization (Vajont Limestone, Southern Alps, Italy). Geosphere.

Birch, J.S., (2006). Using 3DM Analyst mine mapping suite for rock face characterization, in F. Tonon and J. Kottenstette (eds.), Laser and Photogrammetric Methods for Rock Face Characterization, Proc. 41st U.S. Rock Mechanics Symposium, Golden.

Blendinger, W., Blendinger, E., (1989). Windward-leeward effects on Triassic carbonate bank margin facies of the Dolomites, northern Italy. Sedimentary Geology, 64: 143 – 166.

Blendinger, W., (1994). The carbonate factory of Middle Triassic buildups in the Dolomites, Italy: a quantitative analysis. Sedimentology, 41: 1147 – 1159.

Blendinger, W., Brack, P., Norborg, A., Wulff-Pedersen, E., (2004). Three-dimensional modelling of an isolated carbonate buildup (Triassic, Dolomites, Italy). Sedimentology 51(2):297 - 314.

Blendinger, W., Lohmeier, S., Bertini, A., Meißner, E., Sattler, C.D., (2015). new model for the formation of Dolomite in the Triassic Dolomites, Northern Italy. Journal of Petroleum Geology, 38(1): 5-36.

Boriani, A. Giobbi Origoni, E., Pinarelli, L., (1995). Paleozoic evolution of southern Alpine crust (northern Italy) as indicated by contrasting granitoid suites. Lithos 35:47–63.

Bosellini, A., (1968). Paleogeologia pre-anisica delle Dolomiti centro-settentrionali: Memorie dell'Accademia Nazionale dei Lincei, s. 8, v.9: 1 -34.

Bosellini, A. and Rossi D., (1974). Triassic carbonate buildups of the Dolomites, Northern Italy. SEPM Spec. Publ. 18: 209-233.

Bosellini, A., Masetti, D., Neri, C., (1982). La geologia del passo Falzarego. In: A. Castellarin, G.B. Vai (a cura di): Guida alla geologia del Sudalpino centro-orientale. Guide geol. reg. S.G.I. 273-278, Bologna.

Bosellini, A., Doglioni, C., (1986). Inherited structures in the hanging-wall of the Valsugana overthrust (Southern Alps, northern Italy). Journal of Structural Geology 8: 581 - 583.

Bosellini, A., Neri, C., (1991). The Sella Platform (Upper Triassic, Dolomites, Italy). Dolomieu Conference on Carbonate Platforms and Dolomitization, Guidebook excursion B.

Bosellini, A., (1996). Geologia delle Dolomiti. Athesia, 192 pp.

Bosellini, A., Gianolla, P., Stefani, M., (2003). Geology of the Dolomites. Episodes, Vol. 26: 181-185.

Brandner, R., (1991) - Geological setting and stratigraphy of the Schlern-Rosengarten buildup and Seiser Alm basin.In: Brandner, R., Flugel, E., Koch, R., Yose., L.A. (1991): «The northern margin of the Schlern/SciliarRosengarten/Catinaccio platform». Dolomieu Conference on Carbonate Platforms and Dolomitization, Guidebook Excursion A, pp. 61, Ortisei.

Brandner, R., Horacek, M., Keim, L., (2012). Permian-Triassic-Boundary and Lower Triassic in the Dolomites, Southern Alps (Italy). Field Trip Guide 29th IAS Meeting of Sedimentology. Schladming/Austria. Journal of Alpine Geology 54 S. 379-404.

Breda A., Preto N. (2008), A continental/siliciclastic to shallow-marine/carbonate system in the Upper Triassic of Dolomites (Travenanzes Formation, N Italy), Rend. online SGI, 2, Note Brevi, www.socgeol.it, 51-56.

Breda, A., Preto, N., Roghi, G., Furin, S., Meneguolo, R., Ragazzi, E., Fedele, P., Gianolla, P., (2009). The Carnian Pluvial Event in the Tofane area (cortina d'Ampezzo, Dolomites, Italy). Geo.Alp, 6: 80 -115.

Broglio Loriga, C., Masetti, D., Neri, C., (1983). La Formazione di Werfen (Scitico) delle Dolomiti occidentali. Rivista Italiana di Paleontologia e Stratigrafia 88/4: 501–598.

Burnham, B.S., Hodgetts, D., (2018). Quantifying spatial and architectural relationships from fluvial outcrops. Geosphere: vol.15 (n.1).

Cadrobbi, L., Nobile, G., Lutterotti, G., (1995). Studio di supporto alla stesura del piano regolatore generale del comune di Canazei Studio associato di geologia applicata, No. 1995-1. Canazei (Bolzano), pp. 80.

Calanchi, N., Lucchini, F., Rossi, P. L., (1978). The Volcanic Rocks of Mount Agnello Area (Fiemme Valley, Italy): A Contribution to the Knowledge of the Mid-Triassic Magmatism of the Southern Alps, TMPM Tschermaks Min. Petr. Mitt. 25, 131-143.

Caputo, R., (1996).The polyphase tectonics of Eastern Dolomites. Mem. Sc. Geol., 48: 93-106.

Caputo, R., Stefani, M., Dalpiaz, G., (1999). Contractional and transcurrent tectonics in the Marmolada Group (Dolomites, Italy), Mem. Sc. Geol., 51(1): 63-77.

Caputo, R., (2008). Polyphase tectonic in the Cortina d'Ampezzo area, eastern Dolomites. Rendiconti Online Società Geologica Italiana 1(1):57-61.

Casella, E., Rovere, A., Pedroncini, A., Stark, C.P., Casella, M., Ferrari M., & Firpo, M. (2016). Drones as tools for monitoring beach topography changes in the Ligurian Sea (NW Mediterranean). Geo-Marine Letters, 36(2): 151-163.

Casini, G., Hunt, D.W., Monsen, E., Bounaim, A., (2016). Fracture characterization and modeling from virtual outcrops. AAPG Bulletin, 100 (1): 41–61.

Castellarin A., (1979). Il problema dei raccorciamenti crostali nel Sudalpino. Rend. Soc. Geol. It., 1: 21-23.

Castellarin, A., Lucchini, F., Rossi, L., Selli, L., Simboli, G., (1988). The Middle Triassic magmatic-tectonic arc development in the Southern Alps. Tectonophysics,146, Issues 1–4: 79-89.

Castellarin, A., Cantelli, L., Fesce, A. M., Mercier, J. L., Picotti, V., Pini, G. A., Prosser, G., Sartori, R., Selli, L., (1992). Alpine compressional tectonics in the Southern Alps. Relationships with the N-Apennines. Annales tectonicae, Vol. 6, No. 1: 62-94.

Castellarin, A., Selli, L., Picotti, V., Cantelli, L., (1998), La tettonica delle Dolomiti nel quadro delle Alpi Meridionali orientali: Memorie della Società Geologica Italiana, v. 53, 133-143.

Cau A., Fanti F. (2014), A pliosaurid plesiosaurian from the Rosso Ammonitico Veronese Formation of Italy, Acta Palaeontologica Polonica, 59 (3), 643-650.

Cawood, A.J., Bond, C., Howell, J., Butler, R.W.H., Totake, Y., (2017). LiDAR, UAV or compass-clinometer? Accuracy, coverage and the effects on structural models. Journal of Structural Geology,98: 67-82.

Chandler, J., (1999). Effective application of automated digital photogrammetry for geomorphological research. Earth Surf. Process. Landforms24: 51-63.

Chen, J., Zhu, H., & Li, X. (2016). Automatic extraction of discontinuity orientation from rock mass surface 3D point cloud. Computers and Geosciences, 95: 18-31.

Chesley, J.T., Leier, A.L., White, S., Torres, R., (2017). Using Unmanned Aerial Vehicles and Structure-From-Motion Photogrammetry to Characterize Sedimentary Outcrops: An Example from the Morrison Formation, Utah, USA. Sediment. Geol., 354: 1–8.

Colomina, I., & Molina, P. (2014). Unmanned aerial systems for photogrammetry and remote sensing: A review. ISPRS Journal of Photogrammetry and Remote Sensing, 92, 79-97.

Corradetti, A., Tavani, S., Parente, M., Iannace, A., Vinci, F., Pirmez, C., Torrieri, S., Giorgioni, M., Pignalosa, A., Mazzoli, S. (2017). Distribution and arrest of vertical through-going joints in a seismic-scale carbonate platform exposure (Sorrento peninsula, Italy): insights from integrating field survey and digital outcrop model. Journal of Structural Geology, 108: 121-136.

Corradetti, A., Tavani, S., Russo, M., Arbués, P. C., & Granado, P. (2017). Quantitative analysis of folds by means of orthorectified photogrammetric 3D models: a case study from Mt. Catria, Northern Apennines, Italy. The Photogrammetric Record, 32(160): 480–496.

Cousin, M., (1981). Les rapportes Alpes - Dinarides - Les confins de l'Italie et de la Yugoslavie. Soc. Geol. du Nord. Publ. 5 (1): 1 -521.

Cullen, N. D., Verma, A. K., Bourke, M. C., (2018). A comparison of structure from motion photogrammetry and the traversing micro-erosion meter for measuring erosion on shore platforms. Earth Surf. Dynam., 6, 1023–1039.

Dal Corso, J., Mietto, P., Newton, R. J., Pancost, R. D., Preto, N., Roghi, G., Wignall, P. B., (2012). Discovery of a major negative δ13C spike in the Carnian (Late Triassic) linked to theeruption of Wrangelliaflood basalts. Geology, 40: 79–82.

Dal Corso, J., Bernardi, M., Sun, Y., Song, H., Seyfullah, L., Preto, N., Gianolla, P., Ruffell, A., Kustatscher, E., Roghi, G., Merico, A., Hohn, S., Schmidt, A., Marzoli, A., Newton, R., Wignall, P.B., Benton, M., (2020). Extinction and dawn of the modern world in the Carnian (Late Triassic). Science Advances. 6.

De Zanche, V., Gianolla, P., Mietto, P., Siorpaes, C., Vail, P. R., (1993). Triassic sequence stratigraphy in the Dolomites (Italy). Memorie di Scienze Geologiche. 45. 1-27.

De Zanche, V., Gianolla, P., (1995). Litostratigrafia al limite Ladinico-Carnico (Sudalpino orientale).Ann. Univ. Ferrara, Sci. Terra, 5(suppl.): 41-48, Ferrara.

Doglioni, C., and Castellarin, A., (1985). A geologic schematic cross section of the eastern Southern Alps. Rend. Soc. Geol. It., 8: 35-36.

Doglioni, C., (1987). Tectonic of the Dolomites (Southern Alps, Northern Italy). Journal of Structural Geology, 9: 181-193.

Doglioni C., (1984). Tettonica triassica transpressiva nelle Dolomiti. Giornale di Geologia, ser. 3°, vol. 46/2, 47 - 60.

Doglioni C. (1987). Tectonics of the Dolomites (Southern Alps, Northern Italy). Journal of Structural Geology, 9: 181-193.

Doglioni C. & Goldhammer R.K. (1988). Compaction-induced Subsidence in a margin of a carbonate platform. Basin Research, 1/4: 237-246.

Doglioni, C., (2007), Tectonics of the Dolomites. Bull. Angewandte Geol. 12/2, pp. 11-15.

Doglioni, C., Carminati, E., (2008). Structural styles & Dolomites field trip. Memorie descritt. Carta Geol. d'Italia. Volume LXXXII: 300 pp.

Daugherty, D.R., (1986). Characteristics and origins of joints and sedimentary dikes of the Bahama Islands, In: Boardman, M.R. Metzler, C.V. (Eds.), Proceedings of the Symposium on the Geology of the Bahamas 3: 45-56.

Ferry, J.M., Passey, B.H., Vasconcelos, C., Eiler, J.M. (2011). Formation of dolomite at 40-80 °C in the Latemar carbonate buildup, Dolomites, Italy, from clumped isotope thermometry. Geology, 39: 571 -574.

Fois, E., Gaetani M., (1981): The northern margin of the Civetta buildup. Evolution during the Ladinian and the Carnian. Riv. Ital. Paleont. Strat., 86: 469-542.

Ford D, Williams PW (2007) Karst hydrogeology and geomorphology. Wiley, Chichester, pp 576

Franceschi, M., Martinelli, M., Gislimberti, L., Rizzi, A., Massironi, M., (2015). Integration of 3D modeling, aerial LiDAR and photogrammetry to study a synsedimentary structure in the early jurassic calcari grigi (southern alps, Italy). European Journal of Remote Sensing, 48: 527–539.

Franceschi, M., Preto, N., Caggiati, M., Gattolin, G., Riva, A., Gianolla, P. (2020). Drowning of microbial mounds on the slopes of the Latemar platform (middle Triassic). Ital. J. Geosci., Vol. 139: 98 – 108.

Frost, E. L. and Kerans, C., (2009). Platform-margin trajectory as a control on syndepositional fracture patterns, Canning Basin, Western Australia. Journal of Sedimentary Research 79 (2), 44-55.

Frost, E. L. and Kerans, C., (2010). Controls on syndepositional fracture patterns, Devonian reef complexes, Canning Basin, Western Australia, Journal of Structural Geology, 32: 1231-1249.

Gaetani, M., Fois, E., Jadoul, F., Nicora, A., (1981). Nature and evolution of Middle Triassic carbonate buildups in the Dolomites (Italy). Marine Geology Volume 44, Issues 1–2: 25-57.

Gattolin, G., Breda, A., Preto, N., (2013). Demise of Late Triassic carbonate platforms triggered the onset of a tide-dominated depositional system in the Dolomites, Northern Italy. Sedimentary Geology, 297: 38 – 49.

Gattolin, G., Preto, N., Breda, A., Franceschi, M., Isotton M., Gianolla, P., (2015). Sequence stratigraphy after the demise of a high-relief carbonate platform (Carnian of the Dolomites): Sea-level and climate disentangled. Palaeogeography, Palaeoclimatology, Palaeoecology, 423: 1 – 17.

Gianolla, P., De Zanche, V., Mietto, P., (1998). Triassic Sequence Stratigraphy in the Southern Alps (Northern Italy): Defenition of Sequences and Basin Evolution. Special Pubblication - SEPM, 60: 719-748.

Gianolla, P.,(2008a). Nomination of the Dolomites for inscription on the World Natural Heritage List UNESCO: Nomination document. Section 2.a.2: Geology: pp 36- 51.

Gianolla, P., Andreetta, R., Furin, S., Furlanis, S., Riva, A., (2008b). Annex 2.1: The geological contribution: Geology of the Dolomites. In: Nomination of the Dolomites for inscription on the World Natural Heritage List UNESCO.

Gianolla P., Furin S., (2019). Litho - and chrono - stratigraphic scheme of the WHS Dolomites UNESCO, Cover page.

Giordan, D., Manconi, A., Tannant, D.D., & Allasia, P. (2015). UAV: Low-cost remote sensing for high-resolution investigation of landslides. In Geoscience and Remote Sensing Symp. (IGARSS), IEEE, 5344-5347.

Goldscheider, N., Madl-Szonyi, J., Eross, A., Schill, E., (2010). Review:Thermal water resources in carbonate rock aquifers. Hydrogeology Journal, 18:1303 - 1318.

Goldscheider, N., Chen, Z., Auler, A., S., Bakalowicz, M., Broda, S., Drew, D., Hartmann, J., Jiang, G., Moosdorf, N., Stevanovic, Z., Veni, G., (2020). Global distribution of carbonate rocks and karst water resources. Hydrogeology Journal, 28:1661 - 1677.

Gomes, R.K., de Oliveira, L.P., Gonzaga, L., Tognoli, F.M., Veronez, M.R., & de Souza, M.K. (2016). An algorithm for automatic detection and orientation estimation of planar structures in LiDAR-scanned outcrops. Computers and Geosciences, 90: 170-178.

Guido, A., Mastandrea, A., Stefani, M., Russo, F., (2016). Role of autochthonous micrite in depositional geometries of Middle Triassic carbonate platform systems. Geological Society of America Bulletin, 128: 989 – 999.

Guido, A., Russo, F., Miriello D., Mastandrea, A., (2018). Autochthonous Micrite to Aphanodolomite: The Microbialites in the Dolomitization Processes. Geosciences, 8: 451.

Grammer, M.G., Ginsburg, R.N., Swart, P.K., McNeill, D.F., Timothy Jull, A.J., Prezbindowski, D.R., (1993). Rapid growth rates of syndepositional marine aragonite cements in steep marginal slope deposits, Bahamas and Belize. Journal of Sedimentary Petrology, 63; 983-989.

Grammer, G.M., Crescini, C.M., McNeill, D.F., Taylor, L.H., (1999). Quantifying rates of syndepositional marine cemetation in deeper platform environments – new insight into a fundamental process. Journal of Sedimentary Research 69,202–207.

Hodgetts, D., Drinkwater, N. L., Hodgson, J., Kavanagh, J., Flint, S. S., Keogh, K. J., Howell, J. A., (2004). Three-dimensional geological models from outcrop data using digital data collection techniques: an example from the Tanqua Karoo depocentre, South Africa. Geological Society, London, Special Publications, 239: 57-75.

Hodgetts, D., (2013). Laser scanning and digital outcrop geology in the petroleum industry: A review. Marine and Petroleum Geology, 46: 335-354.

Hunt, D., Fitchen, W.M., Swarbrick, R., Allsop, T., (1995). Differential compaction as a primary control of sequence architecture and development in the Permian Basin: geological significance and potential as a hydrocarbon exploration model. In: Garber, R.F., Lindsay, R.F. (Eds.), Wolfcampian – Leonardian Shelf Margin Facies of the Sierra Diablo: Seismic Models for Subsurface Exploration. West Tex. Geol. Soc. Publ., vol. 95-97: 83-104.

Hunt, D. W., Fitchen, W M., Kosa, E., (2002). Syndepositional deformation of the Permian Capitan reef carbonate platform, Guadalupe Mountains, New Mexico, USA. Sedimentary Geology 154: 89-126.

Inama, R., Menegoni, N., Perotti, C., (2020). Syndepositional fractures and architecture of the lastoni di formin carbonate platform: Insights from virtual outcrop models and field studies.Marine and Petroleum Geology, 121.

Jaboyedoff, M., Metzger, R., Oppikofer, T., Couture, R., Derron, M.H., Locat, J. & Turmel, D. (2007). New insight techniques to analyze rock-slope relief using DEM and 3D-imaging cloud points: COLTOP-3D software. In Rock mechanics: Meeting Society's Challenges and Demands Vol. 1:61-68.

Jacquemyn, C., El Desouky. H., Hunt, D., Casini, G., Swennen, R., (2014). Dolomitization of the Latemar platform: Fluid flow and dolomite evolution. Marine and Petroleum Geology, 55: 43 – 67.

James, N.P., Ginsburg, R.N., (1979). The seaward marginal Belize barrier and atoll reefs. International Association of Sedimentologists Special Publication, 3; 191 p.

James, M., Robson, S., (2012). Straightforward reconstruction of 3D surfaces and topography with a camera: Accuracy and geoscience application. Journal of Geophysical Research. 117.

Jordá Bordehore, L., Riquelme A., Miguel Cano, M., Tomás, R., (2017). Comparing manual and remote sensingfield discontinuity collection used in kinematic stability assessment of failed rock

slopes. International Journal of Rock Mechanics & Mining Sciences 97: 24-32.Keim, L., Schlager, W., (1999). Automicrite Facies on Steep Slopes (Triassic, Dolomites, Italy). Facies, 41: 15-26.

Keim, L., Brandner, R., (2001). Facies interfingering and synsedimentary tectonics on late Ladinian–early Carnian carbonate platforms (Dolomites, Italy). International Journal of Earth Sciences, 90: 813–830.

Keim, L., Schlager, W., (2001). Quantitative compositional analysis of a Triassic carbonate platform (Southern Alps, Italy). Sedimentary Geology 139: 261-283.

Kenter, J.A.M., 1990. Carbonate platform flanks: slope angle and sediment fabric. Sedimentology, 37: 777 - 794.

Kerans, C., Hurley, N.F., Playford, P.E., (1986). Marine diagenesis in Devonian reef complexes of the Canning Basin, Western Australia. In: Schroeder, J.H., Purser, B.H. (Eds.), Reef Diagenesis. Springer-Verlag, Berlin; 357-380.

Kosa, E., Hunt, D., W., (2005). Growth of syndepositional faults in carbonate strata: Upper Permian Capitan platform, New Mexico, USA. Journal of Structural Geology 27: 1069–1094.

La Bruna, V., Lamarche, J., Agosta, F., Rustichelli, A., Giuffrida, A., Salardon, R., Mariè, L., (2019). Structural diagenesis of shallow platform carbonates: Role of early embrittlement on fracture setting and distribution, case study of Monte Alpi (Southern Apennines, Italy). Journal of Structural Geology, 131, 103940.

Leonardi, P., (1968). Le Dolomiti. Geologia dei Monti tra Isarco e Piave. Manfrini, Rovereto, 1021 pp.

Lorenz, V., Nicholls, I. A., (1984). Plate and intraplateprocesses of Hercynian Europe during the late Paleozoic. Tectonophysics 107:25–56.

Lowe, D.G., (1999). Object recognition from local scale-invariant features. In International Conference on Computer Vision, Corfu, Greece, pp. 1150-1157.

Lowe, D.G., (2004). Distinctive Image Features from Scale-Invariant Keypoints. International Journal of Computer Vision 60: 91–110.

Marocchi, M., Klötzli, U. S., Morelli, C., Bargossi, G. M., Mair, V. (2005). Zircon geochronology, geochemistry and a new stratigraphic systematic of the lower Permian Athesian Volcanic Group (AG), Southern Alps (Italy). Epitome, Geoitalia 2005, 1:130.

Marocchi, M., Morelli C., Mair, V., Klötzli, U., Bargossi. G. M., (2008). Evolution of Large Silicic Magma Systems: New U-Pb Zircon Data on the NW Permian Athesian Volcanic Group (Southern Alps, Italy).

Martinelli, M., Bistacchi, A., Mittempergher, S., Bonneau,F., Balsamo, F., Caumon, G., Meda, M., (2020). Damage zone characterization combining scan-line and scan-area analysis on a km-scale Digital Outcrop Model: The Qala Fault (Gozo). Journal of Structural Geology 140, 104144.

Massari, F., Grandesso, P., Stefani, C., Jobstraibizer, P. G. (1986) - A small polyhistory foreland basin evolving in a context of oblique convergence: the Venetian basin (Chattian to Recent, Southern Alps, Italy). Spec. Publs. Int. Ass. Sediment., 8: 141-168, Oxford.

Mastandrea, A., Perri, E., Russo, F., Spadafora, A., Tucker, M., (2006). Microbial primary dolomite from a Norian carbonate platform: northern Calabria, southern Italy. Sedimentology, 53: 465–480.

Maurer, F. (2000), Growth mode of Middle Triassic carbonate platforms in the Western Dolomites (Southern Alps, Italy), Sedimentary Geology, 134, 275-286.

Mazzoli, S., Helman, M., (1994). Neogene patterns of relative plate motion for Africa-Europe: some implications for recent central Mediterranean tectonics. Geol. Rund., 83: 275-286.

McCaffrey, K.J.W., Jones, R.R., Holdsworth, R.E., Wilson, R.W., Clegg, P., Imber, J., Holliman, N., Trinks, I., (2005). Unlocking the spatial dimension: digital technologies and the future of geoscience fieldwork. J. Geol. Soc., 162: 927–938.

McKenzie, J.A., Vasconcelos, C., (2009). Dolomite Mountains and the origin of the dolomite rock of which they mainly consist: historical developments and new perspectives. Sedimentology, 56: 205 – 219.

Menegoni, N., Meisina, C., Perotti, C., Crozi, M., (2018). Analysis by UAV Digital Photogrammetry of Folds and Related Fractures in the Monte Antola Flysch Formation (Ponte Organasco, Italy). Geosciences. 8: 299.

Menegoni, N., Giordan, D., Perotti, C., Tannant, D., (2019). Detection and geometric characterization of rock mass discontinuities using a 3D high-resolution digital outcrop model generated from RPAS imagery – Ormea rock slope, Italy. Engineering Geology. 252: 145-163.

Minisini, D., Wang, M., Bergman, S., Aiken, C., (2014). Geological data extraction from lidar 3-D photorealistic models: a case study in an organic-rich mudstone, Eagle Ford Formation. Geosphere 10 (3): 610 - 626.

Ministero dell'Ambiente: Geoportale Nazionale, 2019. Piano Straordinario di Telerilevamento Ambientale.http://www.pcn.minambiente.it/mattm/progetto-piano-straordinario-di-telerilevamento/.

Mollema, P.N., Antonellini M., (1999). Development of strike-slip faults in the dolomites of the Sella Group, Northern Italy. Journal of Structural Geology, 21: 273 - 292.

Montanari, D., Minissale, A., Doveri, M., Gola, G., Trumpy, E., Santilano, A., Manzella, A., (2017). Geothermal resources within carbonate reservoirs in western Sicily (Italy): A review. Earth-Science Reviews, 169: 180-201.

Nemeth, K., Budai, T., (2009). Diatremes cut through the Triassic carbonate platforms in the Dolomites? Evidences from and around the Latemar, northern Italy. Episodes, 32: 74-83.

Neri, C., Gianolla, P., Furlanis, S., Caputo, R. & Bosellini, A., (2007). Note illustrative della Carta Geologica d'Italia. Foglio Cortina d'Ampezzo 029. Scala 1:50.000. Servizio Geologico d'Italia, 200 pp.

Neuweiler, F., Gautret, P., Thiel, V., Lange, R., Michaelis, W., Reitner, J., (1999). Petrology of Lower Cretaceous carbonate mud mounds (Albian, N. Spain): insights into organomineralic deposits of the geological record. Sedimentology, 46: 837-859.

Nolting, A., Zahm, C. K., Kerans, C., Nikolinakou, M. A., (2018). Effect of carbonate platform morphology on syndepositional deformation: Insights from numerical modeling, Journal of Structural Geology,115: 91-102.

Nooitgedacht, C.W., Kleipool, L.M., Andeweg, B., Reolid, J., Betzler, C., Lindhorst, S., Reijmer, J.J.G (2018). New insights in the development of syn-depositional fractures in rimmed flat-topped carbonate platforms, Neogene carbonate complexes,Sorbas Basin, SE Spain. Basin Research 30 (Suppl. 1): 596 - 612.

Pisa G., Farabegoli E. Ott E., (1979). Stratigrafia e paleogeografia dei terreni anisici della Conca di Agordo e dell'alta Val di Zoldo (Dolomiti sudorientali). Mem. della Soc. Geolog. Ital., 18: 63-92.

Pless, J. C., McCaffrey, K. J. W., Jones, R . J., Holdsworth, R. E., Conway, A., Krabbendam, M., (2015). 3D characterization of fracture systems using Terrestrial Laser Scanning: an example from the Lewisian basement of NW Scotland. Geological Society London Special Publications 421(1).

Polino, R., Dal Piaz, G. V., Gosso, G., (1990). Tectonic erosion at the Adria margin and accretionary processes for the Cretaceous orogeny of the Alps. Mem. Soc. Geol. France,156: 345 - 367.

Preto, N., Hinnov, L.A., (2003). Unraveling the Origin of Carbonate Platform Cyclothems in the Upper Triassic Durrenstein Formation (Dolomites, Italy). Journal of sedimentary research, 73: 774 - 789.

Preto, N., Kustatscher, E., Wignall, P.B., (2010). Triassic climates—state of the art and perspectives. Palaeogeogr. Palaeoclimatol. Palaeoecol., 290: 1–10.

Preto, N., Gianolla, P.,Franceschi, M., Gattolin, G., Riva, A., (2017). Geometry and evolution of Triassic high-relief, isolated microbial platforms in the Dolomites, Italy: The Anisian Latemar and Carnian Sella platforms compared. AAPG Bulletin. 101: 475-483.

Pollard, D.D., Segall, P., (1987). Theoretical displacements and stressesnear fractures in rock: with applications to faults, joints, veins, dikes and solution surfaces. In: Atkinson, B.A. (Ed.), Fracture Mechanics of Rock. Academic Press, London, pp. 277±349.

Posenato, R., (2008). Global correlations of mid Early Triassic events: The Induan/Olenekian boundary in the Dolomites (Italy). Earth-Science Reviews 91: 93–105.

Preto, N., Gianolla, P.,Franceschi, M., Gattolin, G., Riva, A., (2017). Geometry and evolution of Triassic high-relief, isolated microbial platforms in the Dolomites, Italy: The Anisian Latemar and Carnian Sella platforms compared. AAPG Bulletin. 101: 475-483.

Quick, J. E., Sinigoi, S., Snoke, A. W., Kalakay, T. J., Mayer, A., Peressini, G., (2003). Geologic map of the southern Ivrea-Verbano Zone, northern Italy. U.S.Geol. Surv. Geologic Investigations Series Map I-2776, 22 p., scale 1:25,000.

Rarity, F., van Lanen, X. M. T., Hodgetts, Gawthorpe, D., R. L., Wilson, P., Fabuel-Perez, I., Redfern, J., (2014). LiDAR-based digital outcrops for sedimentological analysis: workflows and techniques. Geological Society, London, Special Publications 2014, v.387: 153-183.

Remondino, F., El-Hakim, S. (2006). Image-based 3D modelling: a review. The Photogrammetric Record, 21(115), 269-291.

Reitner, J., Neuweiler, F., (1995). Mud mounds, a polygenic spectrum of fine-grained carbonate buildups. Facies, 32, 1-70.

Resor, P. G., Flodin, E. A., (2010). Forward modeling synsedimentary deformation associated with a prograding steep-sloped carbonate margin. Journal of Structural Geology, 32: 1187-1200.

Roghi, G., (2004). Palynological investigations in the Carnian of the Cave del Predil area (Julian Alps, NE Italy). Rev. Palaeobot. Palynol., 132: 1–35.

Roghi, G., Kustatscher, E., Bernardi, M., Dal Corso, J., Forte, G., Franz, M., Hochuli, P., Krainer, K., Petti, F.M., Ragazzi, E., Riva, A., Wappler, T., Gianolla, P., (2014). Field trip to Permo-Triassic Palaeobotanical and Palynological sites of the Southern Alps- Geo.Alp, Vol. 11 2014 29 - 84.

Ross-Brown, D.M., Wickens, E.H., & Markland, J.T. (1973). Terrestial photogrammetry in open pits: 2-an aid to geological mapping. Trans. Inst. Min. Metall., 82, A115-A130.

Rusciadelli, G., Di Simone, S., (2007). Differential compaction as a control on depositional architectures across the Maiella carbonate platform margin (central Apennines, Italy). Sedimentary Geology 196: 133-155.

Russo, F., Neri, C., Mastandrea, A., Baracca, A., (1997). The mud mound nature of the Cassian platform margins of the Dolomites. A case history: the Cipit boulders from Punta Grohmann (Sasso Piatto massif, Northern Italy). Facies, 36: 25-36.

Saller, A.H., (1996). Differential compaction and basinward tilting of the prograding Capitan reef complex, Permian, west Texas and southeast New Mexico, USA. Sedimentary Geology, 101: 21-30.

Salvini, R., Mastrorocco, G., Seddaiu, M., Rossi, D., & Vanneschi, C. (2016). The use of an unmanned aerial vehicle for fracture mapping within a marble quarry (Carrara, Italy): photogrammetry and discrete fracture network modelling. Geomatics, Natural Hazards and Risk, 1-19.

Santantonio, M., Carminati, E., (2011). Jurassic rifting evolution of the Apennines and Southern Alps (Italy): Parallels and differences. Geological Society of America Bulletin 123, no. 3-4: 468-484

Schlager, W., (2003). Benthic carbonate factories of the Phanerozoic. International Journal of Earth Sciences (Geol. Rundsch) 92:445–464.

Schlager, W., Keim, L., (2009). Carbonate platforms in the Dolomites area of the Southern Alps – historic perspectives on progress in sedimentology. Sedimentology, 56:191 - 204.

Schmid, S. M., Pfiffner, O. A., Froitzheim, N., Schonborn, G., Kissling, E., (1996). Geophysical-geological transect and tectonic evolution of the Swiss-Italian Alps. Tectonics, 15:1036 - 1064.

Schonborn, G., (1999). Balancing cross sections with kinematic constraints: The Dolomites (northern Italy). Tectonics, vol. 18(3): 527 -545.

Seers, T. D., Hodgetts, D., (2013). Comparison of digital outcrop and conventional data collection approaches for the characterization of naturally fractured reservoir analogues. Geological Society, London, Special Publications, 374, 51-77.

Shakiba, M., Ayatollahi, S., Riazi, M., (2016). Investigation of oil recovery and CO2 storage during secondary and tertiary injection of carbonated water in an Iranian carbonate oil reservoir. J. Petrol. Sci. Eng, 137: 134 - 143.

Simms, M. J., Ruffell, A. H., (1989). Synchroneity of climatic change and extinctions in the Late Triassic. Geology, 17: 265–268.

Simms, M. J., Ruffell, A. H., (1990). Climatic and biotic change in the late Triassic. J. Geol. Soc.Lond., 147: 321–327.

Slob, S., Hack, R., Van Knapen, B., & Kemeny, J. (2004). Automated identification and characterization of discontinuity sets in outcropping rock masses using 3D terrestrial laser scan survey techniques. In Proc. of the ISRM Regional Symp. EUROCK: 439-443.

Soldati, M., Pasuto, A., (1991). Some cases of deep-seated gravitational deformations in the area of Cortina d'Ampezzo (Dolomites). European Experimental Course on Applied Geomorphology. Vol. 2 - Proceedings: 91-104.

Spetsakis, M., & Aloimonos, J.Y. (1991). A multi-frame approach to visual motion perception. International Journal of Computer Vision, 6(3), 245-255.

Stefani, M., Brak, P., Gianolla, P., Keim, L., Mauer, M., Neri, C., Preto, N., Riva, A., Roghi, G., Russo, F., (2004). Triassic carbonate platforms of the Dolomites: carbonate production, relative sea-level fluctuations and the shaping of the depositional architecture. 32nd International Geologic Congress. Field Guide Book P44. APAT, Roma. 68 pp.

Stefani, M., Furin, S., Gianolla, P., (2010). The changing climate framework and depositional dynamics of Triassic carbonate platforms from the Dolomites. Palaeogeography, Palaeoclimatology, Palaeoecology, 290: 43–57.

Sturzenegger, M., Stead, D., (2009). Close-range terrestrial digital photogrammetry and terrestrial laser scanning for discontinuity characterization on rock cuts. Engineering Geology, 106: 163-182.

Tannant, D.D. (2015). Review of photogrammetry-based techniques for characterization and hazard assessment of rock faces. Int. Journal of Geohazards and Environment, 1(2), 76-87.

Tavani, S., Corradetti, A., Billi, A., (2016). High precision analysis of an embryonic extensional fault-related fold using 3D orthorectified virtual outcrops: The viewpoint importance in structural geology. Journal of Structural Geology 86: 200-210.

Thiele, S.T., Grose, L., Samsu, A., Micklethwaite, S., Vollgger, S.A., Cruden, A.R., (2017). Rapid, semi-automatic fracture and contact mapping for point clouds, images and geophysical data. Solid Earth, 8: 1241–1253.

Tosti, F., Guido, A., Demasi, F., Mastandrea, A., Naccarato, A., Tagarelli, A., Russo, F., (2011). Microbialites as primary builders of the Ladinian-Carnian platforms in the Dolomites: biogeochemical characterization. Geo.Alp, 8: 156 - 162.

Triggs B., McLauchlan P.F., Hartley R.I., Fitzgibbon A.W. (2000). Bundle Adjustment – A ModernSynthesis. International Workshop on Vision Algorithms, Sep 2000, Corfu, Greece. pp.298-372.

Trombetta, G. L., (2016). Analisi di facies ed architettura di una piattaforma carbonatica del Carnico: il Settsass/Richthofen Riff (Dolomiti, Alpi Meridionali, Italia Settentrionale). Quaderni del Museo Civico di Storia Naturale di Ferrara, 4:11-32.

Venzo S. (1939) - Nuovo lembo tortoniano strizzato tra le filladi ed il permiano a Strigno di Valsugana (Trentino meridionale orientale). Boll. Soc. Geol. It., 58, 1, 175-185, Roma.

Visonà, D. (1982). Chilled margins and commingling of magmas in the Bressanone (Brixen) Hercynian granodiorites (eastern Alps, northern Italy). Geology 56:33–44.

Westoby, M.J., Brasington, J., Glasser, N.F., Hambrey, M.J., Reynolds, J.M., (2012). 'Structure-from-Motion' photogrammetry: a low-cost, effective tool for geoscience applications. Geomorphology, 179: 300-314.

Whitaker, F.F., Smart, P.L., (1997). Groundwater circulation in a karstified bank marginal fracture system, South Andros Island, Bahamas. Journal of Hydrology 197.

Wilson, E. N.; Hardie, L. A.; Phillips, O. M. (1990). Dolomitization front geometry, fluid flow patterns, and the origin of massive dolomite; the Triassic Latemar buildup, northern Italy. American Journal of Science, vol. 290, issue 7: 741-796.

Winterer E.L. and Bosellini A., 1981 - Subsidence and Sedimentation on a Jurassic Passive Continental Margin, Southern Alps, Italy. AAPG Bull., v.65, n.3, 394-421.

Wolf, P.R., & Dewitt, B.A. (2000). Elements of Photogrammetry: with applications in GIS (3rd ed). McGraw-Hill, Boston, 608.